

Hyperspectral imaging for heritage: From books to bricks



Ian James Maybury

St Cross College

Thesis submitted for the degree of

MSci

in

Science and Engineering in Arts, Heritage, and Archaeology

Michaelmas Term 2019

Contents

<i>Figures</i>	5
<i>Tables</i>	7
<i>List of acronyms, notations, and abbreviations</i>	8
<i>Glossary of terms</i>	11
Term	11
Definition	11
<i>Abstract</i>	12
<i>Acknowledgements</i>	14
Chapter 1 Introduction	16
1.1 <i>The foundations of the “Heritage science” field</i>	16
1.2 <i>The benefits of the application of science to cultural heritage</i>	20
1.3 <i>The thesis in the context of heritage science</i>	33
1.4.1 <i>A note on peaks, signals, and noise</i>	37
1.5 <i>Imaging and spectroscopic techniques in heritage science</i>	37
1.6 <i>Hyperspectral imaging</i>	38
1.7 <i>Thesis aim, research questions, and overall approach</i>	39
1.8 <i>General approach</i>	40
1.9 <i>Thesis structure</i>	42
Chapter 2 Literature review	43
2.1 <i>Hyperspectral imaging</i>	43
2.2 <i>Reflectance spectra</i>	47
2.3 <i>The pigmentation of heritage artefacts</i>	48
2.4 <i>The photodegradation of pigmentation</i>	49
2.5 <i>The detection of pigmentation</i>	50
2.6 <i>Problems with hyperspectral imaging</i>	50
2.7 <i>Literature review conclusion (summary and implications)</i>	51
Chapter 3 Methods	53
3.1 <i>Analytical techniques</i>	53
3.1.1 <i>General description of principles</i>	53
3.1.2 <i>Instrumentation used</i>	56
3.2 <i>Summary of analytical methods used</i>	62
3.3 <i>Calibration of hyperspectral equipment and sources of error</i>	64
Chapter 4 experiment 1: Assessing the Effectiveness of Hyperspectral Imaging in the Identification of Pigments: Comparing HSI and Raman Spectroscopy in An Analysis of Illuminated Armenian Manuscripts	78
4.0 <i>Abstract</i>	79

4.1 Introduction	81
4.1.1 Pigment analysis.....	81
4.1.2 Raman spectroscopy.....	82
4.1.3 Hyperspectral imaging	84
4.2 Materials and methods	88
4.2.1 Armenian manuscripts.....	88
4.2.2 Workflow.....	91
4.2.3 HSI database	94
4.2.4 Equipment.....	97
4.3 Results.....	104
4.3.1 Confusion matrices.....	111
4.4 Discussion and conclusions.....	115
Chapter 5 experiment 2: Digital restoration using visible and near infrared hyperspectral imaging (VNIR HSI): An investigation into the pigmentation on the west wall of the Shrine of Taharqa	120
5.0 Abstract.....	121
5.1 Introduction	123
5.1.1 The shrine of King Taharqa	123
5.2 Theory.....	126
5.2.1 The digital recolouring of faded artworks.....	126
5.2.2 Identifying pigments on Ancient Egyptian art from the XXVth dynasty.....	127
5.2.3 Analytical methods	130
5.3 Materials and methods	134
5.3.1 Equipment (primary data collection)	134
5.3.2 Secondary data collection methods	142
5.4 Results.....	143
5.4.1 VNIR HSI mapping	143
5.4.2 XRF.....	146
5.4.3 Microscopy	148
5.4.4 Photo-induced Luminescence (PIL)	149
5.4.5 Creating an amalgamated map of pigments on the west wall of the Shrine of Taharqa	150
5.5 Discussion and conclusions.....	153
Chapter 6 Experiment 3: Visible and near infrared hyperspectral imaging for the analysis of colour change in cultural heritage artefacts.....	156
6.0 Abstract.....	156
6.1 Introduction	158
6.1.1 Light induced fading of pigmentation.....	158

6.1.2 Monitoring of collections	159
6.2 Aim & research questions.....	161
6.3 Materials and methods	162
6.3.1 Materials.....	162
6.3.2 Methodology.....	165
6.3.3 Data processing for hyperspectral data	166
6.4 Results.....	176
6.4.1 Analysis of EAX 3873: Faded silk robe.....	176
6.4.2 Analysis of Bodl. 394: Illuminated manuscript	184
6.5 Discussion and conclusion	197
Chapter 7 Overall thesis discussion and conclusions	202
7.1 Experimental decisions.....	202
7.2 Review of the aim and research questions	204
7.2.1 Research question 1.....	204
7.2.2 Research Question 2.....	205
7.3.3 Research Question 3.....	206
7.3 Future research	206
7.4 Concluding remark – take home message	208
Chapter 8 Declaration of Funding	209
Chapter 9 References.....	210
Chapter 10 Appendix Proof of submission of manuscripts to journals	233

Figures

<i>Figure 1.1 The scientific method</i>	21
<i>Figure 1.2 The three periods of development</i>	22
<i>Figure 3.1. Illustration of a data cube</i>	54
<i>Figure 3.2. The HSI equipment used during the thesis</i>	58
<i>Figure 3.3. White light calibration spectra</i>	59
<i>Figure 3.4 Raman spectroscopy equipment</i>	60
<i>Figure 3.5 The DRSP equipment</i>	61
<i>Figure 3.6. The calibration workflow</i>	65
<i>Figure 3.7. The reflectance spectrum of Spectralon®</i>	68
<i>Figure 3.8. MS. Arm. d.3</i>	72
<i>Figure 3.9. A basic diagram of chromatic aberration</i>	73
<i>Figure 3.11. Demonstration chromatic aberration</i>	75
<i>Figure 3.11. Headwall Photonics calibration chart</i>	76
<i>Figure 4.1 Armenian Manuscripts</i>	89
<i>Figure 4.2. Flow diagram experiment 1</i>	94
<i>Figure 4.3. Colour swatches of different pigments</i>	95
<i>Figure 4.4. The HSI equipment</i>	99
<i>Figure 4.5. The Raman spectroscopy equipment</i>	102
<i>Figure 4.6. Map of vermillion pigment</i>	116
<i>Figure 5.1 The HSI equipment during a scan of The Shrine of Taharqa</i>	136
<i>Figure 5.2 The shrine of King Taharqa</i>	138
<i>Figure 5.3 White calibration data (Laboratory)</i>	139
<i>Figure 5.4 White calibration data (field)</i>	141
<i>Figure 5.5. HSI map of red colouration on the west wall</i>	143
<i>Figure 5.6. HSI map of red colouration on hieroglyphics</i>	145
<i>Figure 5.7. XRF showing Cu found on the west wall</i>	146
<i>Figure 5.8. A representative spectra from the pXRF experiment</i>	147
<i>Figure 5.9. The approximate locations of the samples used for microscopy</i>	148
<i>Figure 5.10. Armstrong's photoinduced luminescence results</i>	149
<i>Figure 5.11. Creation of finished figure</i>	152
<i>Figure 5.12. Final image of pigmentation on the Shrine</i>	153
<i>Figure 6.1 The DRSP equipment in use</i>	163
<i>Figure 6.2. Silk robe EAX 3873</i>	164
<i>Figure 6.3. MS Bodl. 394</i>	165
<i>Figure 6.4. Workflow to obtain CIELAB values</i>	169
<i>Figure 6.5. The PCA plot for Bodl. 394</i>	175
<i>Figure 6.6. Endmembers (robe)</i>	176
<i>Figure 6.7. Plot of eigenvalues (robe)</i>	177
<i>Figure 6.8. The most significant Endmembers (robe)</i>	181
<i>Figure 6.9. A false colour image of the robe</i>	182
<i>Figure 6.10. Robe areas of analysis</i>	183
<i>Figure 6.11. Bodl. 394 areas of analysis</i>	184
<i>Figure 6.12. Reflectance spectra taken from Bodl. 394</i>	185
<i>Figure 6.13. Reflectance spectra Comparing day 0, and day 111</i>	189
<i>Figure 6.14 The area of Bodl. 394 that was used to demonstrate the effect of the Radiometric Normalisation process</i>	190
<i>Figure 6.15. Plot of eigenvalues vs principal components Manuscript</i>	192
<i>Figure 6.16. Endmember map for Day 0: Bodl 394</i>	194

Figure 6.17. Spectra of endmembers, Day 0: Bodl.394. 195
Figure 6.18. Spectra of endmembers Bodl. 394: Day 111 196
Figure 6.19. Endmember map Bodl. 394: Day 111 corrected. 197

Tables

<i>Table 1.1 A summary of the analytical techniques.....</i>	<i>32</i>
<i>Table 1.2 List of NDT methods and sampling methods.....</i>	<i>37</i>
<i>Table 2.1 Multispectral vs hyperspectral imaging.</i>	<i>44</i>
<i>Table 2.2 Definitions of terms used to describe colourants.</i>	<i>48</i>
<i>Table 3.1 A comparison of the main techniques in the paper.</i>	<i>64</i>
<i>Table 4.1. Details of the Armenian manuscripts</i>	<i>91</i>
<i>Table 4.2. Contents of databases for Experiment 1.....</i>	<i>96</i>
<i>Table 4.3. HSI vs Raman Spectroscopy.....</i>	<i>104</i>
<i>Table 4.4. The results of Raman spectroscopy</i>	<i>105</i>
<i>Table 4.5. A comparison of percentage agreements</i>	<i>107</i>
<i>Table 4.6. Percentage success: default wavelength range.....</i>	<i>110</i>
<i>Table 4.7. Confusion matrix for the lowest score.....</i>	<i>112</i>
<i>Table 4.8. Confusion matrix for the highest score</i>	<i>113</i>
<i>Table 5.1. A brief comparison of the main study methods.</i>	<i>128</i>
<i>Table 5.2. Pigments from Ancient Egypt and their molecular formulae.....</i>	<i>129</i>
<i>Table 6.1. Eigenvalue analysis for the robe</i>	<i>178</i>
<i>Table 6.2. The pixel count of the endmembers (robe)</i>	<i>180</i>
<i>Table 6.3. Colour change values (Bodl. 394).....</i>	<i>186</i>
<i>Table 6.4. Effect of radiometric normalisation</i>	<i>191</i>
<i>Table 6.5. Eigenvalue data for Day 0: Bodl. 394.....</i>	<i>193</i>

List of acronyms, notations, and abbreviations

AAS	Atomic absorption spectroscopy
AES	Auger electron spectroscopy
BE	Binary encoding
CDT	Centre for doctoral training
DSC	Differential scanning calorimetry
DTA	Differential thermal analysis
ED	Electron diffraction
EELS	Electron energy loss spectroscopy
ENVI	Environment for visualising images
EPR	Electron paramagnetic resonance spectroscopy
EPSRC	European physical sciences research council
FORS	Fibre optic reflectance spectroscopy
FT-IR	Fourier transform infrared
GC	Gas chromatography
HPLC	High performance liquid chromatography
HPLC	High performance liquid chromatography
HSI	Hyperspectral imaging
ICCROM	International centre for the study of the preservation and restoration of cultural property
IR	Infrared spectroscopy
MS	Mass spectrometry
MSI	Multispectral imaging

NAA	Neutron activation analysis
ND	Neutron diffraction
NDT	Non-destructive testing/technique
NIR	Near infrared
NMR	Nuclear magnetic resonance
NRCA	Neutron resonance capture analysis
OES	Optical emission spectroscopy
OM	Optical microscopy
OSL	Optically stimulated luminescence
PGAA	Prompt gamma activation analysis
PIL	Photo-induced luminescence
PIXE	Particle induced x-ray emission
pXRF	Portable XRF
ROI	Region of interest
RS	Raman spectroscopy
SAM	Spectral angle mapping
SEM	Scanning electron microscopy
SFF	Spectral feature fitting
SWIR	Short wave infrared
TEM	Transmission electron microscope
TEM	Transmission electron microscopy
TG	Thermogravimetry
TL	Thermoluminescence
UV	Ultraviolet
VIS	Visible light

VNIR HSI	Visible and near infrared HSI
XAS	X-ray absorption spectroscopy
XPS	X-ray photoelectron spectroscopy
XRD	X-ray diffraction
XRF	X-ray fluorescence

Glossary of terms

Term	Definition
Imaging techniques	<p>Instrumentation that creates an image. An image being defined as “a representation of a physical object formed by a lens, mirror, or other optical instrument”</p> <p><i>Daintith & Martin (2010)</i></p>
Spectroscopy	<p>“The study of methods of producing and analysing spectra using spectroscopes, spectrometers, spectrographs, and spectrophotometers. The interpretations of the spectra so produced can be used for chemical analysis, examining atomic and molecular energy levels and molecular structures, and for determining the composition and motions of celestial bodies.” <i>Daintith & Martin (2010)</i></p>

Abstract

In heritage science one important line of enquiry is the pigmentation of an artefact. Imaging methods have been developed for this purpose and have had success in the investigation of colourants. In particular a great deal of information has been gained by looking at the spectra outside of the visible region, however, visible and near infrared hyperspectral imaging (VNIR HSI) equipment has been developed at a price point that could see widespread use across heritage institutions. This thesis addresses how VNIR HSI is best utilised for the analysis of colourants and evaluates the efficacy of VNIR HSI for characterisation, detection, and monitoring. Advantages and drawbacks of this new technique are highlighted.

VNIR HSI was used to characterise the colouration in illuminated manuscripts from the Bodleian Libraries. VNIR HSI was restricted in its capacity for characterisation by its spectral range but it could analyse a surface more rapidly than Raman spectroscopy. In the case of characterisation VNIR HSI could be useful for mapping heterogeneity of colourants, or to highlight areas of interest to investigate.

To investigate the ability of VNIR HSI to detect traces of pigmentation the shrine of Taharqa, in the Ashmolean Museum, was scanned. VNIR HSI was capable of mapping pigmentation not obvious to the eye. It could therefore act as a useful aid in the reconstruction of works of art, however as it was limited to mapping only pigmentation that it could detect, X-ray fluorescence (XRF), and data from past experiments, were used in conjunction with VNIR HSI in order to more fully evaluate the surface.

To investigate the abilities of VNIR HSI as a method for the monitoring of pigmentation in an artefact, an illuminated manuscript on short display at the Bodleian Libraries, and a partially faded silk robe now in the collection of The Ashmolean Museum, were analysed and it was found that a colour change value was obtainable,

and that VNIR HSI could afford the advantages of being non-contact, full-field, and capable of digitising the scan in comparison to presently used methodology.

Acknowledgements

Thanks to my supervisors Heather, David, and Melissa for their support through the years we have worked together, I'm certain I've learned a great deal.

Thanks also to Prof. Andrew Beeby, and Dr Kate Nicholson for their assistance with Raman spectroscopy throughout the investigation into Armenian manuscripts..

Thanks to Marinita Stiglitz (Head of Paper Conservation, Bodleian Libraries, Oxford University) who introduced me to the Armenian Manuscripts and whose knowledge helped me. To K. Domoney, L. McNamara, and D. Bone of the Ashmolean Museum, who brought the shrine to our attention, gave us help with the logistics, and offered advice on Ancient Egyptian colourants and to the curators and conservators at the Ashmolean Museum and Bodleian Libraries for their help selecting collection items, and assistance with logistics.

Section 1: Introductory Section

Chapter 1 Introduction

1.1 The foundations of the “Heritage science” field

To define Heritage science briefly it can be thought of as the meeting of conservation science, archaeological science, and building science (Strlič 2018) whereby the scientific method is utilised for the characterisation and understanding of the mechanisms and materials involved in cultural heritage (Artioli 2010) in other words the analysis and treatment of an artefact with a view to its preservation (Artioli 2010).

Arguably “heritage science” has been conducted for centuries. As Strlic notes, Faraday’s lecture in 1843 about the contribution of pollution to the degradation of books can be seen as “heritage science” *Strlic (2015)*

A parliamentary science and technology committee publication defines heritage science as the “research and application of science to conservation problems related to moveable... and immovable heritage” *House of Lords (2012)*. In that same report they commended the arts and humanities research council (AHRC), and the engineering and physical sciences research council (EPSRC) for pulling together previously disparate disciplines to form the new research discipline “heritage science” in response to the House of Lords report in 2006 calling for a national strategy to aid the conservation of cultural heritage *House of Lords (2006)*.

The response of the AHRC, and EPSRC to the House of Lords report was to develop a research programme in 2009 *Science and Heritage Programme (2009)* which aimed to “strengthen and develop the hybrid discipline of heritage science” in which the interdisciplinary nature of heritage science is stressed, and it is said that the programme was to embrace researchers and stakeholders who were encompassed by the research aims of both AHRC, and EPSRC, listing 24 distinct subjects *Science and Heritage*

Programme (2009) including chemistry, physics, mathematics, conservation science, materials science, building science, and archaeology. More directly, the programme states that “heritage science is a complex field, requiring input across the full range of disciplines and practices covered by the AHRC and EPSRC” *Science and Heritage Programme (2009)*.

In 2010 a National Heritage Science Steering Committee was set up as a collaboration between academic, and heritage organisations, in response to the House of Lords’ recommendation to formulate a strategy for heritage science, which produced three initial reports which sought to provide an evidence base for a UK wide strategy. The first report, *The role of science in the management of the UK heritage Williams (2009a)* summarises the assets of UK heritage sites including museums, galleries, archives, libraries, archaeological sites, and the built environment. The report also discusses the management of those assets, looking at the mechanisms by which those assets may deteriorate *Williams (2009a)*.

Seeking to improve the management of UK heritage assets the report suggests three “themes” to cover gaps in the knowledge base which they name as understanding material behaviour, understanding environments, and improving practice which respectively indicate the need for research into the effect of deterioration agents and damage thresholds with a focus on modern materials, the improvement of the environmental efficiency and sustainability of the displays and built environments with a view to reducing the effect of deterioration agents in a sustainable and cost effective way, and finally the production of recommendations seeking to improve the range of techniques for monitoring and assessing heritage assets particularly non-destructive testing methods including the desire for a greater availability of information surrounding available techniques *Williams (2009a)*.

This DPhil therefore falls into the third category outlined in the initial report as it could help monitor the effects of the identified deterioration agents, namely water, inappropriate relative humidity, inappropriate temperature, light, fire damage, chemical agents, biological agents, and physical agents *Williams (2009a)*.

Of relevance to this DPhil is that the second report *The Use of Science to Enhance our Understanding of the Past* reviews the drivers for scientific investigation into “detecting and imaging heritage assets” *Williams (2009b)* in which the improvement of precision and accuracy are highlighted as needed by the national strategy and hyperspectral imaging is said to have “significant potential” for the investigation of artwork and suggests learning best practice from other fields *Williams (2009b)*. The third report provided an overview of the heritage scientists currently working, and where they worked in order to assess gaps in capacity *Williams (2009c)*. From these reports the National Heritage Science Steering Group produced a National Heritage Science Strategy, the aim of which was to improve awareness of the heritage science field and increase collaboration to improve the situation surrounding resources, funding, and skills *National Heritage Science Steering Group (2010)*.

A search for papers with the term “heritage science” reveals that the first papers produced in the field were *Brocx & Semeniuk (2007)* which is a paper on the preservation of Earth Science features, *Cotte et al. (2009)* which reviewed the use of μ FT-IR in cultural heritage science, and *Schulz (2009)* which is probably the first paper to explore the desire of scientists to exploit cultural heritage for the investigation of science, and the desire of museums to utilise science for the care of their collections.

The most recent publications include *Vandivere et al. (2020)* which evaluates the art historical relevance of an earlier study into *Girl with a Pearl Earring* by Vermeer and further analyses the painting using a 3D digital microscope with a view to analysing

Vermeer's painting techniques. *Masini et al. (2020)* discuss the challenges surrounding the protection, and location of buried archaeological heritage in urban environments and present a case study of a site in Cusco, Peru. Finally *Dooley et al. (2020)* compared molecular fluorescence imaging spectroscopy to X-ray fluorescence spectroscopy for the identification and mapping of pigments using *The Olive Orchard* by Van Gogh as a case study.

The most popular paper is *Viles et al. (2011)* which is a paper on the comparison of four different tools for measuring rock hardness, a property of rocks that allows a heritage scientist to characterise the rocks as they deteriorate. The next most popular is *Volp & Grassian (2013)* which describes the effect of surface water on the reactions of the surface with atmospheric particles, of particular interest to the heritage scientist is the reaction of the surface with atmospheric pollutants, which can be agents of deterioration. The third most popular paper is *Brocx & Semeniuk (2007)* which has already been discussed.

These papers show a growth in the field, shortly after the House of Lords report *House of Lords (2006)* the papers were focussed on defining the field and its research questions, *Schulz (2009)* is an excellent example of this and the popularity of *Brocx & Semeniuk (2007)* is indicative of the popularity of the earth sciences within the heritage science field, in fact the three most popular papers discussed here all have connotations for the earth sciences. The most recent papers demonstrate that the field has developed into something aligned with the original vision of the House of Lords where scientific principles, and scientifically trained persons are applied to the application of problems affecting the cultural heritage of the UK.

1.2 The benefits of the application of science to cultural heritage

Analytical instrumentation was applied to cultural heritage before the field of heritage science and there are a multitude of different analytical techniques that have been utilised for the work now described as falling under the umbrella of the field of heritage science *Artioli (2010)* and the use of these in heritage institutions has grown over the last couple of decades. A growth in the number of such methods used on artworks was noted in 1995 *Bacci (1995)* and the frequency of publications in conservation journals about scientific analyses has increased recently *ICCROM (2021); Liang (2012)*.

Such analytical techniques have gained in popularity because they can provide quantitative information to conservation teams such as the characterisation and location of pigments. For example, reflectance and luminescence imaging have been used to characterise pigments and locate underdrawings *Ricciardi et al. (2009)*, and Raman spectroscopy has been utilised in the estimation of the concentrations of the constituents of lead based paint in various artworks *Pallipurath et al. (2014)*. The ability of such techniques to reveal hidden information is extremely informative, false colour images have been used to identify restorations and preparatory sketches *Delaney et al. (2016a)*, and fluorescence has been used to improve the readability of a palimpsest attributed to Archimedes *Bloechl et al. (2010)*. Monitoring can be performed by scientific methods, for example Raman spectroscopy has been used to monitor wooden artefacts *Marengo et al. (2003)*, and provenance determination is aided by scientific investigations, for example a multi-technique examination of a painting whose artist attribution is debated contributed to the argument *Burgio et al. (2005)*. Finally, the scientific study of artefacts aids our understanding of the technology of the artist *Royal Society of Chemistry (2020)* with, for example, Raman spectroscopy used to evaluate the techniques of artists *Coupry et al. (1994)*. It is therefore demonstrable that information gained through

application of the scientific method (*Figure 1.1*), and is of importance to heritage professionals *Clark (2002); Zhao et al. (2008)*.

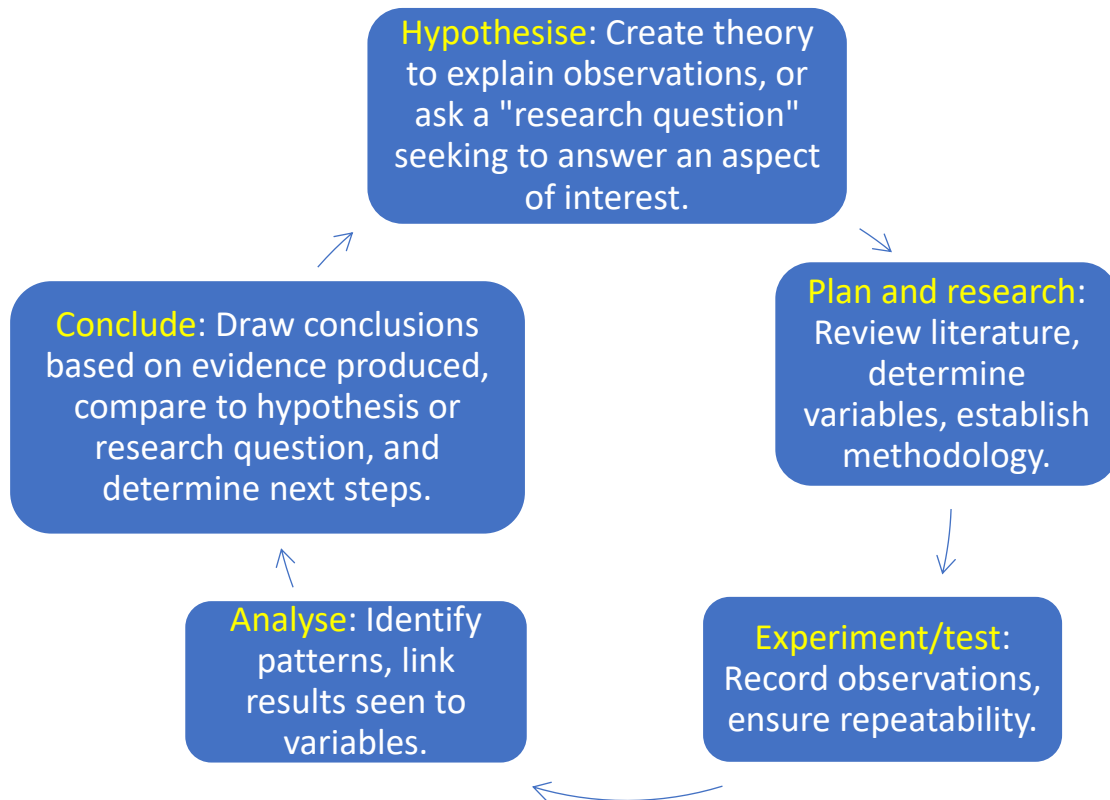


Figure 1.1 The scientific method: The underlying principle of a scientific investigation, common to all scientific fields, and cyclical in nature.

1.3 The introduction of scientific analysis to cultural heritage

Doménech-Carbó & Osete-Cortina (2016) outline three historical periods of development of the “chemical analysis” of cultural artefacts, presented in *Figure 1.2*.

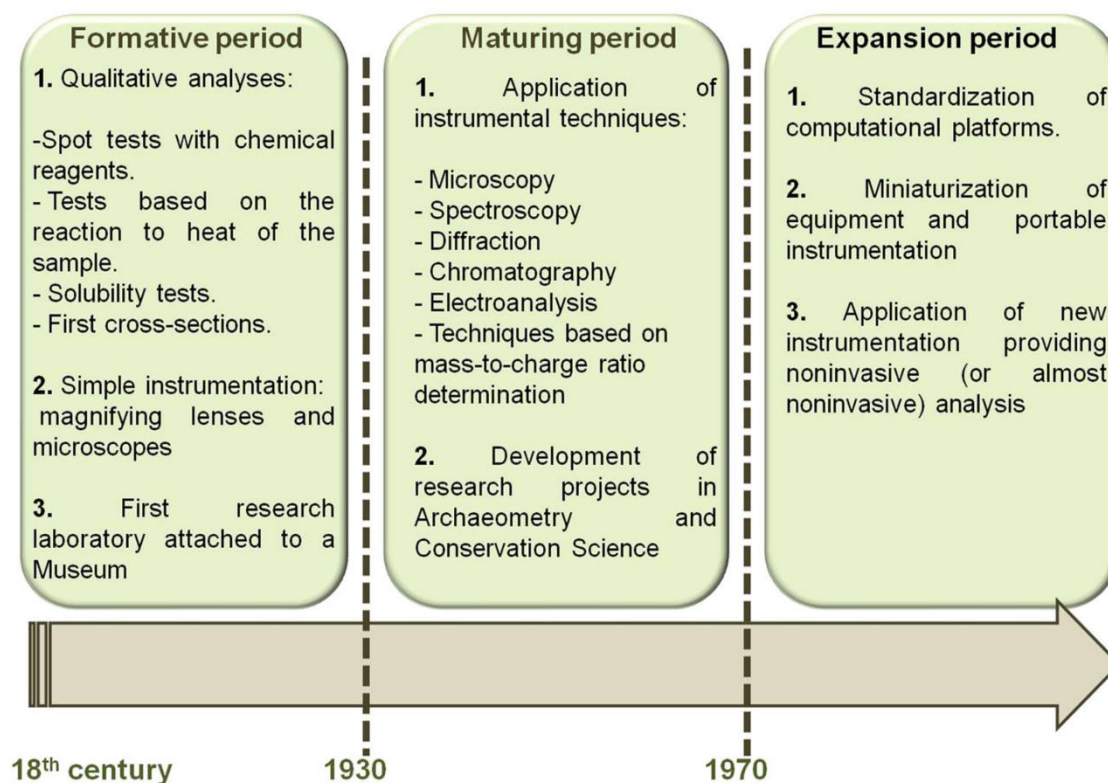


Figure 1.2 The three periods of development of chemical analysis of cultural artefacts as defined by Doménech-Carbó & Osete-Cortina (2016). Figure reproduced from the same.

Doménech-Carbó & Osete-Cortina (2016) claim that the use of chemistry and physics to evaluate cultural heritage dates to the 18th century when the methodology of Winckelmann (1717 – 1768) (historical knowledge based on the study of old documents combined with the examination of archaeological remains) was popularised and indeed the first analytical study by a scientist on a work of art was when Gmelin investigated the pigments and binding medium of a sarcophagus in 1781 *Doménech-Carbó & Osete-*

Cortina (2016); Nadolny (2003) whose analysis consisted of qualitative chemical analyses of the sort described by *Vogel Vogel (1996)* with the first quantitative analysis performed in 1826 by *Vauquelin Doménech-Carbó & Osete-Cortina (2016); Nadolny (2003)* who investigated Egyptian blue in an attempt to generate its molecular formula *Nadolny (2003)*. Also noteworthy is the first research laboratory attached to a museum in 1888, the director of which, Rathgen, was the first to “adopt a scientific appraisal to the treatment of museum objects” *Doménech-Carbó & Osete-Cortina (2016); Gilberg (1987); Plenderleith (1998)*.

Doménech-Carbó & Osete-Cortina (2016) argue that the beginning of the second period is marked by the first use of scientific instrumentation, namely the first instance of the use of spectroscopy is in 1931 when an ongoing investigation into the metallurgy of European relics was begun *Doménech-Carbó & Osete-Cortina (2016); Olin et al. (1969)*. Also noteworthy is the early use of IR spectroscopy by Feller in 1954 *Doménech-Carbó & Osete-Cortina (2016); Feller (1954)* to characterise paintings’ materials.

Doménech-Carbó & Osete-Cortina (2016) argue that the beginning of the third period is marked by a “notable” increase in the analysis of cultural heritage artefacts with scientific instrumentation and that this period continues to the present day owing to advancements in the analytical techniques themselves alongside increasingly powerful computational support for the instruments.

Based on books giving a broad overview of the use of analytical techniques for the investigation of cultural heritage such as *Artioli (2010); Sabbatini & van der Werf (2020)* a summary of analytical techniques for the investigation of cultural heritage is given in *Table 1.1*. Both sampling, and non-destructive techniques are used. There are

techniques that examine a single point, or the whole sample. Equipment can be either portable, or laboratory based, some techniques require a synchrotron.

Method	Description	NDT?	Uses?	Equipment?	Further reading
XRF X-ray fluorescence spectroscopy	Point technique. Interaction of x-rays and core electrons releases secondary x-rays. Spectra are characteristic of elements	✓	Identification, and quantification of elements	Portable devices are available, industrial devices provide higher powers	<i>Namowicz et al. (2009); Szökefalvi-Nagy et al. (2004)</i>
OES Optical emission spectroscopy	The measurement of visible light upon de-excitation. Spectra are characteristic of elements	Sampling technique	Elemental analysis and provenancing of ceramics and metals	Laboratory based	<i>Gaudiuso et al. (2010); Troalen (2013)</i>
AAS Atomic absorption spectroscopy	Measurement of light emitted as sample is vaporised	Sampling technique	Quantitative chemical analysis of samples in solution, identification of trace elements in ceramics and metals	Laboratory based	<i>Bitossi et al. (2005); Varella (2012)</i>

<p>PIXE Particle induced x-ray emission</p>	<p>Measurement of x-rays emitted as a result of bombardment with charged particles</p>	<p>✓</p>	<p>Identification of pigments via bulk elemental composition. Can give chemical micro maps. Used on paintings, metals, manuscripts, ceramics, stones</p>	<p>Requires accelerator</p>	<p><i>Pascual-Izarra et al. (2007); Sokaras (2020)</i></p>
<p>RS Raman spectroscopy</p>	<p>Point technique. Inelastic scattering of photons, spectra characteristic of molecules</p>	<p>✓</p>	<p>Identification of pigments</p>	<p>Portable devices available, use of laser</p>	<p><i>Chiriu et al. (2020); Vandenberghe et al. (2000)</i></p>
<p>IR Infrared spectroscopy</p>	<p>Absorption of radiation by molecules, characteristic spectra</p>	<p>Sampling technique</p>	<p>Identification of pigments</p>	<p>Laboratory based devices</p>	<p><i>Arrizabalaga et al. (2014); Invernizzi et al. (2018)</i></p>
<p>MS Mass spectrometry</p>	<p>The separation of charged particles based on their mass to charge ratio</p>	<p>Sampling technique</p>	<p>The only technique that can identify and quantify individual isotopes. Mainly used for the characterisation of surfaces and their</p>	<p>Laboratory based devices</p>	<p><i>Colombini & Modugno (2009); Krmpotić et al. (2020)</i></p>

			alteration, corrosion, and layers		
XRD X-ray diffraction	The diffraction of x-rays from regular crystal lattices, for the study of atomic structure	Sampling technique (mostly)	Characterisation of synthetic and natural materials, identifies crystalline phases	Laboratory based devices (mostly)	<i>Gianoncelli et al. (2008); Gonzalez et al. (2020)</i>
UV-VIS-NIR Ultraviolet, visible light, and near infrared spectroscopies (incl. HSI, and MSI)	The measurement of colour by probing with photons which interact with electronic transitions that cause colour	✓	For the measurement of colour	Handheld, and laboratory devices	<i>Bitossi et al. (2005); Romani et al. (2020)</i>
ND Neutron diffraction	Probes the nucleus, penetrates tens of centimetres	✓	Evaluates hidden features, alteration and corrosion of surface layers, reconstruction and interpretation of manufacturing processes	Synchrotron required	<i>Bakirov et al. (2020); Kockelmann & Kirfel (2006)</i>
ED Electron diffraction	Performed in a TEM where electrons pass through sample,	Small sample required (nm scale)	For the characterisation of crystal phases	Laboratory based equipment	<i>Pérez-Arantegui & Larrea (2003);</i>

	diffraction pattern analysed				<i>Zacharias et al. (2018)</i>
TG, DTA, DSC Thermal analyses	Thermogravimetry, differential thermal analysis, and differential scanning calorimetry. Study of properties as temperature is changed	Sampling techniques	Provides information on thermal stability, important for understanding the ageing of materials, and the impact of materials' environment	Laboratory based equipment	<i>Messenger et al. (2020); Pires & Cruz (2007)</i>
OM Optical microscopy	Light either reflects off a surface, or transmits through a very thin surface. Observes features down to 0.5 μm scale (1000 mag.)	Does not necessarily need a sample	Investigation of rocks, minerals, pigmentation, metals. Appropriate for all solid samples	Laboratory based equipment	<i>Alfieri et al. (2020); Moropoulou et al. (2013)</i>
SEM/TEM Electron microscopies	Scanning and transmission EM. Scanning (100,000 mag.), transmission (1 x 10^7 mag.). TEM can discriminate atoms	Sampling technique	Investigation of solid materials. Equipment can be used to generate elemental maps of surface	Laboratory based equipment	<i>Burattini & Falcieri (2020); Palamara et al. (2020)</i>

X-ray and neutron radiography	Visualisation of density distribution within object by differential absorption	0.4 % of material irradiated, radiation falls below safe levels within days	Images internal features of objects. Paintings routinely investigated	Laboratory based, industrial equipment can penetrate several cm of Cu, and bronze. Synchrotron required for neutrons	<i>Casali (2006); Festa et al. (2020)</i>
X-ray and neutron computed tomography	Mathematical technique where 2D radiographic images are reconstructed as 3D image	✓	Images internal space of an object	Computational technique	<i>Casali (2006); Morigi et al. (2010)</i>
Photogrammetry	Mathematical technique where 2D images are reconstructed as 3D images	✓	Mainly used on buildings and archaeological sites for the determination of geometric properties	Computational technique	<i>Sebar et al. (2020); Yastikli (2007)</i>
C¹⁴ dating	Upon death an organism's C ¹⁴ /C ¹³ and C ¹⁴ /C ¹² ratios decrease at a	Sampling technique	Measurement of the current ratios of C ¹⁴ /C ¹³ and C ¹⁴ /C ¹² can therefore be used	Laboratory based technique	<i>Boudin et al. (2015); Mori et al. (2006)</i>

	known rate modelled by the universal radioactive decay equation		to calculate the approximate age. Determines age up to 60,000 years old		
TL, OSL Thermoluminescence, and optically stimulated luminescence	Dating based on accumulation of radiation dose within materials. Irregularities within a lattice cause electrons to become trapped upon excitation by ionising radiation. These traps can last for thousands of years.	✓	Thermoluminescence examines deeper traps, and can provide a date for the last ‘firing event’ of ceramics and clays (i.e. the date of manufacture). Optically stimulated luminescence is much more sensitive, and can reveal the objects last exposure to daylight.	Laboratory based technique	<i>Feathers (1997); Huisman et al. (2019)</i>
EPR Electron paramagnetic resonance spectroscopy	Similar to NMR, but focusses on electrons, not nuclei. Magnetic moments are studied as they are oriented by a magnetic field.	Sampling technique	Dating ceramics, bones, teeth. Characterisation of white marbles, paper. Assessment of degradation of paper.	Laboratory based technique	<i>Javier & Hornak (2018); Zoleo et al. (2010)</i>

<p>NAA, PGAA, NRCA</p> <p>Neutron based analyses</p>	<p>Measurement of gamma rays after irradiation by neutron beam.</p> <p>Neutron activation analysis (NAA), Prompt gamma activation analysis (PGAA), Neutron resonance capture analysis (NRCA)</p>	<p>Not necessarily sampling.</p> <p>Radioactivity negligible</p>	<p>Characterisation, authentication, provenancing of pottery, geological materials, glass, metals. Determines bulk composition</p>	<p>Requires synchrotron</p>	<p><i>Festa et al. (2020); Kardjilov & Festa (2017)</i></p>
<p>XPS</p> <p>X-ray photoelectron spectroscopy</p>	<p>Analysis electrons released upon irradiation with x-rays</p>	<p>Requires cleaning, may be considered minimally destructive?</p>	<p>Measures elemental composition, and characterises surfaces contaminants. For understanding corrosion, patinas, treatments, of metals, glass, pottery, ceramics</p>	<p>Laboratory based technique</p>	<p><i>Balta et al. (2009); Maravelaki-Kalaitzaki et al. (2002)</i></p>
<p>AES, EELS</p> <p>Electron spectroscopies</p>	<p>Auger electron spectroscopy (AES), electron energy loss spectroscopy (EELS).</p>	<p>Sampling technique</p>	<p>Characterisation of metal surfaces</p>	<p>Laboratory based</p>	<p><i>Casadio et al. (2011); Janssens & Van Grieken (2004)</i></p>

	Measurement of the energy of electrons emitted as a result of electron bombardment				
XAS X-ray absorption spectroscopy	Measures incident, and transmitted photons as a function of energy, giving information on geometry at an atomic scale	Sampling technique	Examination of glasses and glazes, particularly colourants therein	Requires synchrotron	<i>Cotte et al. (2009); Farges & Cotte (2016)</i>
NMR Nuclear magnetic resonance	The detection of resonant absorption on susceptible nuclei upon application of a strong magnetic field	Sampling technique	For determining the chemical composition	Laboratory based	<i>Blümich et al. (2010); Capitani et al. (2012)</i>
HPLC High performance liquid chromatography	Efficient at the separation of complex organic mixtures. Mixture is passed through a column (stationary phase) with a	Sampling technique	Separation and identification of dyes, amino acids, proteins, carbohydrates, oils, fats, waxes, tannins, acids	Laboratory based	<i>Karapanagiotis & Chryssoulakis (2006); Mazzuca et al. (2020)</i>

	mobile phase (liquid). Mixtures separated based on affinity for stationary or mobile phase				
GC/MS Gas chromatography/mass spectrometry	Chromatography where the mobile phase is gaseous, followed by MS which identifies unknowns and measures their concentration	Sampling technique	Identification of unknowns	Laboratory based	<i>Bonaduce et al. (2016); Palla et al. (2020)</i>

Table 1.1 A summary of the analytical techniques commonly applied to cultural heritage. Information is taken from Artioli (2010) and Sabbatini & van der Werf (2020). The further reading provided consists either of methodological summary papers, or of papers considered particularly interesting.

1.3 The thesis in the context of heritage science

Manikowska et al. (2020) argue that the one of the most significant challenges for the field of cultural heritage is the uptake of digitisation technology. Both nationally, and internationally the digitisation of cultural heritage is changing the way in which people interact with and approach heritage *Manikowska et al. (2020)*. Digitisation can aid preservation efforts, and improve access and education *Manikowska et al. (2020)*. The abilities of the VNIR HSI equipment used in the thesis with respect to the digitisation of cultural heritage were not directly stated in the main body of the experiments but nonetheless the advantages of such equipment for effective communication and the remote analysis of works of cultural heritage are inferred. HSI data was used in all three experiments to capture data on the current state of objects, and to characterise and map the location of constituents. This data could in theory be used internationally to allow access to collections for analysis thus aiding conservation collaborations, an important consideration given that the International centre for the study of the preservation and restoration of cultural property (ICCROM) reports that the heritage sector publishes 9 times more papers per annum than it did 20 years ago and that a third of these are from international collaborations *Heritage et al. (2014); ICCROM (2021)*.

Stakeholders, and policy makers in the field of heritage science are ensuring that the continuing professional development of skills and knowledge in the latest areas of technology is keeping pace with the newest developments, and is a priority for the sector *Manikowska et al. (2020)*. From this perspective the involvement of conservation teams in the design of experiments for this thesis benefitted the experiments by increasing the relevance of the experiments to practitioners, and by increasing the awareness of the techniques used within conservation teams.

Bratasz, who defines heritage science as a new field which answers the questions of the humanities with the tools and methods of science *Bratasz & Manikowska (2020)* argues that while there has always been care for collections there is an increasing awareness of the economic importance of the heritage sector and its non-renewable nature. Separating heritage science into two streams, the development of new knowledge and information, and the preservation of information or values of aesthetic, historic, scientific or economic importance it can be seen that this thesis matches elements of both. In examining the utility of the VNIR HSI equipment new knowledge about its applications has been generated, and through the application of the techniques to genuine collection items information about them has been preserved.

The main challenges identified by *Bratasz & Manikowska (2020)* going forward are a push toward sustainable heritage (the preservation of heritage while balancing financial, social, and environmental costs), the application of new computational technologies and tools, and the monitoring of environmental factors. VNIR HSI has been shown in this thesis to have utility in the monitoring of collections and is by its nature a computational technology. The improvement of computational analysis for VNIR HSI data has been discussed throughout.

ICCROM believes that the key focusses of heritage science at present ought to be the strengthening of its professional identity as a sector (arguably achieved through increased publications and networking, both of which were core aspects of the DPhil), the improvement of strategies which link research to needs i.e. the steering of scientific research toward meeting the requirements of conservators as this thesis has done, the increased participation of stakeholders has also been demonstrated in these experiments, proving the benefits of the application of the scientific method to issues facing the humanities and delivering as has been discussed at length in this thesis, and an increased

awareness of the capacity of the field. This thesis could be argued to highlight the capabilities of the Bodleian, opening up possibilities of collaboration for international audiences.

The National Heritage Science Forum recently called for the involvement of heritage science in the answer to five societal challenges, sustainable development, the climate emergency, improved wellbeing, increased equality and inclusivity, and the development of a digital society *National Heritage Science Forum (2021)*. It is this last call, specifically to “Transform the way that collections, buildings, and archaeology are managed, accessed, and understood” that is of most relevance to the thesis which broadly has aimed to highlight a methodology for aiding the management of collections and which, owing to its inherent digitisation, could be used to improve access.

Generally the increased awareness of the capability and availability of VNIR HSI equipment through experiments such as those detailed in this thesis can increase collaboration, and digitisation, and help to demonstrate the utility of the equipment, not just for local resource management but for the increased sharing of knowledge internationally.

1.4 Non-destructive testing methods

“An art object or ancient artefact cannot be replaced, and the consumption or damaging of even a small part of it for analytical purposes must be undertaken only where vital data cannot otherwise be obtained” *Adriaens (2005)*.

The non-destructive nature of some techniques makes them favourable to cultural heritage custodians. Of those techniques in

Table 1.1 thirteen are non-destructive, listed in

Table 1.2.

Non-destructive methods	Sampling methods
XRF	AAS
PIXE	IR
RS	MS
UV-VIS	XRD
ND	ED
OM	Thermal analyses
Radiography	Electron microscopies
Tomography	C ¹⁴ dating
Photogrammetry	EPR
TL	Electron spectroscopies
OSL	XAS
Neutron based analyses	NMR
XPS	HPLC
	GCMS
	OES
Single point analysis techniques	Full field analysis techniques
XRF	UV-Vis spectroscopies
RS	OM
PIXE	Tomography
ND	Photogrammetry
Neutron based analyses	Radiography
XPS	TL
	OSL

Table 1.2 Listing the NDT methods and sampling methods commonly used for the analysis of cultural heritage.

1.4.1 A note on peaks, signals, and noise.

Spectra of various analytical techniques are discussed throughout this thesis, it is at this point worth defining a few of the terms used. Signal is defined by *Daintith & Martin (2010)* as “The variable parameter that contains information and by which information is transmitted in an electronic system or circuit. The signal is often a voltage source in which the amplitude, frequency, and waveform can be varied”. It is more concisely defined by *Owen (2007)* as “a varying quantity whose value can be measured and which conveys information”. Noise can be defined as “irregular fluctuations accompanying and tending to obscure an electrical signal or other significant phenomenon” *Stevenson & Waite (2011)*, a corruption of the signal akin to interference *Owen (2007)* and the cause of random variations in the signal which “masks the lowest detectable true intensity value” *Gonzales & Woods (2010)*. Lastly a peak is defined as “a point in a curve or on a graph, or a value of a physical quantity, which is higher than those around it” *Stevenson & Waite (2011)*.

1.5 Imaging and spectroscopic techniques in heritage science

It is a given that the ultimate goal of heritage scientists is to prevent harm to the artefacts in their care *Creagh et al. (2017)* and as such it is obvious that a heritage scientist would find it preferable to use a non-destructive technique (NDT) when carrying out their investigation. NDTs can be defined as techniques which do not cause damage, and do not prevent any future application of the artefact under investigation *Hum-Hartley (1978)*. Because NDT does not damage the artefact under scrutiny it becomes possible to analyse more of the artefact than would be tested by a comparative

sampling technique. This broader sampling can give a more representative view of the artefact, and multiple NDT methods can also be utilised to provide a deeper understanding of the object *Amat et al. (2013)*. NDT methods generally involve some form of spectroscopy where the artefact is radiated with photons and the emission is then monitored *Creagh et al. (2017)*. Spectroscopy can be a powerful technique informing the user of the molecular constituents of the sample *Bitossi et al. (2005)* and such techniques have become increasingly commonplace in heritage studies *Možina et al. (2013)*. Imaging techniques in particular can be advantageous, as they provide digital reconstructions of artefacts which enhance visitor interaction at cultural heritage sites *Barrile et al. (2018)*.

1.6 Hyperspectral imaging

This thesis investigates the use of hyperspectral imaging (HSI) in the heritage science field. HSI is a technique that combines imaging, and spectroscopy. HSI generates a data cube with two spatial dimensions and one spectral dimension. This data cube can be read as one reflectance spectrum for each pixel in an image *Creagh & Bradley (2007)*. It is either the analysis of these reflectance spectra *Cavaleri et al. (2013)*, or the utilisation of false colour images *Hayem-Ghez et al. (2015)*, that the HSI data cube is generally used for. HSI is therefore both a spectroscopic technique, and an imaging technique, where the analytical capability of HSI relies on the usefulness of the reflectance spectra it produces.

1.7 Thesis aim, research questions, and overall approach

This thesis has been produced within the framework of the EPSRC-funded CDT in Science and Engineering for the Arts, Heritage and Archaeology in association with the Bodleian Libraries and Headwall Photonics. Given the current state of the art in the topic of HSI and heritage science and the interests of the supervisory team, the overall thesis aim is as follows;

What is the efficacy of VNIR HSI for the evaluation of the pigmentation of items of cultural significance in museum and archive collections?

The aim can be further broken down into the following research questions:

- Research Question 1: What is the accuracy of the equipment in terms of chemical characterisation? To what extent can reflectance spectra produced by VNIR HSI be differentiated so that different chemicals may be identified? (Experiment 1)
- Research Question 2: Can the utilisation of the VNIR HSI equipment for the purpose of identifying the spatial location of pigments be of use for the study of cultural heritage items? (Experiment 2)
- Research Question 3: Can the utilisation of the VNIR HSI equipment for the purpose of monitoring cultural heritage items that have been on display be of use to institutions wishing to study the effect of the photo-induced degradation on their collections (Experiment 3)

It is also noteworthy that each of the research questions answer genuine inquiries from members of the Bodleian Libraries, or the Ashmolean Museum's conservation teams about

either specific pieces in their collections or for the application of the equipment to more general cases.

1.8 General approach

It was desirable that the three projects were rooted in the three main uses of HSI for conservation as evidenced from within the literature. It was also desirable that the projects would have real world applications, and therefore be of genuine use to the conservation teams in the Bodleian Library and Ashmolean Museum who collaborated in this research. They were consulted for each project to determine which items from their collections were of interest and what the key issues facing them were.

It was decided to compare the VNIR HSI equipment to the techniques that conservation professionals within the Bodleian Libraries and Ashmolean Museum were already using. The goal was to examine the advantages of the new VNIR HSI equipment and to suggest how it could be best used as part of the conservation team's selection of scientific analyses. By comparing it to well-established techniques it could be clearly shown why they should, or sometimes shouldn't, use VNIR HSI instead of, or as well as, other techniques.

Experiment 1 was carried out to determine if VNIR HSI could characterise colouration, something that conservation professionals are frequently interested in. For a case study the Bodleian conservators suggested a collection of Armenian illuminated manuscripts. There had been a recent exhibition in the Weston Library (part of the Bodleian) which displayed the manuscripts, and as part of the exhibition the colouration on the manuscripts had already been analysed by Raman spectroscopy. This provided an ideal opportunity to investigate whether VNIR HSI was capable of the same characterisation.

Experiment 2 was set up to investigate the efficacy of VNIR HSI with regards to the location of colouration, particularly on faded artworks. Curatorial and conservation staff at the Ashmolean Museum were able to suggest a suitable case study. They had received funding to install a new display which was intended to project the original colour scheme of the Shrine of Taharqa onto the shrine in situ within the museum using a range of lighting. Furthermore the west wall of the shrine had undergone analysis previously, and so there was a wealth of data to use to aid with the investigation and with which to compare the VNIR HSI data.

Finally experiment 3 was designed to evaluate the ability of VNIR HSI to monitor the fading of colouration over a length of time useful to conservators in the Ashmolean Museum and Bodleian Library. An initial meeting with the conservation teams revealed that the method currently used is a point-based, contact method which greatly limits the number of collection items to which it could be applied, and their attempts to use a scaffold to overcome this had proved unsuccessful. It was also difficult for them to examine the same spot before and after display, and the size of the sample spot was too large for the intricate designs on many of their collections. Therefore if VNIR HSI could be shown to be useful in this capacity it would offer many advantages to the conservation teams.

Because the overarching goal of the thesis was to investigate how VNIR HSI could practicably answer research questions posed by conservation teams, choices of the materials for each experiment were made based on the usefulness of the studies to those teams. For example illuminated manuscripts were examined for the Bodleian libraries as these form the bulk of the Libraries' collection and are the focus of interest for the conservators. Similarly, pigments have been chosen based on the principle of which were most likely to be of use to the conservators. Experiments have always been

performed on collection items to increase the applicability of the results to real artefacts within the library and museum collections and also on samples where possible as these give greater control over experimental factors.

Success was judged by how the VNIR HSI equipment performed in relation to the techniques that otherwise would have been used. Success criteria included the data obtained, the ease of use, and the impact on the conservation of the artefact, and generally the conclusions provide advice on the best use of the equipment within each field evaluated.

1.9 Thesis structure

The DPhil was produced as a ‘thesis by papers’, and can be divided into three sections.

Section 1: Introductory section

In this section the topic is introduced, and the literature is reviewed. The knowledge gap and the reasoning for undertaking the investigations forming the thesis is explained. The aims and objectives are set out.

Section 2: Experimental section

The methodological approach is explained, and the three research papers are presented.

Section 3: Concluding section

The findings of the papers are discussed in light of the overall research goals, and they are discussed within the frame of reference of the theses aims and objectives. This is a review of the collective conclusions that can be drawn from the project as a whole.

Chapter 2 Literature review

This literature review briefly covers the main topics looked at during the course of the investigations forming the thesis, however as literature reviews were conducted for each individual paper this literature review is necessarily brief, and generalised to the overall thesis. More in depth literature on each experiment can be found within the papers reproduced below.

2.1 Hyperspectral imaging

It is at this point useful to define the terminology used in this thesis. Hyperspectral imaging as used herein, refers to a technique that produces a reflectance spectrum for each pixel in an image with a spectral resolution good enough to resolve any peaks that might be expected in such spectra. This is distinct from multispectral imaging where the spectral resolution would be much lower, analysis might perhaps be carried out on a smaller number of wavelengths, ten or so for example. There are other differences. Multispectral imaging tends to have a much higher spatial resolution as the technique makes use of high resolution cameras, and multispectral imaging also tends to use multiple light sources, so that the subject may be examined in ultraviolet or infrared light. In the case of hyperspectral imaging a single, broad spectrum light source is used. A brief comparison is given in *Table 2.1*.

	Hyperspectral Imaging	Multispectral imaging
Number of wavelengths analysed	Often hundreds, they are contiguous and can be used to produce a spectrum	Tens of non-contiguous bands. Reflectance data cannot be used to produce a continuous spectrum
Light source	A single broad-band source	Often multiple different sources such as UV and IR lamps
Data	A reflectance spectrum for each pixel	Multiple false colour images
Equipment	A light source and a detector	Light sources, high resolution camera, filters

Table 2.1 A comparison of basic facts about multispectral and hyperspectral imaging techniques.

Furthermore it is useful to define what is meant by the terms used to describe the different types of hyperspectral imaging sensors that are available. A VNIR HSI sensor is capable of the detection of the reflectance spectra of the surface of the subject between 400 and 1000 nm covering the entire visible spectrum with a little of the ultraviolet and the infrared parts of the electromagnetic spectrum. Another sensor in common use is the short wave infrared (SWIR) which is typically a sensor for wavelengths between 1000 and 2500 nm which would give a reflectance spectra with characteristic peaks useful for the characterisation of components of the surface such as pigmentation.

A review of recent literature reveals that hyperspectral imaging is typically used for the safety inspection of foodstuffs *Femenias et al. (2020); Kang et al. (2020); Shen*

et al. (2020), or the characterization of remote sensing data for things such as foliage and bodies of water *Boukezzoula et al. (2020)*; *Song et al. (2020)*; *Tan et al. (2020)*. The other most common papers released on the topic are technical papers discussing new methods for dealing with the vast amount of data produced by hyperspectral imaging *Elkholy et al. (2020)*; *Laban et al. (2020)*; *Xie et al. (2020)*.

In the field of cultural heritage previous work has focussed on adapting HSI for the heritage field *Cucci & Casini (2020)*; *Piccolo et al. (2020)* and improving the technological capabilities *Piccolo et al. (2020)*. HSI is used mainly for revealing hidden information *Bayarri et al. (2019)*; *Hou et al. (2019)*; *Wu et al. (2019)*, the identification and mapping of constituents in polychrome, multi-material works *Bayarri et al. (2019)*; *Cucci & Casini (2020)*; *Piccolo et al. (2020)*; *Sandak et al. (2021)*, the tracking of interventions *Sandak et al. (2021)*, the monitoring of colour change *Bonifazi et al. (2019)*; *Sandak et al. (2021)*, and assessment and digitisation *Bayarri et al. (2019)*; *Cucci & Casini (2020)*; *Piccolo et al. (2020)*; *Sandak et al. (2021)*. The detection of wavelengths further into the IR has the demonstrable advantage of revealing more due to its increased penetration *Piccolo et al. (2020)*; *Sandak et al. (2021)*; *Wu et al. (2019)*, and a superior ability to characterise constituents owing to the increased information from spectra of functional groups *Bonifazi et al. (2019)*; *Sandak et al. (2021)*.

The most recent literature from teams evaluating HSI for heritage applications generally agrees on the benefits of HSI. Large areas can be analysed in a short time *Palomar et al. (2019)*, it is non-contact *Sandak et al. (2021)*, and provides detailed spatial analysis *Sandak et al. (2021)* offering support for those persons working in the heritage field *Cucci & Casini (2020)*.

There is, however, a requirement for multiple, complex processing steps *Cucci & Casini (2020); Hou et al. (2019); Picollo et al. (2020); Sandak et al. (2021)*, and there is presently a limitation in the detector sensitivity, data storage, and ability to determine *Sandak et al. (2021)*. HSI is often used to give an overview before using complementary techniques to reduce cost, and save time *Cucci & Casini (2020); Sandak et al. (2021)*. Owing to the complexity of the heterogenous surfaces involved in heritage, data from other techniques is often necessary *Males et al. (2019); Picollo et al. (2020)*.

It is interesting that literature from the last couple of years (after the bulk of the experimental was carried out for the thesis, certainly long after the planning stage) speak of HSI as “widely applied” *Palomar et al. (2019)*, “well established”, “a mature technology” *Cucci & Casini (2020)*, “standard practice” *Males et al. (2019)*, “no longer experimental” *Picollo et al. (2020)*, and a simple extension of conventional photography *Sandak et al. (2021)* whilst providing the information of multiple techniques *Bonifazi et al. (2019); Cucci & Casini (2020)*.

Future work efforts are directed toward automation through artificial intelligence (AI) *Picollo et al. (2020); Sandak et al. (2021)*, higher resolution, new processing algorithms, and multisensory systems *Sandak et al. (2021)*, and the expansion of the use of HSI to other heritage mediums such as a greater body of work on rock art, and industrial heritage objects *Bayarri et al. (2019)*, and the expansion of its use to less well used methodologies such as the monitoring of colour change *Bonifazi et al. (2019)*.

In summary HSI is well-placed to be heavily utilised to answer heritage science questions but there is nonetheless a desire for improved technological capabilities. In the light of this recent literature this DPhil can be viewed as an investigation into the capabilities of HSI equipment typical of its time.

2.2 Reflectance spectra

Reflectance is defined as “The ratio of the radiant flux reflected by a surface to that falling on it” with the spectral reflectance being the radiant reflectance for a specific wavelength of the incident radiant flux *Daintith & Martin (2010)*. A reflectance spectrum therefore is simply the spectral reflectance plotted against wavelength.

When incident light in the UV-VIS-NIR range interacts with matter it can cause the excitation of electrons whose transitional energy matches that of the incident photons *Burrows (2009)* thus causing an electronic transition which upon de-excitation emits a photon. These are the interactions responsible for the colour of molecules, it is very rare that such interactions lead to a colour change in the molecules *Burrows (2009)*, and because different pigments absorb at different wavelengths, their reflectance spectra can be used to tell them apart *Burrows (2009)*. Spectroscopies dealing with this range therefore quantify the colour of items, the colour being caused by the selective absorption or re-emission of light *Artioli (2010); Burrows (2009)*.

Importantly, spectroscopy in the VNIR wavelength range cannot identify molecules based on properties other than colour. Infrared light for example could interact with the bond vibrations of molecules and could therefore be used to identify molecules based on a molecular fingerprint *Burrows (2009)*, however in the VNIR range used in this thesis it is only the colour that is analysed, which may not be enough to distinguish between two similar pigments *Aceto et al. (2014); Vitorino et al. (2015)*.

2.3 The pigmentation of heritage artefacts

The terminology used when referring to colourants is summarised in *Table 2.2* below.

Term	Definition as used in this thesis
Colourant	A general term referring to all chemicals, or mixtures of chemicals, used to alter the colour of an artefact.
Pigment	A colourant used to paint onto the surface. A pigment can be either organic or inorganic depending on the molecular structure. Pigments (in powdered form) are mixed with binders (a glue) before being applied to the surface, usually with a brush.
Dye	A chemical which forms a coordination complex with a mordant (a complexing agent). It is the Mordant-Dye complex which then binds to the fabric. It is the mordant that provides the bonding to the fabric, and the dye that provides the colour. Dyes and pigments are sometimes the same chemical, madder for example is used as both. To dye the fabric, the fabric is submerged in a dye bath.

Table 2.2 Definitions of terms used to describe colourants.

It is the vivid colouration of d-block metal compounds such as HgS (Vermillion) and $\text{CoO} \cdot \text{Al}_2\text{O}_3$ (Cobalt blue) that has encouraged their use for centuries in the pigmentation of historic works of art *Burrows (2009)* and it is the limitation of the use

of certain compounds to a certain period or area that allows their identification to inform the analyst as to the date of the artwork, or alert them to forgery *Kühn (1963)* as well informing them about the science and technology of the period and culture *Berrie (2012)*. Generally speaking, more modern pigments can be distinguished from older ones based on their particle size, and the prevalence of impurities *Kühn (1963)*. Colourants were highly valued in ancient times, blue pigments in particular due to their rarity *Berke (2002)*. This situation forced the production of the first synthetic pigment, Egyptian blue ca 5200 years ago *Berke (2002)* and continued until the 19th century mass industrialisation of pigment production *Berke (2002)*, the first synthesis of note being that of mauve in 1856 *Lomax & Learner (2006)*. Further advances in pigmentation came from the dying industry *Berrie (2012)*. The modern palette now consists of the earth pigments (used in prehistoric cave paintings, the oldest known form of art), natural pigments (used in the middle ages), and modern organic compounds *Barnett et al. (2006)*.

2.4 The photodegradation of pigmentation

It was the Russel and Abney report in 1888 which first persuaded people that light was a cause of fading *Brommelle (1964); Miliani et al. (2018)*. Nowadays the different mechanisms of photodegradation are much better understood *Artioli (2010); Miliani et al. (2018)* and it has been shown that the components mixed with the pigments (binders for example) can have an effect on their photodegradation *Saunders & Kirby (1994)*. Other factors can affect the degradation of pigmentation such as the temperature *Artioli (2010)*, relative humidity *Saunders & Kirby (2004)*, and atmospheric pollutants *Whitmore et al. (1987); Whitmore & Cass (1989)*.

2.5 The detection of pigmentation

The chemical analysis of pigmentation began with Michael Faraday and others *Berrie (2012)*. Since then much of the emphasis in instrument improvement has been placed on the improvement of the limit of detection so that ever smaller samples could be tested. The improved determination of impurities has aided understanding of manufacturing methods and raw materials *Berrie (2012)*. Nowadays scientific analysis of pigmentation is fundamental to the conservation of cultural heritage *Bitossi et al. (2005)*.

Spectral imaging techniques such as hyperspectral imaging are becoming increasingly sophisticated but remain difficult to apply to heterogenous, multi-phased systems (as many heritage artefacts are). Improvements in spatial resolution and the mathematical analysis of the data are improving characterisation and identification *Berrie (2012)*. Generally speaking non-destructive tests are better suited to the identification of inorganic pigments *Berrie (2012)*, with the identification of organic pigments being substantially more difficult *Kühn (1963)*.

2.6 Problems with hyperspectral imaging

Hyperspectral data cubes can be composed of different wavelength ranges. As discussed infrared radiation will provide more information on the composition of the subject than visible light radiation and is therefore advantageous for scientific analysis *Delaney et al. (2009)*. However, HSI equipment covering the visible and near infrared (VNIR, 400-1000 nm) region has become widely used in recent years *Cséfalvayová et al. (2011)*. This is likely due to the increased cost involved with detectors for the SWIR range *Liang (2012)*. VNIR HSI is therefore the more likely technique to be utilised by heritage institutions and should be the focus of investigation to determine its efficacy.

2.7 Literature review conclusion (summary and implications)

The reflectance spectra generated by HSI have three main uses. The characterisation of pigments, the generation of images detailing the location of pigmentation that the naked eye cannot see, or finds it difficult to see, and for the monitoring of the degradation of pigmentation over a period of time. HSI imaging can be carried out at multiple wavelength ranges, including far enough into the IR (2500 nm) so as to provide characteristic peaks in the spectra. More commonly the equipment utilised for heritage science enquiries is limited to mainly visible spectra (400 – 1000 nm) reducing the ease with which constituents are characterised and necessitating the combination of results with those of other, complementary, techniques.

There is a lack of knowledge about the efficacy of HSI in this wavelength range for identification, mapping, and colour change purposes, and therefore a detailed investigation would be of value to heritage professionals seeking to take advantage of recent advances in the technology by incorporating this cost effective solution into their array of analytical techniques and indeed the research questions presented in this thesis were formed based on queries from conservation staff of partner institutions in order to elucidate the utility of the spectral data produced in this range to the institutions. Such an investigation will help to introduce the technique both in the context of HSI as an imaging technique, and HSI as a tool for spectroscopy, to the heritage science field whilst suggesting the most effective uses of the equipment. Comparison of VNIR HSI with techniques already in use, provides a point of reference for readers.

Even prior to considering the disadvantages of VNIR compared to SWIR, HSI is difficult to apply to heterogenous, multi-material surfaces such as those that heritage objects represent and so an investigation into VNIR HSI for heritage is worthwhile for the advancement of the field, especially as VNIR HSI specifically has become more

widespread owing to the comparable low price of VNIR HSI equipment, compared to SWIR HSI equipment.

It is noteworthy that the most common papers are those detailing new methodology for the analysis of the large datasets produced, and that there continues to be a push in this direction for future work. HSI is only as useful as the spectra it produces and the commentary that this thesis attempts to provide, on the utility of visible spectra, closely aligns with the most common uses mainly seen in the literature.

This thesis will therefore address the efficacy of the current equipment, and the computational aids (initially developed for remote sensing) for the analysis of the data generated for the purposes of characterisation, location, and monitoring of pigmentation in heritage artefacts.

Chapter 3 Methods

3.1 Analytical techniques

3.1.1 General description of principles

3.1.1.1 HSI

Hyperspectral imaging (HSI) is a technique which records data both spatially and spectrally. An image is generated and for each pixel within that image, the reflectance of the area covered by the pixel is recorded for a number of contiguous wavelengths such that a reflectance spectra may be produced for that pixel. Thus the end result of HSI is a 3D data cube the 3 axis of which are comprised of 2 spatial axis relating to the real world geometry of the image taken, and 1 spectral axis covering the wavelength range recorded by the equipment. The analyst can therefore ask for the reflectance value, at a certain wavelength, of the area covered by a pixel. In practice this data is used to build a reflectance spectrum of the area covered by the pixel which is then used for further analysis, either by way of comparison to a database of such spectra, or through comparison with other spectra in the data cube thus allowing the user to characterise the surface captured by the HSI scan. An illustration made by *Liang (2012)* of a hyperspectral data cube is shown in *Figure 3.1*.

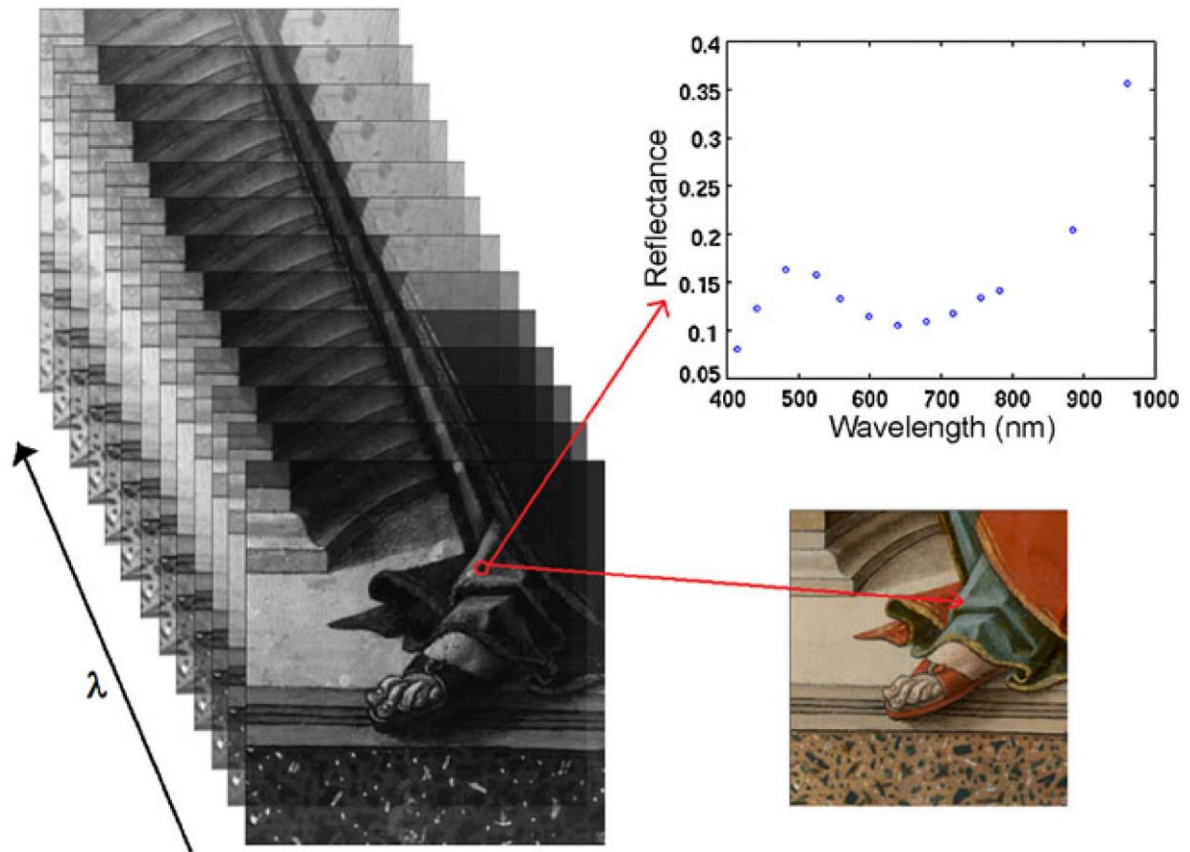


Figure 3.1. Illustration of a data cube acquired by HSI Liang (2012). On the left are a stack of greyscale images taken at different wavelengths, RHS (top) the reflectance spectrum of the highlighted pixel, RHS (bottom) an RGB image of the area scanned.

First developed for remote sensing, heritage scientists have developed HSI for their own purposes. It has the advantage of being non-destructive and full-field, and in addition to the characterisation and location of constituents, HSI can be used to reveal hidden features depending on the wavelength range detected.

3.1.1.2 Raman spectroscopy

Raman spectroscopy is a non-destructive technique for point analysis. It produces spectra that are characteristic of the molecules in the area under analysis. It relies upon the phenomena of Raman scattering. Named after its discoverer *Daintith & Martin (2010)* Raman scattering is the inelastic scattering of radiation (where the scattered radiation is not equal in energy to the incident radiation). Because it is a weak effect in nature, a laser source (a monochromatic source) is used as the incident radiation to increase the ease of its detection. Equipment is small, portable, and single spots are rapidly analysed. The main problem for Raman spectroscopists is the elimination of fluorescence, a competing phenomena which can obscure the signal from Raman scattering.

3.1.1.3 XRF

X-ray fluorescence (XRF) is a non-destructive technique for point analysis. The data it provides is used to determine, to an extent, the elemental composition of the area under analysis. XRF relies upon the excitation of atoms and the subsequent emission of X-rays *Artioli (2010)*. Upon bombardment of the atom with either X-rays, high energy electrons, or other particles *Daintith & Martin (2010)* core electrons (electrons tightly bound to the nucleus not involved in bonding) are expelled from the atom creating an ion in an excited state. Relaxation of the excited state to a lower energy state expels X-rays, the energy of which is characteristic of the atom and dependent on the element. In portable XRF (pXRF) the bombardment is carried out by X-rays, and the range of elements able to be detected is dependent on the energy of the excitation X-rays. XRF cannot provide quantitative results, it is not an imaging technique and so cannot be used as a mapping tool (without scanning the surface), it does not penetrate the surface to any

great extent, and it does not inform the analyst as to how the elements are combined into molecules *Artioli (2010)*.

3.1.1.4 DRSP

Diffuse reflectance spectrophotometry (DRSP) is a non-destructive method for the analysis of colour in materials. Similarly to HSI it produces reflectance spectra, however, given the focus on colour the wavelength range of these spectra is limited to visible light (400 – 740 nm) though equipment also often provides tristimulus values. It is a point analysis technique, and requires contact with the surface under analysis which can complicate readings, and compromise consistency. It is best deployed on a flat surface as it is sensitive to undulations.

3.1.2 Instrumentation used

3.1.2.1 HSI

HSI was performed using a Headwall Photonics VNIR 1003B – 10147. The data cube provided consists of 972 contiguous wavelengths from 400 nm to 1000 nm (a spectral resolution of 0.64 nm). A Schneider XNP 1.4/17 – 0303 lens with a headwall ACOBL – 380 – 49X, 075 filter was equipped to the camera. The light source is a halogen bulb controlled by a Techniquip 21DC, and cooled by a Minebea Motor Manufacturing Corporation 3110KL – 04W – B50 fan. This HSI equipment is line-scanning, data is acquired for 1600 pixels along one spatial axis before moving the object, using a stage controlled by a stepping motor, along the second spatial axis, thus acquiring the 3 dimensions of the data cube. The stepping motor is a Vexta PK264A2A – SG3.6 controlled by a Velmex VXM stepping motor controller. All aspects of the setup were supplied by Headwall Photonics, including the light source and stepping motor.

White and dark calibrations were performed at the beginning of use and were used to transform raw data into reflectance data by the acquisition software. For white calibration Spectralon® is scanned multiple times and an average taken, for dark calibration multiple scans are taken with the lens cap on, and an average is taken. Equipment calibration (such as signal linearity and accuracy of the wavelength axis) are performed by Headwall prior to shipping. The room lights are off during calibration and scanning as the fluorescent lights produce unwanted lines in the scan.

The spatial resolution depends on the distance between the detector and the subject which can be adjusted at the operator's discretion. The speed of the stage is calculated based on the distance between the stage and the detector in order to ensure firstly that the pixels produced represent square sections of the object (i.e. there is no stretching or squashing effect produced) and secondly to ensure that no part of the object is missed by the scan, given that at set intervals a snapshot is taken in order to build up the hyperspectral data cube. This setup is shown in *Figure 3.2*.



Figure 3.2. The HSI equipment used during the thesis.

3.1.2.1.1 The Halogen light source

The spectrum of the halogen bulb used throughout the thesis was never measured directly, however, an approximation of the light source can be achieved through observation of the white calibration spectrum. Prior to taking the white calibration the light source is left to warm up for longer than 5 minutes. The spectrum is then recorded as an average of 100 scans to minimise the impact of random noise on the final calibration spectrum by imaging a calibration target of known reflectance. Spectralon® was used throughout to provide the calibration target as it has consistent reflectivity over the wavelength range measured *Labsphere (2021)* and it is this property that allows the resultant white calibration spectrum to approximate the light source spectrum.

Figure 3.3 shows two white calibration spectra taken over an hour apart. The spectra are consistent with halogen bulb spectra seen in the literature *Retzlaff et al. (2017); Tehfe et al. (2012); Thoms & Girwidz (2013)*. The output of halogen bulbs has

been found to be consistent over a period of hours *Langenkämper et al. (2018)* and the two spectra here differ by no more than 6.2 %.

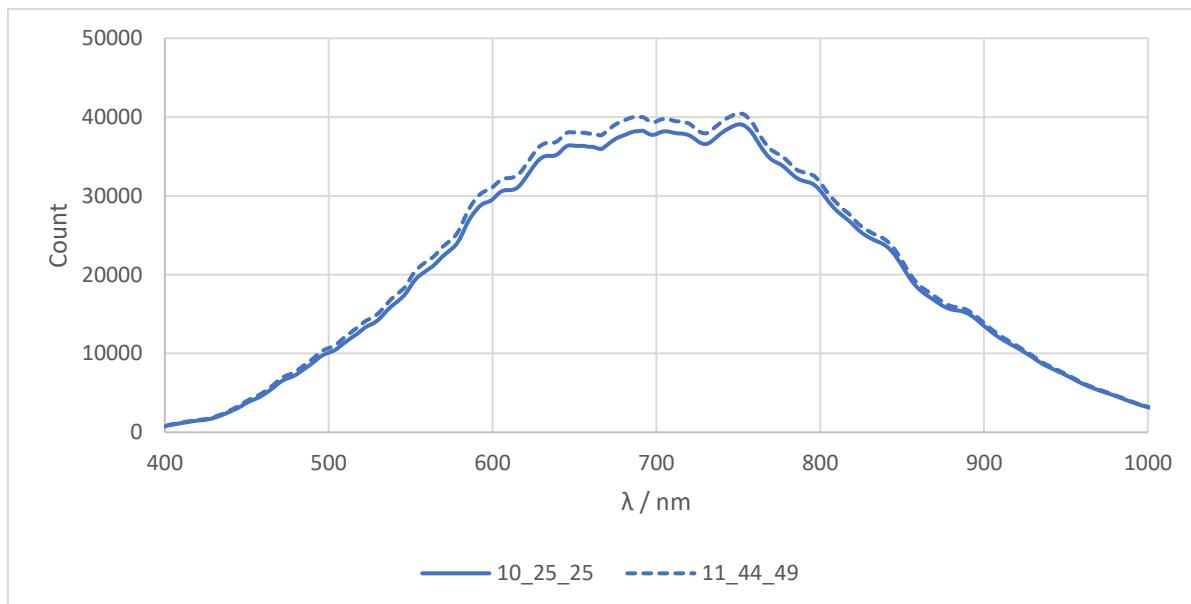


Figure 3.3. White light calibration spectra for scans taken 1hr 20min apart. The spectra are labelled after the time they were taken in the format HH_MM_SS.

3.2.1.2 Raman

The Raman spectroscopy equipment used for experiment 1 was bespoke, developed by *Beeby et al. (2016)*. It was developed specifically for the identification of pigments in objects of cultural heritage, and is unique in its construction, designed to allow large manuscripts to fit under the detector with ease, and to be portable. The device is shown in *Figure 3.4*. The lightweight frame construction allows movement of the detector in two spatial dimensions through repositioning, either of the frame, or of the detector on the frame.

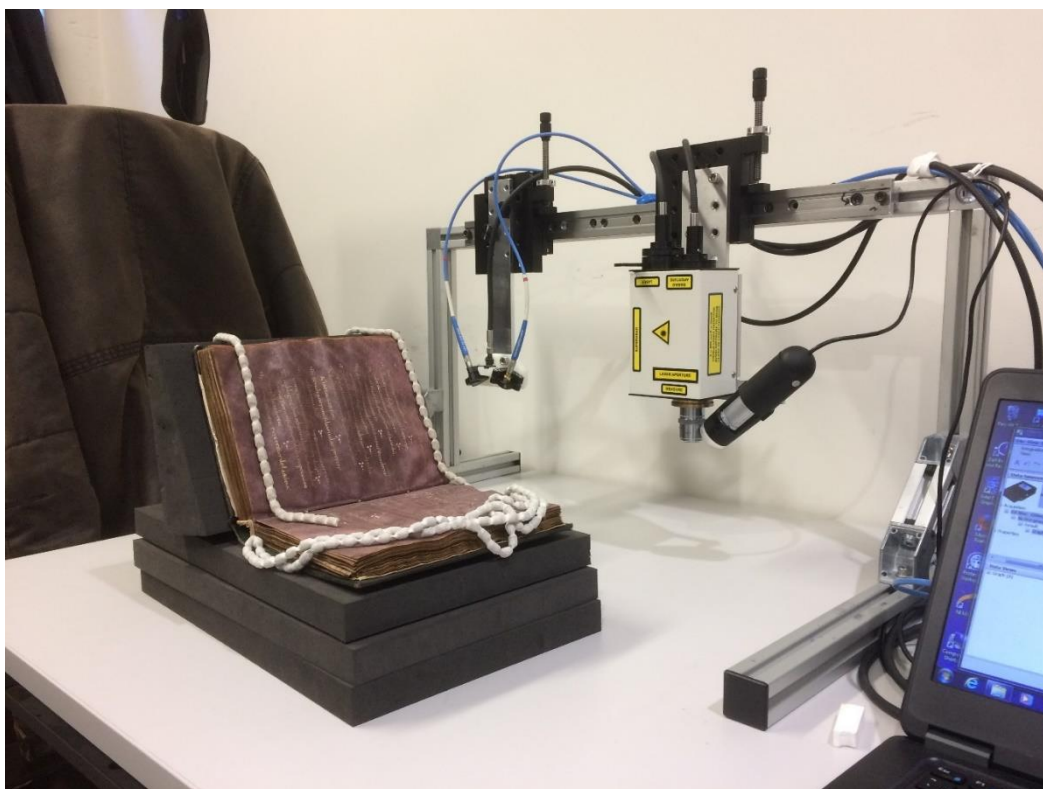


Figure 3.4 Raman spectroscopy equipment as used in experiment 1.

The excitation source is a JDSU 1 mW HeNe laser with a wavelength of 632.8 nm . The detector measures in the range of $2577.367 \text{ cm}^{-1} - 91.14842 \text{ cm}^{-1}$ and is an Andor Shamrock 163/iDus 416 camera CCD spectrograph with a Horiba Ltd Superhead sampling accessory. A USB microscope (Veho Discovery VMS-004 deluxe, 400x, 2 megapixels magnification) generates a live image on the laptop, stills of which are used to record the exact location of the laser spot measurement.

Light and dark calibration are performed and a reference sample is used to correct for any shift from true peak values. All Raman measurements require a blacked-out room to minimise interference.

3.1.2.3 XRF

The pXRF equipment used was an Oxford Instruments X-MET 8000 series light element handheld pXRF analyser, 5 mm spot size, in air. Calibration has been performed on an ongoing basis as per the manufacturers recommendations to ensure the equipment is up to standard. The software used to analyse the pXRF spectra was Bruker Spectra Artax Version 7.2.0.0.

3.1.2.4 DRSP

DRSP was performed using a Konica Minolta CM 600 d connected to a Windows 10 pro 1903 laptop running SpectraMagic NX. White and black calibrations were performed at the beginning of use using the provided reference samples. Reflectance spectra are in the range of 360 – 740 nm, spectral resolution 10 nm, spatial resolution diameter 3 mm. This equipment is shown in *Figure 3.5*.



Figure 3.5 The DRSP equipment in use, analysing the robe EAX 7873.

3.2 Summary of analytical methods used

Table 3.1 reviews techniques commonly used for pigment characterisation, location, and monitoring and compares their characteristics and performance. For each of the three experiments, techniques were chosen based on their popularity for the required purpose. Not all limitations and benefits of each technique can be listed in such a table, for example Raman spectroscopy works only on certain pigments (mainly inorganic pigments), and so the table has focussed on those advantages and disadvantages that were relevant to their being the technique of choice for each of the three applications that have been investigated during my DPhil.

	VNIR HSI	Raman spectroscopy	XRF	Diffuse reflectance spectrophotometry (DRSP)
Data given	Reflectance spectrum for each pixel in an image, 400 – 1000 nm detection range. Spectra easily affected by chemicals mixed with the pigment.	Definitively identifies certain pigments, results easily obscured by fluorescence. Generally better at organic structures, than inorganic.	Informs the user about chemical elements present in sample area, can be used to suggest which pigments are present.	Provides reflectance spectrum in the VNIR region for one spot 3 or 8 mm in diameter, similar to VNIR HSI expect that it is a contact method.
Use <u>FOR</u> CHARACTERISATION Techniques used in paper 1 highlighted	Can be used to give an indication of colour, the characterisation of pigments based on this wavelength range is very complex.	Very good, can be used to provide the exact pigment. Sometimes molecules do not exhibit the Raman phenomena thus making them unidentifiable.	Provides only the elements present, and is penetrative, other methods (Raman spectroscopy, FTIR) require less interpretation.	Gives the same data as VNIR HSI but only in one spot.
Use <u>FOR</u> LOCATION	Provides data on the entire area of interest,	Many points are needed to provide good coverage, best used to	Many points are needed to provide good	Gives the same data as VNIR HSI but only in one spot.

Techniques used in paper 2 highlighted	useful in the creation of false colour images used as maps of colouration.	characterise visible colouration.	coverage. Can be penetrative which must be taken into account in interpretation of results.	
Use <u>FOR</u> <u>MONITORING</u> <u>G</u> Techniques used in paper 3 highlighted	The whole surface of the object can be observed over time, in a non-contact, non-destructive manner.	Will only identify the pigment present, not the percentage of it faded, or ΔE value.	Cannot be used to determine fading, only provides data on the elements present.	This is the current methodology used for the monitoring of fading, but as a contact method it can be difficult to obtain consistent results.

Table 3.1 A comparison of the utility of the main techniques in the paper, and their relevant uses.

3.3 Calibration of hyperspectral equipment and sources of error

A comparison of the calibration workflow used for this thesis with those found in the literature confirms that it is a standard procedure. The utilisation of white and dark references to calculate the relative reflectance as the initial pre-processing step is the most common calibration approach *Nouri et al. (2013); Pillay et al. (2019); Wang et al. (2012)*. Of particular relevance is the round robin test (RRT) conducted by *Pillay et al. (2019)* with members of cultural heritage institutes who perform hyperspectral imaging on artefacts which focussed on the calibration workflow. *Pillay et al (2019)* discuss both

the spectral and spatial calibration of hyperspectral systems, and their proposed “ideal” workflow mirrors that which has been used throughout this thesis and the most common elements of the workflows of those heritage institutes involved in the study. *Figure 3.6* shows how the workflow proposed by Pillay et al (2019) differs from the workflow used throughout this thesis.

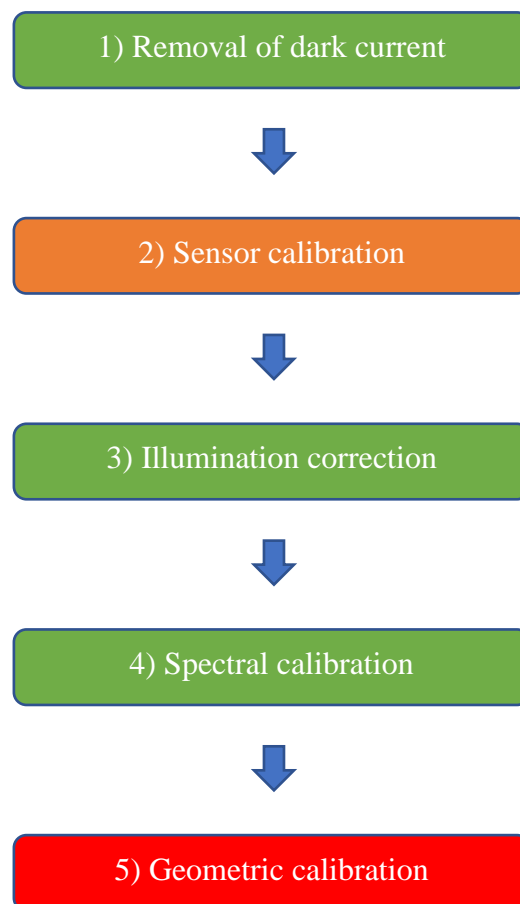


Figure 3.6. The workflow suggested by Pillay et al. (2019) based on the results of their RRT. Steps shown in green were used explicitly throughout this thesis, step 2 (orange) was used implicitly as it was accounted for by the manufacturer’s image acquisition software, and step 5 (red) was not used in this thesis as it was considered unnecessary.

In step 1, removal of dark current, a dark reference image is captured by covering the lens with the lens cap and capturing an image whilst all other parameters are kept the same as during the scan of the intended subject. Several scans are taken in order to produce a mean dark current value for each pixel, which is then subtracted from subsequent scan data. In this, the methodology used throughout this thesis is identical to that proposed by *Pillay et al. (2019)*.

In step 2, sensor calibration, a correction is applied for errors caused by the variability in the sensitivities of each pixel. This is normally performed by the manufacturer owing to the prohibitive equipment requirement that the image be acquired under uniform and constant lighting such as that provided by an integrating sphere. It is therefore corrected for by the acquisition software *Pillay et al. (2019)*.

In step 3, illumination correction, the data is scaled according to the results of the white reference image to account for the spatial variability in the illumination and optics. The white reference is taken under the same conditions as the scan of the intended subject and is ideally of a target that is diffuse, uniform, and of known reflectance *Pillay et al. (2019)*. It is noteworthy that *Pillay et al. (2019)* investigated the use of targets of 99 %, 50 %, 25 %, and 12.5 % reflectance and found that, owing to the less reflective nature on average of heritage material compared to remote sensing data, it was beneficial to calibrate the hyperspectral equipment to a reference target with different values, allowing the system to use a greater extent of its dynamic range thus improving SNR, and data quality. This could have been a cost effective method of improving the data quality of scans taken using the Bodleian Libraries' equipment and is a recommendation of this thesis. Regrettably it cannot retrospectively be applied to

scan data as the re-scanning of artefacts used throughout the thesis is currently impracticable^a.

In step 4, spectral calibration, an image of a target of known spectral reflectance is used to transform the raw hyperspectral data into reflectance data *Pillay et al. (2019)* as per *Equation 3.1*

$$I = 100 \times \frac{R-D}{W-D}$$

Equation 3.1. To calculate the reflectance values from raw data using the white and dark calibration scans. I is the converted relative spectral image (reflectance data), R is the spectral image of the subject (raw data), W is the white reference image, D is the dark current (dark reference). Adapted from the equation presented by Wang et al.

(2012)

In most cases, including in this thesis, this is done using the same target as for step 3. Both step 3 and step 4 share the same drawbacks, as the target will not have perfectly uniform reflectance across the range of the equipment (owing to manufacturing constraints) but this is easily compensated for by incorporating the true reflectance spectrum of the target. Spectralon[®] is the most commonly used white reference *Pillay et al. (2019)* and *Figure 3.7* shows the reflectance spectrum of this. A further drawback is that the calibration will be impacted should the target become dirty though this is easily prevented by routine maintenance and the impact can be minimised by scanning the entire target (normally only one line is scanned) and averaging the results.

^a Restrictions imposed due to the COVID-19 pandemic including social distancing, lockdowns, and the closure of certain services has prevented access to both the equipment held at the Bodleian Libraries, and the subject material.

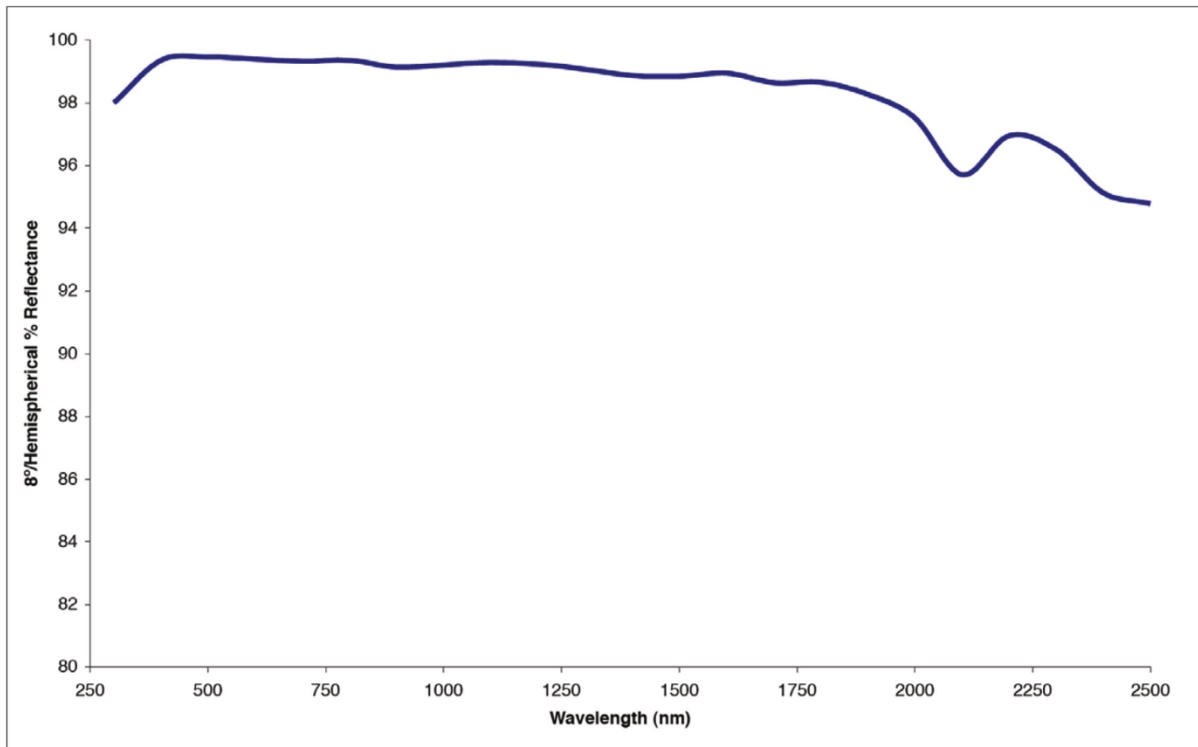


Figure 3.7. The reflectance spectrum of the “99 %” reflective Spectralon[®] used throughout the thesis tested for $\lambda = (250 - 2500 \text{ nm})$ Labsphere (2021). The Labsphere datasheet lists the reflectance as between 0.975 and 0.995 for 350 – 500 nm, 0.985 – 0.995 (500 – 700 nm), and 0.975 – 0.995 (750 – 1600 nm).

Finally step 5 is geometric calibration. Hyperspectral imaging systems may have geometric distortions as a result of the scan motion, the arrangement of dispersion optics, the lens, errors in alignment with respect to the target, and geometric distortions introduced as a result of an incorrectly calculated scan speed causing an error in the aspect ratio *Pillay et al. (2019)*. For errors in the aspect ratio, a geometric calibration target may be imaged alongside the subject so that the aspect ratio may be corrected later. However, in order to correct for distortions caused by the equipment a complex characterisation of the sensor model, obtained by measuring the angle of view of each pixel using a micrometer, must be obtained. As with step 2, this is performed by the manufacturer but in this case the demand for geometric calibration is much lower and so

it is not generally included in the software. Generally it is only carried out if multiple images are to be mosaiced which is not often the case for heritage users. Interestingly in the RRT performed by *Pillay et al. (2019)* the image geometries were described as being “highly variable”.

The standard calibration workflow of a hyperspectral imaging system is concerned with the reduction of signal variations arising from uncontrolled, or undesirable, variables. Such variations can be a product of both noise *Nouri et al. (2013); Pillay et al. (2019); Wang et al. (2012)*, and signal variations caused by non-uniformities in the illumination, and in the focal plane array of the camera *Nouri et al. (2013); Pillay et al. (2019)*. Hyperspectral imaging is particularly prone to noise, especially at the extreme wavelengths, owing to the narrow spectral bands and the large variability in the quantum efficiency across the spectral range *Pillay et al. (2019)*.

The evaluation of noise in an imaging system is primarily concerned with dark current noise *Nouri et al. (2013); Pillay et al. (2019)*. The term dark current noise refers to electronic noise in the system which increases with an increased integration time, and with an increase in temperature *Pillay et al. (2019)*. Dark current noise is caused by the movement of electrons arising from thermal energy in the system when no light is incident on the sensor *Hui (2020)* and is primarily reduced by cooling *E. Kokkinou et al. (2001)*. Other sources of noise such as read noise are reduced by increasing the number of scans per image, increasing the scan time, increasing the exposure, and binning *Bai et al. (2019); E. Kokkinou et al. (2001); Wang et al. (2012)*.

The white and dark calibration described above will account for dark current noise *Nouri et al. (2013); Pillay et al. (2019); Wang et al. (2012)* however it does not account for all noise. For example shot noise caused by background thermal radiation

cannot be removed WANG *et al.* (2010) and noise due to temperature and voltage variations in the equipment will always be present Wang *et al.* (2012).

The signal to noise ratio (SNR) presents a quantitative evaluation of the noise in a system and was calculated here using the method presented by Wang *et al.* (2012) shown in Equation 3.2.

$$SNR = \frac{1}{N} \sum SNR(\lambda) = \frac{1}{N} \sum \frac{\mu(\lambda)}{\sigma(\lambda)}$$

Equation 3.2. For calculation of the SNR of hyperspectral data where N is the number of spectral bands, $SNR(\lambda)$ is the SNR at wavelength λ , $\mu(\lambda)$ is the mean reflectance value at wavelength λ , and $\sigma(\lambda)$ is the standard deviation of the reflectance values at wavelength λ .

An image of MS. Arm. d.3 (10r) Gospels (dated 1304), shown in Figure 3.8 (a) was used for the calculation of the typical SNR of the equipment used in this study. Ideally for this calculation the same scan is performed multiple times, the analysis of the SNR of a single pixel over different scans would thus provide the operator with an evaluation of the “random noise” of the machine, caused by temperature and voltage variations within the equipment. A region of interest (ROI) consisting of 77 neighbouring pixels was created as an approximation of this approach and the mean and standard deviation for the calculation were taken from this data. The spectra for the ROI are shown in Figure 3.8 (b) where it is seen that the noise appears to be more accentuated in regions of approximately $\lambda < 460$ nm, and $\lambda > 790$ nm. From Equation 3.2 the SNR of these 77 pixels is 23.8. Wang *et al.* (2012) calculated the typical SNR of their hyperspectral imaging system to be 68.84 prior to correction of their system, and 80.16 after corrective measures such as increasing the camera exposure, and applying

digital gains at each spectral band. The SNR of the Bodleian system as set up for the scanning of MS. Arm. d.3 (10r) is lower than that achieved by *Wang et al. (2012)*, 23.8 compared to compared to 68.84. The ideal value of an imaging system's SNR is difficult to define but it is commonly thought that SNR must be ≥ 5 in order for the features to be viably detectable by a human observer *Burgess (1999)*, an SNR of 23.8 therefore, is still sufficient for analysis.

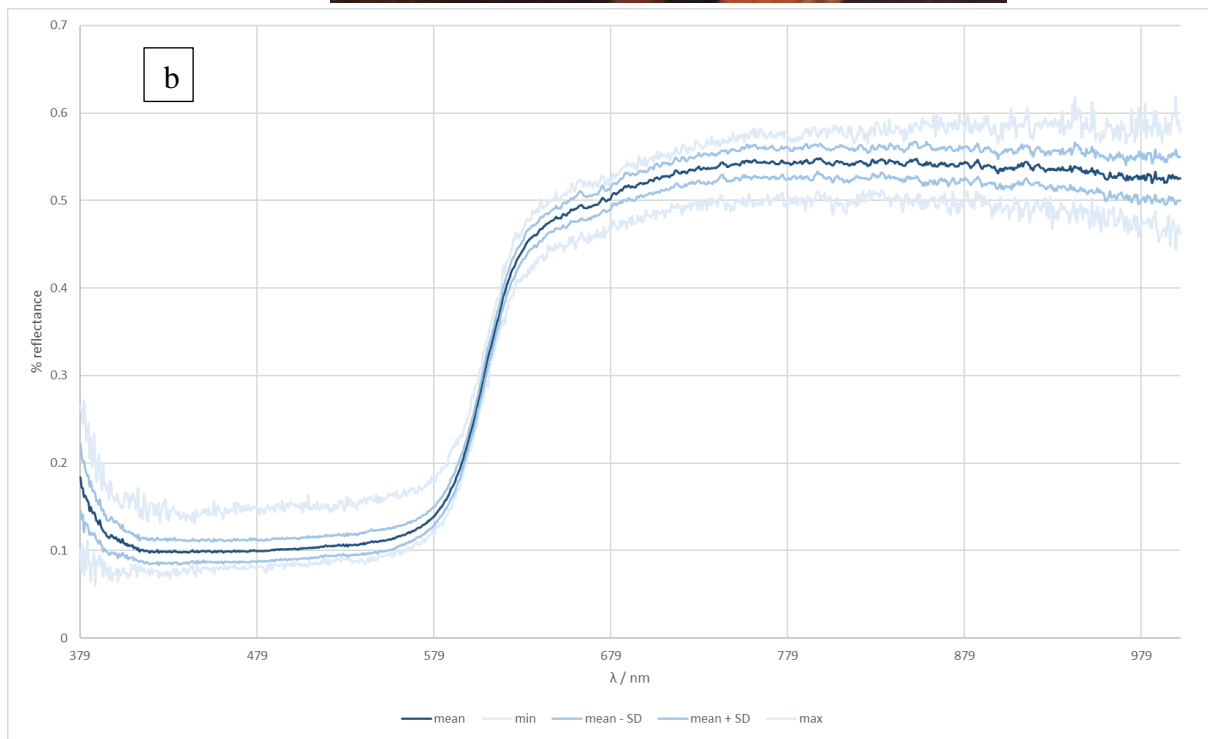
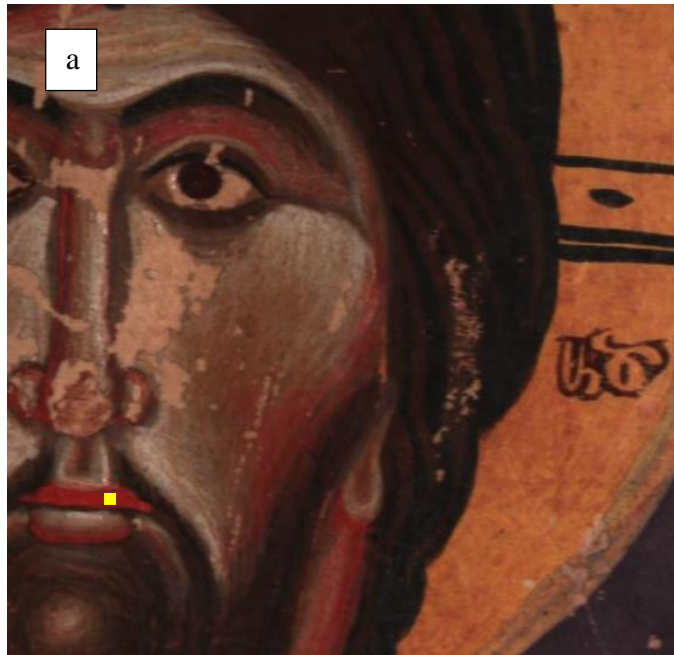


Figure 3.8. a) MS. Arm. d.3 (10r) Gospels (dated 1304) showing the region of interest used for the determination of SNR for this scan (yellow square bottom left), b) showing the spectra obtained from this region, along with the maximum, minimum, and standard deviations.

Another error common to hyperspectral imaging systems in the heritage field is blur introduced as a cause of chromatic aberration (*Figure 3.9*). Hyperspectral images are typically captured with a low f number and an open aperture in order to collect as much light as possible. The resultant low depth of field is not normally an issue for remote sensing applications where the system is focussed at infinity however, when imaging at close range, as in the cultural heritage field, the image will not be in focus across the spectral range *Pillay et al. (2019)*. Focus is often a compromise across the detection range but can be improved through techniques such as focus stacking *Pieper & Korpel (1983)* where the image cube is created from multiple images each taken at a different focal length, obviously this is more feasible for some systems than others.

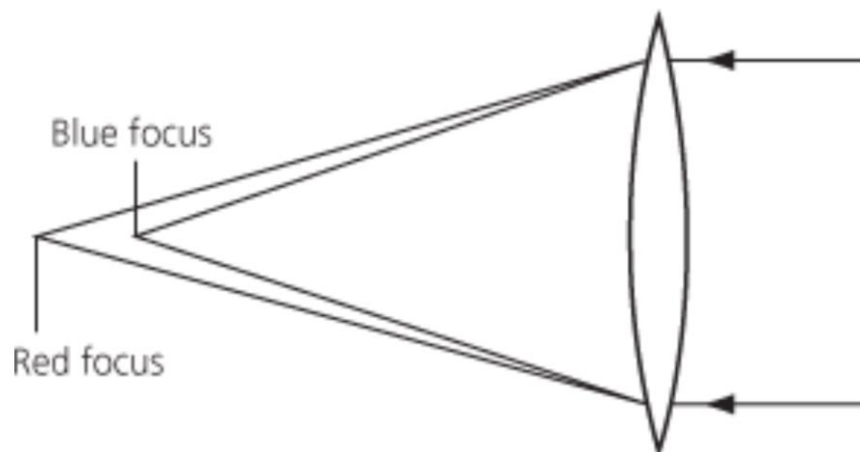


Figure 3.9. A basic diagram of chromatic aberration Ridpath (2018). The focal length of the blue light transmitted through the lens is shorter than that of the red light.

Figure 3.10 shows 5 greyscale images of Bodl. 394. (examined for paper 3) produced every 150 nm from 400 – 1000 nm. Images produced from data at the extremes of the wavelength range (400 nm, and 1000 nm) are the most out of focus. This is expected given that the equipment was focussed using data from the visible

region and indeed the best focussed image presented in *Figure 3.10* is that produced from data at 550 nm with the other greyscale images falling somewhere between.

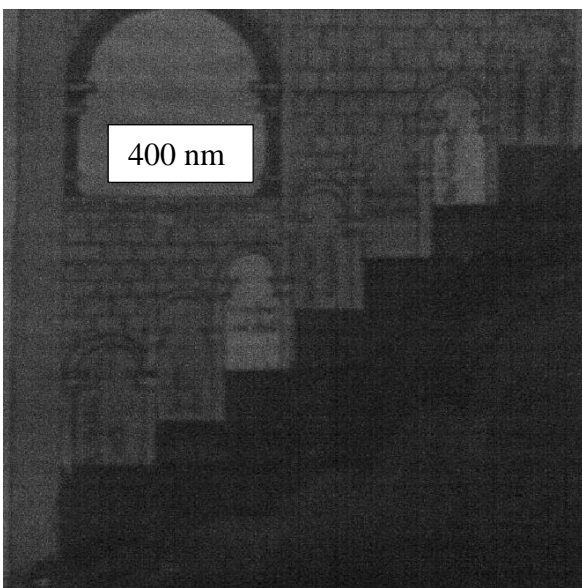
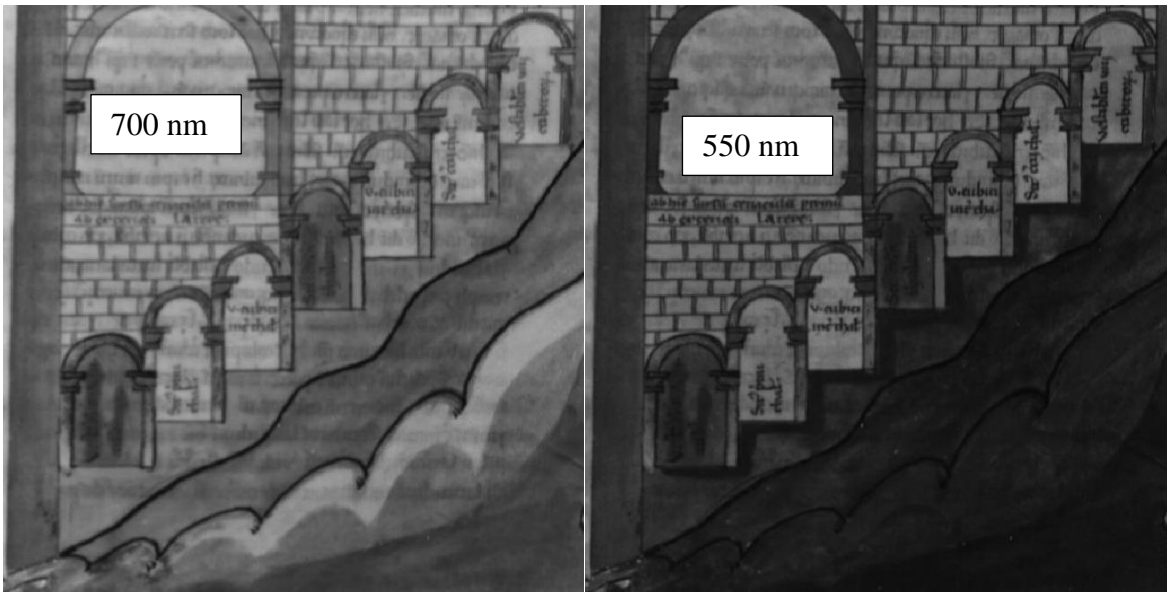
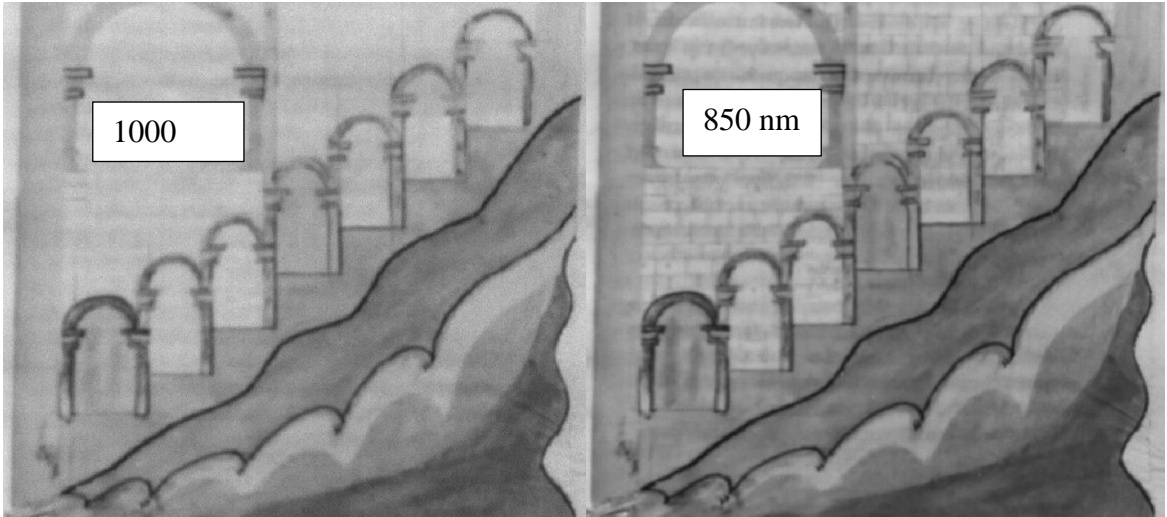


Figure 3.10. A greyscale image taken every 150 nm from 400 to 1000 nm to demonstrate the effect of chromatic aberration on the focus of the image.

A discussion of errors is not complete without mentioning dropped frames. This can be a serious issue for hyperspectral imaging and manufacturers must prevent dropped frames *Martin Chamberland et al. (2004)*. This was encountered during experiments conducted at the same time as this DPhil. It was discovered that dropped frames were occurring as a result of there not being enough space on the hard drive to which the files were being written. After consultation with the manufacturer an indication of disk space usage was added to the software to avoid repetition of this mistake.

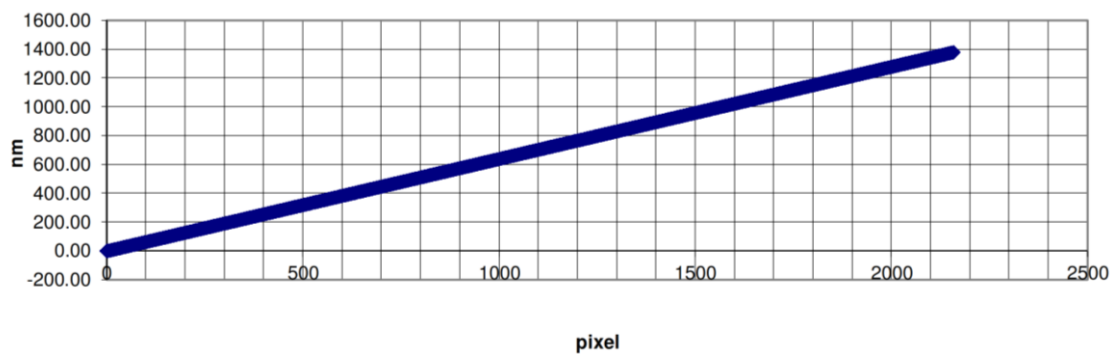


Figure 3.11. A “wavelength to pixel” calibration chart offered to consumers by the hyperspectral imaging equipment manufacturer (Headwall Photonics)

As has been mentioned certain aspects of calibration are carried out by the manufacturer, wavelength to pixel calibration is one such process and the results of this calibration for the equipment held at the Bodleian Libraries, University of Oxford are shown in *Figure 3.11*. This calibration graph was provided by Headwall Photonics upon receipt of the hyperspectral imaging equipment. The purpose of this calibration is to assign wavelengths to pixels on the CCD sensor array *Sun et al. (2019)* and as can be seen there is a strong linear relationship over the wavelength range as is desirable.

Section 2: Experimental Section

Chapter 4 experiment 1: Assessing the Effectiveness of Hyperspectral Imaging in the Identification of Pigments: Comparing HSI and Raman Spectroscopy in An Analysis of Illuminated Armenian Manuscripts

This paper is reproduced from the publication in the journal Heritage Science (Date of publication: 6th July 2018, DOI: 10.1186/s40494-018-0206-1). This journal was selected as it was felt that the aims and scope of Heritage science matched the research question well. In particular the development of non-destructive analytical methods for the identification of constituent components is of interest to a wide range of heritage scientists.

Ian J. Maybury^a, David Howell^b Melissa Terras^{c, d} c Heather Viles^d

- a. Corresponding author: *ian.maybury@stx.ox.ac.uk*, School of Geography and the Environment, Oxford University Centre for the Environment, University of Oxford, South Parks Road, Oxford, OX1 3QY
- b. *david.howell@bodleian.ox.ac.uk*, Weston Library, Broad Street, Oxford, OX1 3BG
- c. *m.terras@ed.ac.uk*, College of Arts, Humanities and Social Sciences, University of Edinburgh
- d. *heather.viles@ouce.ox.ac.uk*, School of Geography and the Environment, Oxford University Centre for the Environment, University of Oxford, South Parks Road, Oxford, OX1 3QY

4.0 Abstract

There is great practical and scholarly interest in the identification of pigments in works of art. This paper compares the effectiveness of the widely used Raman Spectroscopy (RS), with Hyperspectral Imaging (HSI), a reflectance imaging technique, to evaluate the reliability of HSI for the identification of pigments in historic works of art and to ascertain if there are any benefits from using HSI or a combination of both.

We do so by undertaking a case study based on six Armenian illuminated manuscripts (11th -18th centuries CE) in the Bodleian Library, University of Oxford. RS, and HSI (400 – 1000 nm) were both used to analyse the same 10 folios, with the data then used to test the accuracy and efficiency of HSI against the known results from RS using reflectance spectra reference databases compiled by us for the project.

HSI over the wavelength range 400 – 1000 nm agreed with RS at best 93 % of the time, and performance was enhanced using the SFF algorithm and by using a database with many similarities to the articles under analysis.

HSI is significantly quicker at scanning large areas, and can be used alongside RS to identify and map large areas of pigment more efficiently than RS alone. HSI therefore has potential for improving the speed of pigment identification across manuscript folios and artwork but must be used in conjunction with a technique such as RS.

Keywords

Hyperspectral imaging, Raman spectroscopy, pigment identification, illuminated Armenian manuscripts, manuscript studies, multispectral imaging, special collections

List of abbreviations

HSI	Hyperspectral imaging
RS	Raman spectroscopy
FORS	Fibre optic reflectance spectroscopy
FT-IR	Fourier transform infrared spectroscopy
HPLC	High performance liquid chromatography
GCMS	Gas chromatography mass spectrometry
SAM	Spectral angle mapping
BE	Binary encoding
SFF	Spectral feature fitting
ENVI	Environment for visualising images
XRF	X-ray fluorescence spectroscopy
ROI	Region of interest
UV-VIS	Ultraviolet-visible light

4.1 Introduction

4.1.1 Pigment analysis

Technical investigations of works of art are of great value to conservators and researchers. Scientific techniques have been applied to pigment identification as part of conservation since the late twentieth century *Bacci (1995); Liang (2012)* aiding: characterisation of the palette of an artist or workshop *Pallipurath et al. (2014); Ricciardi et al. (2009)*; art historical understanding of the artist *Coupry et al. (1994)*; identification of restorations or interventions *Delaney et al. (2016a); Ricciardi et al. (2009)*; monitoring degradation *Clark (2002)*; detailing the conservation state of an item *Ricciardi et al. (2009)*; and revealing preparatory sketches *Delaney et al. (2016a)*, underdrawings *Ricciardi et al. (2009)*, or palimpsests *Snijders et al. (2016)*. Such knowledge is of value to researchers and can also aid in effective conservation strategies and restoration *Clark (2002)*, and answer questions of provenance (*Ricciardi et al. 2009; J. K. Delaney et al. 2016a; Pallipurath et al. 2014; Clark 2002; Burgio et al. 2005; Liang et al. 2011; Douma, 2008.*). In the broader sense it can also help determine trade routes and cultural interactions (*Douma, 2008.; Royal Society of Chemistry, 2020*), and give some idea of the technology of the period with respect to pigment manufacture *Douma (2008b); Royal Society of Chemistry (2020)*.

Sampling-based techniques such as gas-chromatography-mass spectrometry (GC-MS) and high performance liquid chromatography (HPLC) provide considerable data *Aceto et al. (2014)* however a combination of non-destructive techniques generates desirable data without harming the item (an obvious advantage for conservators) *Aceto et al. (2014); Mounier et al. (2014)*. A combination of techniques is most often used, as any one technique has limitations. For example, Mosca et al used Raman spectroscopy and X-ray fluorescence spectroscopy (XRF) to identify pigments in different layers of

illuminated manuscripts *Mosca et al. (2016)*. Other techniques include: Fibre optic reflectance spectroscopy (FORS) *Aceto et al. (2014)*, and Fourier transform infra-red spectroscopy (FT-IR) *Buti et al. (2013)*.

Access to these techniques and approaches for cultural heritage imaging can be restricted due to their cost, availability, and the complex nature of interdisciplinary research *Terras (2010)*. It is therefore useful to assess which approaches are most feasible, cost-effective, efficient, and accurate for our purpose of pigment identification, as this will help scholars understand the affordances of different systems and aid in the scoping and management of programs of research.

4.1.2 Raman spectroscopy

Raman Spectroscopy (RS) is a common and relatively accessible method in pigment identification *Centeno (2015)*; *Goler et al. (2016)*; *McCreery (2000)*; *Pallipurath et al. (2014)*; *Smith & Clark (2004)*; *Vandenabeele et al. (2006)*. RS relies upon the initialisation and detection of the inelastic scattering of radiation at an atomic level. The energies at which this occurs are dependent on the atom under observation, the energy of which is altered (in a calculable manner) by the neighbouring atoms. In this way each unique orientation (on an atomic level) of a molecule gives a unique spectrum for RS. Therefore when an identification is made, using characteristic peaks, fingerprint regions and any reasonable assumptions of the contents of the subject, it can be taken as confirmed that the molecule is present. RS therefore is a justifiable analytical technique to be used as a benchmark when assessing the application of HSI to this problem. RS has been used to look at significant works of art by artists such as Picasso *Centeno (2015)*; *Muir et al. (2013)* and Vermeer *Burgio et al. (2005)*, and also at high value items such as the Lindesfarne Gospels *Brown & Clark (2004)* and high profile forgeries

Chaplin et al. (2004); Coupry et al. (1994). RS has proved to be efficient at pigment identification *Clark (2002); Coupry et al. (1994)*, although there are some exceptions such as lakes^b and other organic pigments which have poor Raman scattering, making identification difficult *Aceto et al. (2014)*. Where Raman scattering is poor, useful results have been obtained by combining with XRF *Ricciardi et al. (2009)*. RS has also been used to investigate the distribution of pigments and extent of restoration by looking at cross sections of objects *Centeno (2015)*.

Since its introduction as an analytical technique for the study of heritage in the 1970s, RS has become smaller, portable, and simple enough to be used by those who are not considered experts or analysts *Colomban (2012); Smith & Clark (2004)*. Although accurate, it is also very time consuming to use RS to identify pigments across large areas, as sample points are small and have to be repeated. Raman mapping has been used to examine areas on the micrometre scale over several hours. For example, one archaeological study examining rust took 21 hours to image a 52.2 x 46.2 µm rectangle *Neff et al. (2006)*, another looking at cross sections of a sixteenth century painting took 4.5 hours to image a 60 x 45 µm rectangle *Lau et al. (2008b)*. An area can be mapped simultaneously by defocussing the laser beam, but this greatly reduces the intensity and as such is limited to a field of view on the order of micrometres *Brambilla et al. (2011)*. In general using Raman spectroscopy as a mapping tool is unusual *Ernst (2010)*. XRF has also been used for mapping but is also very slow, with an area of 36 x 34 mm scanned in 45 minutes in one study *Mosca et al. (2016)*. In contrast, hyperspectral imaging can image an A4 sheet (210 x 297 mm) in roughly fifteen minutes. It is therefore worth considering if other techniques such as HSI can be used in

^b A class of organic pigments made by precipitating a dye with a binder, the name derives from lac (a resinous secretion) and so is an interesting misnomer, having nothing to do with bodies of water.

conjunction with RS to increase efficiency in identifying pigments, particularly across larger areas.

4.1.3 Hyperspectral imaging

Hyperspectral imaging (HSI) is a reflectance technique which, for each pixel in an image, produces a reflectance spectrum for the wavelength range detected *Liang (2012)*. This holds many potential advantages for pigment identification on a large scale given that it scans large areas quickly, and it is this property (or affordance) that we wish to investigate, within the context of pigment identification. The spectra produced can be used to characterise the materials at the surface of the image and produce maps of these materials, but hyperspectral imaging has also been used to reveal hidden images and text, given its ability to detect several wavelengths, often including wavelengths outside of the visible range *Cucci et al. (2015); Liang (2012)*. Originally a remote sensing technique *Cucci et al. (2015)* it has been developed over the years for astrophysics, military applications, medical imaging, and more recently for the non-destructive investigation of works of cultural heritage *Delaney et al. (2016a); Fischer & Kakoulli (2006); Moutsatsou & Alexopoulou (2014); Schlamm & Messinger (2010)*. HSI has been successfully applied to a range of heritage material including The Declaration of Independence *France (2011)* where alterations to text were revealed, and Edvard Munch's "The Scream" where the pigments used were characterised and mapped *Deborah et al. (2014)*.

Multispectral imaging (MSI), and HSI have both been used as the first step in investigations to provide spatial and spectral data on the pigments in a manuscript. This then allows one to examine and map the entire surface of an object *Delaney et al. (2016a); Janssens et al. (2016b); Moutsatsou & Alexopoulou (2014)* thus guiding the

use of techniques such as Raman spectroscopy *Daniel et al. (2016); Mounier & Daniel (2015)*, XRF *Catelli et al. (2017); Rebollo et al. (2013)*, and FORS *Melo et al. (2016)* which give a more detailed analysis *Aceto et al. (2014); Clarke (2001); Ricciardi et al. (2013); Trumpy et al. (2015)*. Using HSI as a preliminary technique to provide an overview in this manner can alleviate concerns that the assumption that site specific techniques represent the whole may not be sufficient to demonstrate the diversity of colourants in such works *Ricciardi et al. (2009)* thus working with a combination of techniques allows for the best results to be generated *Balas et al. (2003); Cardeira et al. (2016)* and it is mainly recommended to use HSI as the first technique in combination with others *Aceto et al. (2014); Delaney et al. (2016a)*.

The identification of materials in works of art via HSI can be done by comparing the reflectance spectra for the relevant pixel to those of a reference database or by the creation of false colour images from the hyperspectral data as per *Hayem-Ghez et al. (2015)*. Such false colour composite images have recently been successfully used to aid the identification of watercolour pigments in eighteenth century botanical illustrations by Ferdinand Bauer *Mulholland et al. (2017)*, this study however focusses on the former identification method. There is no such database suitable for the identification of pigments and so one must be manufactured by the analyst for each new study. Ideally this would contain all possible combinations of colourants, binders, etc. likely to be found in the studied object and would also be historically accurate (e.g. using the same substrate as found in historic artworks). Such a level of detail is required because the signal is a combination of everything within the pixel and is not molecularly specific and in mixtures one peak may obscure the peak of another compound. Despite this the differentiation of two colourants which are similar visually but chemically distinct

(metamers) by HSI has been demonstrated *Aceto et al. (2014); Balas et al. (2003); Centeno (2015); Montagner et al. (2016); Vitorino et al. (2014)*.

The question of whether or not the algorithms being used in the industry at present to analyse hyperspectral data cubes give the best results has been raised, and newer algorithms have been suggested which can take full advantage of the increasing information *Schlamm & Messinger (2010)*. Doubts about the ability of HSI to definitively identify a pigment have been raised due to the complications of mixtures or degraded pigments *Liang (2012)*. For example, for the identification of mixtures, linear spectral unmixing was designed for remote sensing (the collection of surface data from afar, for example the geological survey of several kilometres of land using sensors on an aeroplane) where the signal is a combination of the spectral responses of spatially separated materials *Liang (2012)*. In such a study a pixel may be several meters across and cover both a patch of grass and some tarmac, whereas for paint materials this is not the case, as pigments are uniformly dispersed in the binding media and the spectral response is not a simple linear mixture of the reflectance. Algorithms not typically applied to remote sensing technologies are being applied to HSI data of heritage artefacts with some success, for example the Kubelka-Munk (KM) theory, which is used in the paint industry to calculate the ratios of paints to match a given colour *Liang (2012)*, has been shown to be superior to the more frequently used spectral angle mapping for the mapping of paints in artworks *Liang (2012); Zhao et al. (2008)*. The effect of binding medium, particle size, and concentration have been systematically studied and dirt and varnish can also have an effect *Liang (2012)*.

Reflectance spectra of pigments in the UV VIS range have relatively few broad bands for use in fingerprinting (compared to IR and RS) and cannot therefore always provide unambiguous identification especially when two or more absorbing species are

present in a mixture. It is interesting to note that the HSI equipment used in this study has a spectral resolution of 0.67 nm which is more than sufficient *Blackburn (2007)*; *Cavaleri et al. (2013)* to discern such peaks and troughs as may be present in the reflectance spectra involved and may even lead to data redundancy *Blackburn (2007)*. This would slow down any computational work done on the reflectance spectra (as the computer would carry out calculations on all the data regardless of its redundancy). Care must also be taken to ensure that relevant analysis is done, techniques used for multispectral image analysis may not be appropriate.

Identification can therefore rely on the fact that relatively few colourants could be used in any one piece due to limitations of geography, availability, and time period *Aceto et al. (2014)*. Unusual or unexpected colourants can create a need for the use of multi-technique analyses *Aceto et al. (2014)*. On the other hand, HSI has been shown to successfully differentiate between colourants that other techniques find difficult *Vitorino et al. (2015)*. Red lake pigments (madder for example) are very light sensitive and so their characterisation and any data on their degradation can be of utmost help *Vitorino et al. (2015)*. HSI was used to discriminate between madder, cochineal, and brazilwood however the addition of binding media etc. made it more ambiguous. A more comprehensive database was recommended *Vitorino et al. (2015)*.

This study therefore investigates how well HSI can be applied to pigment identification given the questions raised about the appropriateness of algorithms designed for other uses, and databases which are unlikely to be complete.

4.2 Materials and methods

4.2.1 Armenian manuscripts

Hyperspectral imaging has been used here to identify pigments used in a set of Armenian illuminated manuscripts from the Bodleian Library, University of Oxford, and the identifications made were compared to data obtained from Raman spectroscopy analysis of the same texts. These texts were part of an exhibition entitled “Armenia: Tales From an Enduring Culture” *Lint & Meyer (2015)* which marked the centenary of the Armenian genocide during WW1 and displayed manuscripts felt to be representative of Armenian culture *Lint & Meyer (2015)*. The texts were surveyed prior to exhibition and it was desired to learn about the palette used in their illumination. As a result of analysis prior to this study the exhibition was able to display the raw ingredients for the palette alongside the manuscripts in the exhibition hall.

Illuminated manuscripts of Armenia, while visually stunning, have not been the subject of many scientific studies *Cabelli & Mathews (1982); Orna & Mathews (1988)* yet they are historically varied and of much scholarly interest *Casey (1931); Kurdian (1956); Mathews (1981); Mathews et al. (1994); Royse (2009); Tumanyan (1967)*. The Bodleian Library has over 140 manuscripts, and over 250 early printed books in its Armenian collection with a date range of over 1000 years acquired from 1635 onwards *Baronian & Conybeare (1918)*. A few examples of these, used during this study and displayed during the exhibition, are shown below in *Figure 4.1*.



Figure 4.1 Armenian Manuscripts held by the Bodleian Library. a) MS Arm. d13 (1609 CE) folio 4r: The adoration of the Magi, b) MS Arm. d13 folio 33r: Eusebian canon table. This manuscript was the work of Mesrop, a famous Armenian illuminator, c) MS Arm. e34 folio 4r: The first page of the Armenian translation of the classical Greek grammar attributed to Dionysius Thrax “Concerning Grammar”. Dated 18th Century.

Armenian illuminators have left no written account of how they prepared their pigments Mathews (1981). One study begun in 1979 identified six pigments as the staple Armenian palette with differences in recipes and quality accounting for differences in locale and era. They are gold, white lead, vermillion, orpiment, ultramarine, and red

lake^c. Mixtures of these six pigments are commonly used to create different hues and shades *Mathews et al. (1994); Orna & Mathews (1981)*. It should be noted the study was of 24 manuscripts, which is a small percentage of the total known today. Two things may strike the art historian as odd about the palette: firstly, the use of ultramarine as the standard pigment *Cabelli et al. (1984)*. In European art, ultramarine is rare *Cabelli et al. (1984)*. It is made from lapis lazuli mined in present day Afghanistan, making it more expensive for European artists than for Armenian artists where it is thought that the close proximity to the mines meant that costs were kept low *Cabelli et al. (1984)*. Secondly, the lack of a natural green pigment (organic or inorganic) such as verdigris, which meant the artists had to use a mixture of other pigments to achieve the green colour instead *Cabelli et al. (1984); Mathews (1981)*. Mixtures of mineral yellow, orpiment, and blue (either ultramarine or an organic blue) with lead white to alter the shades were used to produce an olive green which was duller than that found in western manuscripts *Cabelli et al. (1984); Cabelli & Mathews (1982); Orna (2013); Orna & Mathews (1981)*.

The Bodleian Library's collection, spanning all of the aforementioned periods of production makes it ideal for carrying out a study of the palette used. Working with a curator, a range of 6 manuscripts dated between the 14th and 18th centuries, including works by well-known artists such as Mezrop (MS. Arm. d.13, Gospels, 1609) were chosen for this study.

^c Pigments Explained:

Gold: Usually gold leaf but also shell gold which is powdered gold mixed with a binder, so named because it was traditionally prepared in a shell.

White lead: The oldest white pigment, a by-product of lead production.

Vermillion: A red man-made pigment of mercuric sulfide.

Orpiment: A yellow pigment made from heating and grinding the orpiment stone.

Ultramarine: Significantly also called lapis lazuli, made from a semiprecious stone of the same name

Red Lake: A transparent red made from the root of the Madder plant (*Rubia Tinctoria*) hence it is also called madder.

The corpus studied is replicated in *Table 4.1* below, and ranges from the eleventh to the eighteenth century.

Shelf Mark	Page	Date	Title
MS. Arm. e.34	4r	18 th century	Grammatical and philosophical tracts 18 th century
MS. Arm. d.13	22r	1609	Gospels
MS. Arm. d.3	10r	1304	Gospels
MS. Arm. g.4	N/a	1706-7	Phylactery
MS. Arm. d.22	8r	Late 16 th century	Gospels
MS. Arm. c. 3	1r	16 th century	Menologium 16 th Century

Table 4.1. Details of the Armenian manuscripts from the Bodleian Libraries selected for this study

4.2.2 Workflow

To evaluate the utility of HSI with respect to the identification of pigments using the software ENVI^d and the characterisation algorithms contained within in comparison to RS it was necessary to first gather the point-based RS data. HSI could then be carried out on the folios from which RS data had been gathered. It was then necessary to either compile a database of reflectance spectra or utilise an available one. This database could

^d ENVI: Environment for Visualising Images, (accessed via University of Oxford site license), is a software package for remote sensing and dealing with hyperspectral datacubes containing a number of statistical and image processing algorithms.

then be used for the identification of the HSI reflectance spectra by way of a comparison between the data gathered and the known spectra in the database. This comparison is done by way of three computer algorithms available in the ENVI software (Spectral Angle Mapping (SAM), Spectral Feature Fitting (SFF), and Binary Encoding (BE)[°]), which are to be compared to each other in order to suggest which one is the most applicable to this data. The HSI data could then finally be compared to the RS data (which is identified separately by way of characterising peaks in the RS spectra).

Comparison algorithms are all spectral matching techniques chosen by ENVI for the software's Spectral Analyst toolkit as, between the three algorithms provided, a range of options have been made available to increase the chances of a successful application on a variety of spectra. For instance SFF is more suited to spectra with absorption features *Harris Geospatial Solutions, Inc. (2020g)*.

Pigments in the manuscripts were identified based on their spectral signature from Raman spectroscopy. 90 sample spots in total were analysed. 10 folios from 6 manuscripts were chosen to analyse (One would normally analyse fewer spots to characterise the pigments in the manuscripts but more were desired to give this study sufficient data). Spots were chosen for comparison based on the availability of a confirmatory RS identification. As wide a selection as possible was analysed by RS but owing to the unsuitability of some pigments for identification by RS only 90 were able to be carried forward. Furthermore these points are not spread evenly throughout the

[°] Statistical analysis methods: Briefly, SFF, or spectral feature fitting, is a least squares technique which uses methodology based on the absorption features of the spectra *Harris Geospatial Solutions, Inc. (2020i)*, Spectral angle mapping, or SAM, treats each spectrum as a vector and calculates the angle between two spectra, thus determining spectral similarity. Smaller angles represent better matches and the technique is relatively insensitive to illumination effects *Harris Geospatial Solutions, Inc. (2020h)*, Binary encoding (BE) samples the data based on whether a band falls below or above the spectrum mean: the greater the number of bands which match the reference spectrum, the more likely it is that the spectra match *Harris Geospatial Solutions, Inc. (2020a)*.

manuscripts, some manuscripts having been made with more illuminations than others. For the same reasons the spread of points in terms of the variety of pigments is not even, there is much more vermilion than other pigments. Vermillion is very common, and easily identified by RS.

Setting up RS takes about ten minutes and a further 5 to 10 minutes for analysis of each subsequent spot. Not all pigments provide strong Raman scattering signals and so this study focused on those which gave good signals using the Raman spectroscopy equipment available (see below), in order for the HSI setup to be compared to a technique known to be accurate. The six pigments the study focussed on were vermilion, indigo, lapis lazuli, red lead, red lead/vermillion mixture, and indigo/orpiment mixture. Gilded regions of the manuscripts generated unwanted specular reflectance and so analysis was done on regions unaffected by this phenomenon. HSI was then performed on the same manuscripts and used for the identification of the same pigments as the Raman spectroscopy equipment. The two results were then compared directly and if a pigment was characterised as the same pigment by HSI as it was Raman spectroscopy it was considered correct. The percentage of the total characterised which were correct (were the same as Raman spectroscopy) was considered to be the percentage accuracy. In order to classify reflectance spectra a comparison to a reference database is carried out, as explained below. Raman spectroscopy did not require the creation of a database from scratch. The workflow is represented diagrammatically below in *Figure 4.2*.

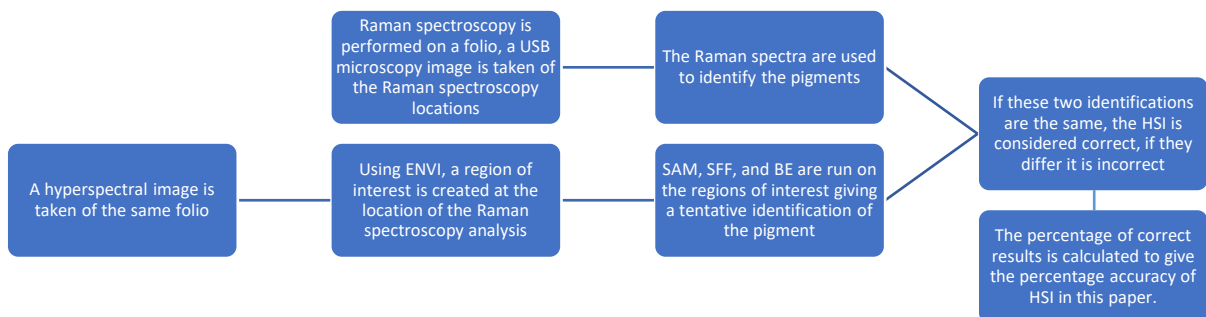


Figure 4.2. A flow diagram of the experiment, explaining the origin of the percentage accuracy for HSI.

4.2.3 HSI database

Reference libraries were needed for the characterisation of the reflectance spectra obtained from hyperspectral imaging. An initial reference library for reflectance spectra was therefore made, using 113 colour swatches painted using Kremer paints (a sample of which are shown below in *Figure 4.3*) on a paper thought to be similar to an eighteenth-century artist's in order to replicate as closely as possible the spectra expected from the genuine manuscripts.

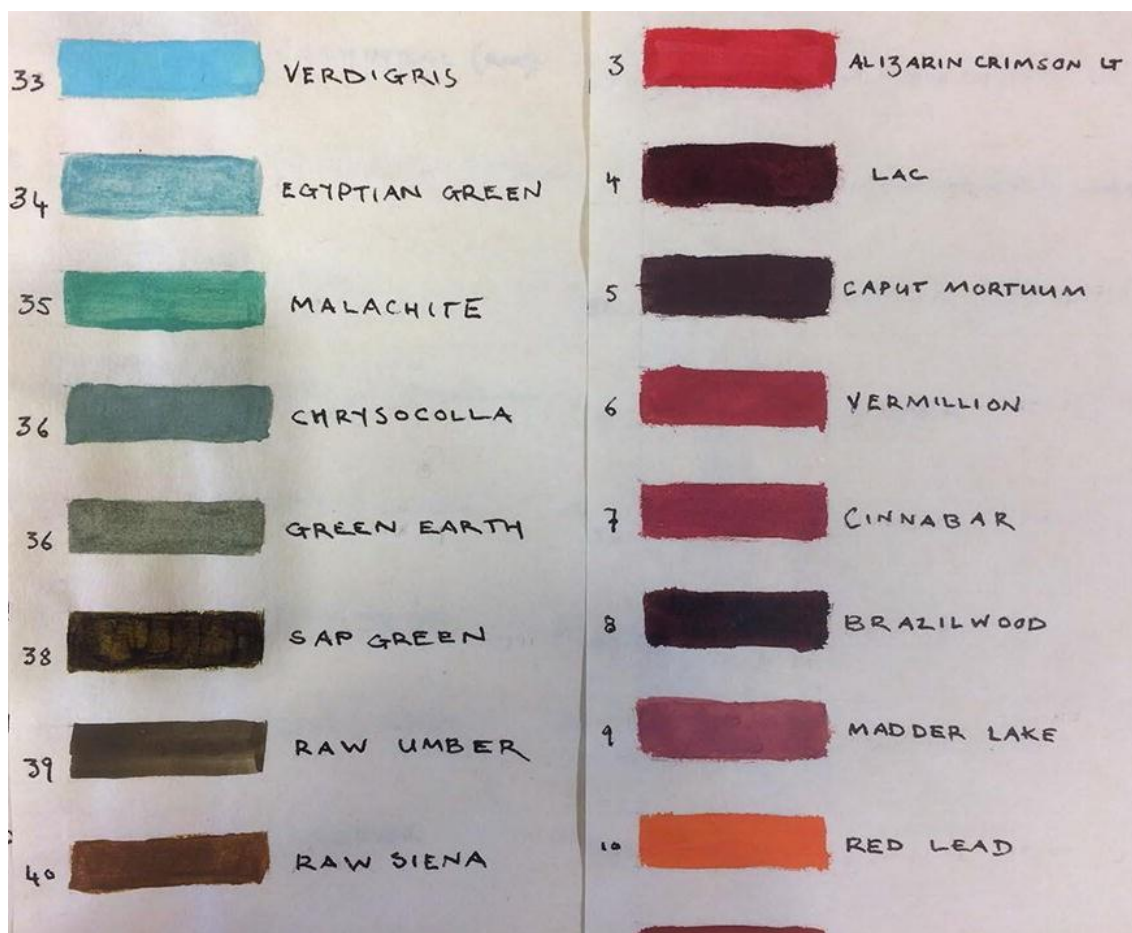


Figure 4.3. Colour swatches of different pigments including common mixtures. These were used to make database 1 (and part of 3).

The first database was created from these colour swatches taking the most likely pigments to be found in Armenian texts based on studies of Armenian illuminated manuscripts *Cabelli et al. (1984); Orna & Mathews (1981)*, and eliminating the ones which were not expected to be found (synthetic pigments for example). This first database was later improved upon once some HSI scans had been taken of some of the Armenian manuscripts and used to create another, more up to date database which included the Armenian spectra, and a further database created which had exclusively the Armenian spectra in it. These three databases were compared with each other in order to see the effect of a change in database on the identification accuracy. Two further databases were also used. A database was downloaded online *Cosentino (2014)* to form database

4, and of these the more likely pigments for Armenian illuminated manuscripts were taken to form database 5. These were used so that externally made references could be compared to those created for the paper. The spread of pigments in databases is shown in *Table 4.2*.

Database	1	2	3	4	5
Spectra from Kremer paints	40	0	40	0	0
Spectra from Armenian manuscripts	0	18	18	0	0
Spectra from online database	0	0	0	55	11
Total number of spectra	40	18	58	55	11

Table 4.2. Showing which spectra are in which database and how many spectra each contains.

Spectra from Kremer paints were of the following pigments: Smalt, gamboge, azurite, verdigris, yellow lake, realgar, massicot, orpiment, alizarin crimson, cochineal, lac, vermillion, madder, red lead, Chilean lapis, indigo, verdigris + indigo, lac + vermillion, red lead + vermillion, realgar + indigo, vermillion + cochineal, lead white.

Spectra taken from the manuscripts and used for database 2 (and later 3) were: indigo, indigo + orpiment, red lead, lapis lazuli, vermilion, red lead + vermilion.

Database 4 contained burnt umber, raw umber, vandyke brown, burnt sienna, raw sienna, red ochre, red lead, cadmium red, alizarin, madder lake, lac dye, camine lake, vermilion, realgar, yellow lake, massicot, yellow ochre, gamboge, naples yellow, lead tin yellow (2 variations), saffron, orpiment, cobalt yellow, cadmium yellow, chrome green, cobalt green, cadmium green, green earth, viridian, phthalogreen, verdigris, malachite, blue bice, cobalt blue, azurite, Egyptian blue, ultramarine, phthaloblue, smalt, indigo, maya blue, Prussian blue, cobalt violet, ivory black, vine black, boneblack, lamp black, gypsum, chalk, lead white, zinc white, titanium white, lithopone, cardboard.

Database 5 contained red lead, madder lake, vermilion, realgar, massicot, orpiment, Verdigris, azurite, ultramarine, smalt, indigo.

The databases were made within the ENVI software by selecting pixels from the area of the pigment, averaging the spectra, and adding this averaged spectrum to an ENVI database file. Databases 4 and 5 were simply downloaded and saved in ENVI database file format.

4.2.4 Equipment

4.2.4.1 Hyperspectral Imaging

The hyperspectral camera used was a Headwall Photonics VNIR 1003B – 10147 which detects 972 contiguous wavelengths from 400 nm to 1000 nm and has a spectral resolution of 0.64 nm. The lens used is a Schneider Xenoplan lens (model XNP 1.4/17 – 0303) with a Headwall Photonics filter (model ACOBL – 380 – 49X, 075).

The setup is a line scanning method, and there are 1600 pixels per line scanned. The spatial resolution depends on the distance between the detector and the subject which can be adjusted at the operator's discretion. A typical pixel size during this study was 110 μm across (this is the "ground sampling distance" the detector's pixel size is 0.65 nm).

The light source is a halogen bulb controlled by a Techniquip 21DC, and cooled by a Minebea Motor Manufacturing Corporation 3110KL – 04W – B50 fan.

The detector remains stationary while the subject is placed on a stage which moves along only one axis, thus scanning the object. The speed of the stage is calculated based on the distance between the stage and the detector in order to ensure firstly that the pixels produced represent square sections of the object (i.e. there is no stretching or squashing effect produced) and secondly to ensure that no part of the object is missed by the scan, given that at set intervals a snapshot is taken in order to build up the hyperspectral data cube. The stage is moved by means of a motor pushing the stage along a screw. As the screw rotates, the stage is moved from one end to the other. The motor used to generate the movement of the stage is a Vexta PK264A2A – SG3.6 stepping motor controlled by a Velmex VXM stepping motor controller. All aspects of the setup were supplied by Headwall Photonics, including the light source and stepping motor.

As HSI gives values of reflectance, calibration is performed by giving the software an example of 100 % reflectance, and 0 % reflectance, these are the white and dark calibrations respectively. White calibration is carried out using a piece of Spectralon®^f, and dark calibration is performed by covering the lens with its lens cap.

^f Spectralon® is the brand name of a fluoropolymer material which has a very high diffuse reflectance (99 %) and reflects evenly across the UV-Vis-NIR range.

The room lights are off during calibration and scanning as the fluorescent lights produce unwanted lines in the scan, ideally the room would be in darkness so that any fluctuations in light intensity and thus reflectance values are eliminated. Equipment calibration (such as signal linearity and accuracy of the wavelength axis) are performed by Headwall prior to shipping. This experimental setup is shown below in *Figure 4.4*. During the scan the manuscript was supported when needed by manuscript grade archival book supports.



Figure 4.4. The HSI equipment during a scan of MS Arm. d13. For the purpose of taking this photo of the equipment the room lights have been left on, during a scan the room lights are always off.

4.2.4.2 Data processing

For processing the Hyperspectral data cube (post-acquisition) the software ENVI was used (version 5.3.1). The spot scanned by RS had been recorded by taking a picture using a USB microscope (Veho Discovery VMS-004 delux, 400x, 2 megapixels magnification) and using the ENVI region of interest tool an average spectrum was calculated from the pixels in the same area of the RS measurement. The RS measurement had a diameter of 30 μm thus analysing an area of 707 μm^2 (from area = $\pi \times r^2$) and the pixels of the HSI camera covered an area of ca. 78 – 130 μm wide (mean pixel size: 110 μm). The HSI pixel data was analysed using the spectral analyst feature in ENVI which compared, using SAM, SFF, and BE, the average spectrum for each region of interest with the spectra held in HSI reference libraries made by us. Each computational method produced a ranking where the highest score represents the closest match to the reference spectra. All rankings are between 0 and 1, the higher the score the closer the match for the spectra. The algorithms match the spectra in the database to the spectrum obtained during experimentation. Thus, if a relevant, trustworthy database is used a likely candidate for the identity of the pigment is given. It is worth noting that although a higher score does indicate a closer match, there are other factors that prevent this score from being used as a measure of confidence. Firstly multiple results can have the same score (they could not be discriminated), or a similar score (this may indicate a mixture). Secondly smaller separation between adjacent scores indicates a lower confidence in the similarity i.e. if the top two results have similar scores then there is a lower certainty that the spectra is correctly identified compared to if the top two had very dissimilar scores. Thirdly the process cannot identify a pigment that is not included in the database, in this instance a high score could be attributed to a similar (though

incorrect pigment). Because of these reasons the score was not used as a measure of confidence.

Using the software it was also possible to select the wavelength range over which the calculations (SAM, SFF, and BE) were performed and this was done in order to remove from the calculation either noise, or large components which were common to all scans, thus improving the agreement between the hyperspectral data and the Raman spectroscopy data. For example spectra tended to level out after 800 nm. These parts of the spectra also coincided with the noisy regions and so the wavelength range upon which the calculations were performed was reduced in order to focus on the areas which gave identifiable peaks or troughs in the data and eliminate areas which were similar in all spectra, thus aiding the computational differentiation process ('tailored wavelength range' in *Table 4.5*).

This reduction was made on a case by case basis in order to account for any variation in major peak positions between the different pigments, however it was found that this took a very long time as it had to be done manually. By way of comparison the computations were run again using the region between 400 and 800 nm each time to see if results could be improved upon without having to tailor the wavelength range to each individual spectrum ('400-800 nm' in *Table 4.5*).

The techniques are included in the software as standard as they have been used for the analysis of remote sensing data (SFF *Kokaly et al. (2003); van der Meer (2004); Pan et al. (2013)*, SAM {*Davies & Calvin (2017); Garg et al. (2017); Gürsoy & Kaya (2017)*, BE *Hadavand et al. (2016); Nidamanuri & Ramiya (2014); Singh & Ramakrishnan (2017)*). For the analysis of heritage based hyperspectral data only SAM appears to have been used previously *Catelli et al. (2017); Cucci et al. (2016); Wu et al. (2017)*.

4.2.4.3 Raman Spectroscopy

The Raman spectroscopy equipment used in this study has been developed specifically for the identification of pigments in objects of cultural heritage, and is unique *Beeby et al. (2016)*. It differs from commercial equipment primarily in that large manuscripts can fit under the detector in-situ and it is extremely portable. The device shown in *Figure 4.5* demonstrates the sensor is attached to a lightweight frame which allows the sensor to move along in one direction with movement in the other direction being achieved through repositioning of the frame. As per HSI the manuscript is supported, if needed by archival grade foam book supports.

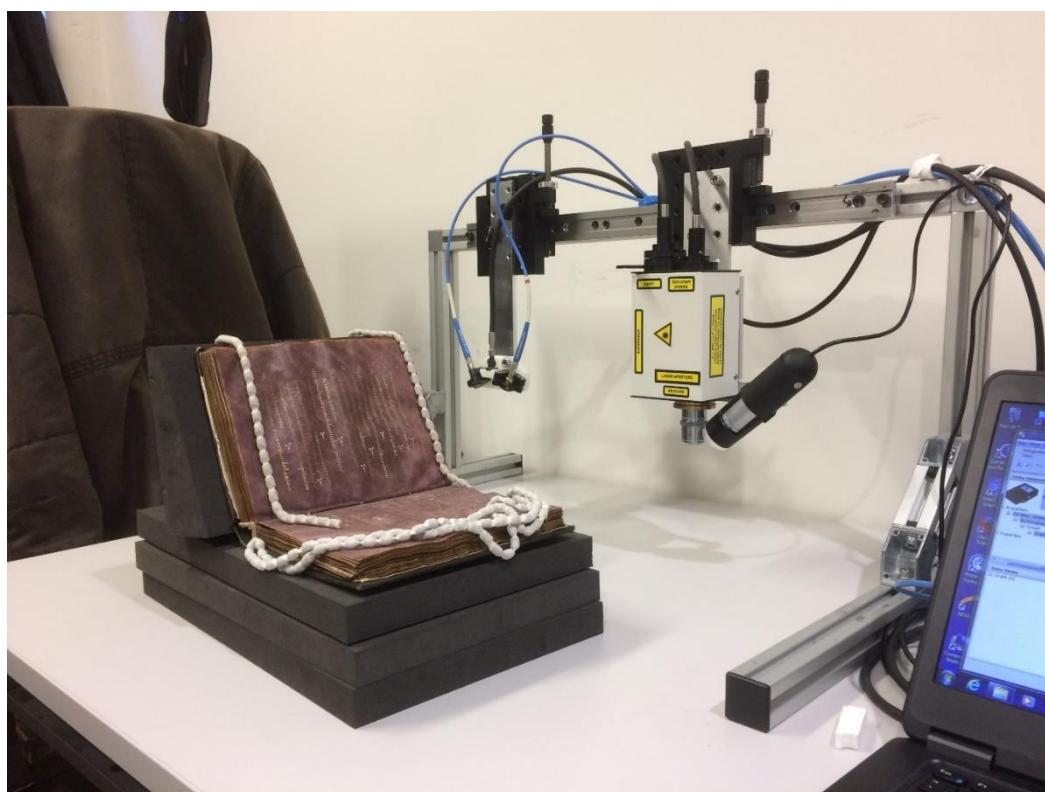


Figure 4.5. The Raman spectroscopy equipment used during the project

Light and dark calibration are performed and a reference sample is used to correct for any shift from true peak values. All Raman measurements require a blacked-out room to minimise interference for this very sensitive technique.

The spot size of each measurement is ca. 30 μm in diameter and a JDSU 1 mW HeNe laser source is used with a wavelength of 632.8 nm. The detector measures in the range of 2577.367 cm^{-1} – 91.14842 cm^{-1} and is a Andor Shamrock 163/iDus 416 camera CCD spectrograph with a Horiba Ltd Superhead sampling accessory. A USB microscope generates a live image on the laptop, stills of which are used to record the exact location of the laser spot measurement.

It may be useful at this point to directly compare the two techniques used during the study as summarised in *Table 4.3*. The advantages and disadvantages given concern the specific equipment used in this study. Differences in equipment specification may alter the usefulness of a technique for example if HSI which produced reflectance spectra further into the IR was used instead then the identification of pigments could be done more independently of a secondary technique.

	Raman spectroscopy	HSI
Analysed area	Spot size: 30 μm diameter	Pixel size 110 μm across
Analysis time by spot or surface unit	≈ 5 min	$\approx 0.33 \text{ mm s}^{-1}$
Irradiance	0.4 mW	$\approx 3.5 \text{ lux h}$
Identification	Identification can be made unequivocally through the use of characteristic peaks	Identification relies upon the comparison of reflectance spectra and must be backed up by another method of analysis
Coverage	Limited spots can be analysed in a reasonable time frame	Larger areas can be scanned in a reasonable time allowing the user to 'map' important features

Table 4.3. A Summary of key differences between HSI and Raman spectroscopy as used in this study.

4.3 Results

Table 4.4 shows the distribution of the Raman spectroscopy analysis across the 6 manuscripts and the pigments which were identified using Raman spectroscopy. These results are taken as correct and were compared to the results generated by the characterisation of reflectance spectra from hyperspectral data cubes by way of the three computational algorithms designed to compare experimental spectra to those in a database. Five Such databases were used as detailed above in Section 4.2.2. If the

algorithm identified the same pigment as Raman spectroscopy then it was considered correct, in this way a percentage success was derived for each configuration.

Shelf mark	Pigments identified through Raman spectroscopy						Total
	Red lead	red lead + vermilion	lapis	indigo + orpiment	vermillio n	indigo	
MS Arm g4	1	1	3	0	2	0	7
MS Arm e34	1	0	5	0	2	0	8
MS Arm d3	0	0	0	0	0	5	5
MS Arm d22	0	1	0	0	1	2	4
MS Arm c3	0	0	2	0	3	2	7
MS Arm d13	1	0	0	1	56	1	59
Total	3	2	10	1	64	10	90

Table 4.4. The results of the Raman spectroscopy survey showing the distribution of inspection points across the manuscripts involved in the study. Not all manuscripts had the same number of illuminations (MS Arm d13 was particularly lavishly decorated). Note the chemical formulas and common names; red lead (Pb_3O_4 , minium), vermilion (HgS , cinnabar), lapis lazuli (S_3 , ultramarine (differentiation between synthetic (ultramarine), and natural (lapis) not possible with this Raman setup), orpiment (As_2S_3), indigo ($C_{16}H_{10}N_2O_2$).

Table 4.5 shows the percentage success of the 3 algorithms with the 5 databases applied to all the manuscripts. The settings and parameters of the algorithms could be manipulated to increase the likelihood of a match by way of eliminating noise or focussing on characteristics of the spectra, and this was also done. *Table 4.6* gives the results of the analysis carried out using default settings broken down into the different manuscripts.

Database	Algorithm	Default settings	Tailored wavelength range	400 – 800 nm	Difference (400 – 800 and default)	Difference (tailored and default)	Difference (tailored and 400 – 800)
1	SFF	20	66	22	2	46	44
1	SAM	9	47	15	7	38	32
1	BE	13	67	16	3	54	51
2	SFF	71	89	71	0	18	18
2	SAM	49	89	49	0	40	40
2	BE	37	93	37	0	56	56
3	SFF	60	89	42	-18	29	47
3	SAM	23	81	33	10	58	48
3	BE	22	92	19	-3	70	73
4	SFF	27	81	26	-1	54	55
4	SAM	14	66	16	2	52	49
4	BE	18	65	30	12	47	35
5	SFF	43	89	47	4	46	42
5	SAM	44	87	43	-1	43	44
5	BE	44	84	48	4	40	35
Sample size		91 (73 for databases 2 and 3)	91 (73 for databases 2 and 3)	91 (73 for databases 2 and 3)			

Table 4.5. A comparison of the percentage agreement obtained using the different methods, databases, and wavelength ranges. The difference between 400 – 800 and default was calculated as the percentage success of the 400 – 800 nm range minus the percentage success of the default wavelength range, similarly Difference (tailored and default) was %tailored - %default and difference (tailored and 400-800) was %tailored - %400 – 800.

As can be seen the majority of pigment regions identified were vermilion: this is because Raman spectroscopy very easily identifies this pigment but also because the Armenian manuscripts analysed here are very red in colour, so vermilion is probably the most prolific pigment throughout the manuscripts. It can also be seen from *Table 4.5* that the majority of pigments were taken from MS Arm d13. This is because there were so many illuminations in this manuscript compared to the others, thus it provided a wealth of experimental material.

Focussing on results from Database 1 (*Table 4.5*) we can see that using the algorithms on a “tailored” wavelength range increased the accuracy of reflectance spectra identification by 38 – 54 %. The best algorithm in this case was the most simple algorithm, binary encoding (67 % success) when used over a tailored wavelength range. SAM was the worst algorithm if applied with the default settings (9 % success). This is true, on the whole, for all the databases with the best percentage success being for Database 2, BE, Tailored wavelengths (93 % success), and the worst being 9 % as above. Spectral feature fitting (SFF) scored higher than spectral angle mapping (SAM) in most cases and is also the one most likely to be correct under default settings which suggests that SFF deserves more consideration when analysing hyperspectral data, presently SAM is the more utilised algorithm.

Database 2 provided the most matches under all parameters: we can also see that Database 5 provided more than Database 4. These results lead us to believe that the database most likely to produce a correct characterisation is one which contains spectra obtained from material matching the experimental material as closely as possible (same binder, same age paper, same age pigments etc.) and containing only the most relevant spectra i.e. a database can be too large for the application.

Table 4.6 shows us the results for all 3 algorithms applied to all 6 manuscripts, but only for the default wavelength range. Here we see as before that on the whole BE was the least successful whilst used across the full wavelength range available. This trend is expected because binary encoding would only really work on data in which the peak is the main feature. In this data that is not the case however as noted above it does improve when the algorithm is focussed on a smaller wavelength range. This too is expected from BE because the main absorption feature would be focussed upon becoming a larger factor in the algorithms' final result. As before we see that SFF is commonly the most successful for the full wavelength range. It has achieved 100 % in places but it is to be noted that these datasets are rather small on their own. On the largest dataset, that of MS Arm d13, SFF still outperformed the others, but was far from achieving perfection. It is interesting then that SAM has become the more popular algorithm.

Database	Algorithm	Total	MS Arm e34	MS Arm d13	MS Arm d3	MS Arm g4	MS Arm d22	MS Arm c3
1	SFF	20	38	10	100	0	50	29
1	SAM	9	35	7	20	0	0	14
1	BE	13	13	9	20	0	50	43
2	SFF	71	n/a	68	100	n/a	50	100
2	SAM	49	n/a	45	60	n/a	50	86
2	BE	37	n/a	34	80	n/a	0	57
3	SFF	60	n/a	55	100	n/a	50	86
3	SAM	23	n/a	13	60	n/a	50	71
3	BE	22	n/a	13	80	n/a	25	57
4	SFF	27	38	32	0	0	0	43
4	SAM	14	13	20	0	0	0	0
4	BE	18	0	27	0	0	0	0
5	SFF	43	38	49	0	43	25	43
5	SAM	44	38	47	80	29	25	29
5	BE	44	25	44	80	14	50	71
Sample size		91 (73 for databases 2 and 3)	8	59 (56 for Databases 2 and 3)	5	7	4	7

Table 4.6. Showing the percentage success of the databases and algorithms with the default wavelength range used separated out into the different manuscripts' results. The difference in sample sizes is due to databases 2 and 3 not being used on some folios from MS Arm D13, MS Arm e34, and MS Arm g4, this is discussed in the text.

It is interesting to note from *Table 4.6* that seemingly the most difficult manuscript to obtain high percentage results from is MS Arm g4, one of the later manuscripts. It should be remembered though that the best databases (as before Databases 2, and 3 outperformed the others) could not be used on the ROIs from this manuscript because it was from these ROIs that the databases were formed, and this perhaps has created challenges. It would be interesting to obtain more ROIs for MS Arm g4, and MS Arm e34 for application of Databases 2, and 3 to these manuscripts. No manuscript consistently provided a greater percentage accuracy than others.

4.3.1 Confusion matrices

The data was further analysed through the use of confusion matrices, allowing the calculation of the statistical values recall, precision, accuracy, and f-measure. This was done for the identification of the pigment vermilion, as it was the most prevalent pigment in the selection of illuminations. Two setups were analysed in this manner, the setup that lead to the lowest accuracy result (*Table 4.7*), and the setup that lead to the highest accuracy result (*Table 4.8*).

Worst				
Database 1	Default settings			
For vermillion as identified by Raman spectroscopy				
		Actual values		
		Positive (is vermillion)	Negative (is not vermillion)	Total
Characterised by HSI (SAM)	Positive (identified as vermillion)	4	0	4
Predicted values	Negative (not identified as vermillion)	58	26	84
	Total	62	26	88
	Recall	0.07		
	Precision	1		
	Accuracy	0.34		
	F-measure	0.12		

Table 4.7. Confusion matrix for the lowest scoring combination of settings, algorithm, and database. Default settings, SAM, and database 1.

Best				
Database 2	Tailored wavelength range			
For vermillion as identified by Raman spectroscopy				
		Actual values		
		Positive (is vermillion)	Negative (is not vermillion)	Total
Characterised by HSI (BE)	Positive (identified as vermillion)	57	0	57
Predicted values	Negative (not identified as vermillion)	3	6	9
	Total	60	6	66
	Recall	0.95		
	Precision	1		
	Accuracy	0.95		
	F-measure	0.97		

Table 4.8. Confusion matrix for the highest scoring combination of settings, algorithm, and database. Tailored wavelength range, BE, and database 2.

The values for accuracy for the pigment vermillion are 34 % and 95 % for the worst, and best setups respectively comparable to 9 % and 93 % overall indicating that the inclusion of other pigments into the calculations reduced the accuracy overall. Both setups have a calculated precision of 100 % meaning that if a pigment were identified as vermillion by the analysis of the hyperspectral data, it was never wrong in this

experiment. The recall value is a measure of how many pigments that actually were vermilion correctly identified as such and this is increased from 7 % to 95 % by the change in setup. Finally, the f-measure is a means of combining the recall and precision values to give a means of comparing two data sets and this value is increased from 0.12, to 0.97 for the change in setup.

4.4 Discussion and conclusions

In this paper, the ability of HSI to identify pigments based on their reflectance spectra (400 – 1000 nm) has been assessed. Results were compared directly with Raman spectroscopy and for the first time an attempt was made to provide a percentage accuracy for the use of HSI in this application. This percentage accuracy was found to vary between 9 % and 93 % in total dependent upon the configuration of the algorithms applied to the data and the database used for characterisation.

Taking the identification of pigments by Raman spectroscopy to be “true” and modelling this use of HSI as a test for the pigment vermilion identified by RS, confusion matrices were constructed that revealed the precision of the technique to be 1 in the best case scenario. The “HSI test” for vermilion was 95 % accurate, had a recall value of 0.95, and an f-measure of 0.97.

The best use of the algorithms required a great deal of manipulation of algorithm parameters, thus lending itself not to identification, but to mapping known pigments. The database most likely to provide a high percentage accuracy was one that was as close as possible to the pigments studied, and contained only relevant spectra. Databases 2, and 3 were consistently high performers, interestingly their data was taken from the most recent manuscripts.

This data highlights some pigment knowledge is needed to be certain that HSI is correctly characterising data, and that best practice would be to use techniques such as Raman spectroscopy to identify pigments, and HSI to map the pigments across the surface of the manuscript, or conversely for the mapping of areas of interest prior to spot analysis techniques. Therefore, based on this research, HSI should not be used exclusively to give an overview of pigments but should be used in conjunction with other techniques.

Other studies have used HSI successfully to identify pigments but they have always applied another technique to aid the identification, and occasionally a larger wavelength detection range has been used, detecting longer IR wavelengths *Aceto et al. (2014)*; *Delaney et al. (2016a)*. This study confirms that the visible wavelength range is not enough for a characterisation but it does offer hope that using hyperspectral data to map pigments can be accurate if used in conjunction with other techniques, which is our major recommendation. One such pigment map is given below in *Figure 4.6*.



Figure 4.6. Showing the map of vermillion pigment across MS Arm e34, folio 4r using SAM.

From this research HSI appears to not be as accurate for pigment analysis as Raman spectroscopy on a point by point basis but on the other hand HSI is vastly quicker at scanning a large area: we therefore recommend the use of the two processes together if a full quantification of the surface is required, with Raman for identification of pigments, and HSI to map, confirm similarity over a large area, or to identify areas for point analysis as has been done in the past *Daniel et al. (2016)*; *Mounier & Daniel*

(2015). For HSI the accuracy of pigment identification could be improved by increasing the range of wavelengths scanned and by way of a more relevant database, again this would require the use of additional techniques such as Raman spectroscopy, suggesting that the best results are obtained firstly by making sure that the techniques at hand are used for purposes suiting their limitations, and secondly that a combination of techniques will yield superior results in a more efficient timescale. In general HSI could also benefit from greater spatial resolution and increased ease of use if it were to be used more frequently in a heritage environment.

A possibility for extending the study further would be to investigate and compare the accuracy and efficiency of other techniques (FTIR for example) and more work could be done with the SFF algorithm which gave a higher percentage accuracy here than the more popular SAM algorithm. This was expected for the reflectance data produced. SFF is designed to work best on absorption features such as those seen. It is perhaps surprising that SAM performed so poorly given its popularity but this could be explained by a lack of spectral features in general and the fact that the default settings in this software would be geared towards remote sensing data. Binary encoding did better than SAM, and this is perhaps because the simplistic algorithm did not require much adjustment.

Only one wavelength was used for the excitation laser for Raman spectroscopy, 635 nm. Previous studies *Marucci et al. (2018)*; *Mulholland et al. (2017)*; *Stanzani et al. (2016)* have shown that different lasers may increase the identifiable range of pigments, with 532 and 785 nm being other commonly used wavelengths. 785 nm has proven to be the most effective at pigment identification but requires an increase in the applied power *Marucci et al. (2018)*; *Mulholland et al. (2017)*; *Stanzani et al. (2016)* (to achieve good S/N ratios) which can cause damage to the object of analysis

Mulholland et al. (2017). 532 nm has been shown to be better than 635 nm only for the identification of blue pigments *Marucci et al. (2018)*; *Mulholland et al. (2017)* but in general suffers from increased fluorescence *Stanzani et al. (2016)*. It is therefore possible that the use of an excitation laser with a wavelength of 785 nm would identify more pigments, but it may also require the application of more power than we are comfortable with for valuable historic documents. 532 nm would be the logical one to try but could be of limited use because it is not as good all round and the manuscripts are predominantly red. The study compares HSI to Raman, if more pigments were found with Raman then more comparisons could be made, this would obviously have an effect on the end result, though it is difficult to predict how. In a similar vein a study incorporating manuscripts from of a more varied origin would expand the study in terms of pigments analysed (Armenian artists used lapis lazuli more prolifically than others for example) but on the whole the study results reflect the dynamic between two techniques and is applicable to other investigations, especially considering similar situations have been shown in the literature.

HSI has a great potential to be useful in the analysis of pigments. The database used was shown to be the most important single factor in increasing the match and a larger quantity of spectra but a smaller more focused number of pigments i.e. ones relevant to the object of study in terms of its chemical composition gives the best results. Caution must be used however, and a combination of analytical techniques is required to properly characterise a pigment and 93 % was only possible with prior knowledge of the target pigment. Using default settings, the percentage accuracy was not sufficient.

When studying such documents HSI is a great advantage, it is a non-destructive technique which is capable of efficiently mapping the entire surface of an object. When

a combination of techniques is used the setup can be a very powerful investigative tool and we recommend using HSI as a mapping tool prior to other techniques, or after them to give a complete picture of the pigment distribution. On a point by point basis however, point techniques such as RS offer clear advantages.

Chapter 5 experiment 2: Digital restoration using visible and near infrared hyperspectral imaging (VNIR HSI): An investigation into the pigmentation on the west wall of the Shrine of Taharqa

This is reproduced from the manuscript submitted for review by the Journal of the American Institute for Conservation. This journal was chosen because of its interest in the presentation of multidisciplinary research for the conservation and exploitation of cultural heritage. This manuscript was of interest to the journal but revisions were suggested.

Ian J. Maybury^a, David Howell^b, Melissa Terras^c, Heather Viles^d

- a. Corresponding author: ian.maybury@stx.ox.ac.uk, School of Geography and the Environment, University of Oxford, South Parks Road, Oxford, England, OX1 3QY
- b. david.howell@bodleian.ox.ac.uk, Weston Library, Bodleian Libraries, University of Oxford, Broad Street, Oxford, England, OX1 3BG
- c. m.terras@ed.ac.uk, College of Arts, Humanities and Social Sciences, University of Edinburgh, Scotland
- d. heather.viles@ouce.ox.ac.uk, School of Geography and the Environment, University of Oxford, South Parks Road, Oxford, England, OX1 3QY

5.0 Abstract

Historians, Museum curators and heritage site managers are interested in identifying faded pigmentation on Ancient statues and structures. We investigate the contribution visible and near infrared hyperspectral imaging (VNIR HSI) can make to this process, focussing on the Ancient Egyptian Shrine of Taharqa (dating from ca 684 BCE) in the Ashmolean Museum, University of Oxford. We use VNIR HSI and portable X-ray fluorescence (pXRF), both non-destructive, non-contact, imaging techniques, to investigate faded remnants of pigmentation on the west wall of the shrine. We complement this investigation with results from previous studies on the wall, whose original samples and results were available to us.

The results demonstrate the need for multiple techniques. VNIR HSI allowed us to map the red pigmentation, whilst XRF and photo-induced luminescence (PIL) from a previous study, were used to detect copper-based Egyptian blue pigmentation. Results from previous microscopy provided us with a fuller colour palette. We demonstrate that a conjunction of these different methods allows us to suggest a portion of the original colour scheme of the wall, which differs greatly from the faded patches visible today. We show that non-contact imaging techniques such as VNIR HSI provide data that can be used to detect and visualise faded pigments across the surface of Ancient statuary not easily visible to the naked eye, but there are limitations to this approach. We therefore demonstrate that hyperspectral imaging is a useful additional tool for the analysis of statuary pigmentation, but needs to be used in conjunction with other analytical methods and art historical expertise in order to reconstruct probable original colours, which will be of interest to those wishing to investigate the polychromy of other Ancient statuary. Our combined analysis allows us to synthesise a probable original colour scheme of the

west wall of the Shrine of Taharqa, which will be of use to the museum, but also for scholars of Ancient Egyptian art and sculpture.

5.0.1 Keywords: Hyperspectral imaging, XRF, photo-induced luminescence, SEM-EDX, Egyptian art

5.1 Introduction

1.1 The digital restoration of artwork

It is well known in art historical and archaeological circles that Ancient statuary was often painted *Bradley (2009); Gasanova et al. (2018)*, in particular colour was of significance to Ancient Egyptian sculpture *Hägele (2013)*, and that investigation into this colour can provide valuable information for researchers *Gasanova et al. (2018)*. Whilst apparent to researchers, it is clear through the response to exhibits and news articles, that public awareness of the coloured nature of statuary is limited *Bradley (2009); Kopczynski et al. (2017)*. Investigation into polychrome statuary is considered to be a multidisciplinary field which has burgeoned over the last twenty years, owing to the development of non-destructive testing methodology with this purpose in mind *Brecoulaki (2019)*. While some reconstructions utilise only the remaining traces of pigmentation, and conservation techniques such as cleaning to reveal them, a great deal more information can be obtained through scientific investigation *Bradley (2009)*. Indeed techniques such as XRF, Raman spectroscopy, FTIR, and imaging spectroscopy have all been used with success *Gasanova et al. (2018)*. This study demonstrates the abilities of visible and near infrared hyperspectral imaging (VNIR HSI) as an aid to colour restoration.

5.1.1 The shrine of King Taharqa

Taharqa was pharaoh of the Twenty-fifth Dynasty of Egypt and qore of the Kingdom of Kush between 690-664 BCE *Kitchen (1996); The Ashmolean Museum (2015)*. During his reign (ca. 684 BCE *Anon (1992); Hanna & Norman (1990)*) he instructed that a shrine be built to honour the sun and fertility god Amun-Re. The shrine was abandoned around the 3rd century BCE after being attacked and burned *Kirwan (1936)*. It was

rediscovered (buried in sand) by the Egyptologist Francis Llewellyn Griffith in Kawa, modern day Sudan in 1930 *Armstrong (2015); Kirwan (1936); The Ashmolean Museum (2015)*. The shrine is made of 236 blocks of sandstone and is approximately 4 x 4 x 3 m in size *The Ashmolean Museum (2015)*. It has decorated figures and hieroglyphs carved in raised relief and is thought to originally have been covered in bright colours *The Ashmolean Museum (2015)*. Only the main decorated blocks of the original 4 walls were transported to the University of Oxford in 1936 *Hanna & Norman (1990)*, the rest being left behind *Macadam (1949)*, and the shrine was reconstructed in its current position in the Ashmolean Museum soon afterwards. It is the largest pharaonic structure in the UK.

Upon excavation, the original pigmentation on the shrine was very faded *Leeds (1942); Macadam (1949)*. Today the shrine appears to the viewer as unpainted carved relief. Our aim is to investigate which methods are best to detect any remaining pigmentation, to create a reconstruction of the likely original pigmentation, which the Ashmolean Museum intends to use to produce a new lighting display which, using a projector, will superimpose an artist's impression of the original palette onto the shrine in situ. The investigation focussed on the west wall because it has undergone analysis previously (in 1990, and 2015), and has a few traces of visible pigment remaining, and was thus a good candidate for further investigation.

The shrine has endured various conservation treatments. In 1936 it was soaked in cellulose nitrate mixed with amyl acetate and acetone for the move but by 1968 this was discoloured and cracking *Hanna & Norman (1990)* so it was removed and replaced with paraffin wax on 3 walls (the paint on the 4th wall (the west wall) was too fragile). This coating suffered the same fate as the original and by 1983 serious loss of paint and discolouration were observed *Hanna & Norman (1990)*. This led to a study in 1990

Hanna & Norman (1990) to remove the coatings from all four walls and reattach the flaking paint *Hanna & Norman (1990)*. Samples were taken from the west wall at the time of the 1990 study which were analysed to determine the colour palette of the shrine. One other study was carried out on the Shrine: photo induced luminescence (PIL) was carried out on numerous artefacts in the Ashmolean Museum, University of Oxford, in 2015 and the results on the west wall of the Shrine suggest the location of the fluorescent pigment Egyptian blue *Armstrong (2015)*. Results of these previous studies (1990, and 2015) are detailed below in sections 5.3.2.1 and 5.3.2.2. The previous research involved physical sample analysis and photo-induced luminescence (PIL), however, the study detailed here provides an opportunity to demonstrate how VNIR HSI can contribute to the field of digital conservation.

Research aim

This research aims to establish how VNIR hyperspectral imaging can be used as part of a suite of non-destructive analytical techniques such as pXRF and PIL, to analyse the remaining pigmentation on faded works of Ancient statuary and to further understand their original presentation. We aim to demonstrate how the results compare to those from micro-destructive sampling-based techniques. Can our non-destructive tests reveal how the image may have looked when new?

5.2 Theory

5.2.1 The digital recolouring of faded artworks

It is well known that artwork is fugitive *Brommelle (1964); Giles (1965); Moussa & Ali (2013)* and it is an obvious extension of that fact that art historians wish to know the original nature and appearance of artwork *Inglis-Arkell (2019); Prisco (2017)*. The digital restoration of artwork is effective and practical *Ando et al. (1997)* while avoiding the ethical conflict inherent in physically reconstructing art *Maynard (1975)*. Commonly, an analytical approach utilising multiple techniques is used to identify faded pigmentation *Abdrabou et al. (2018)* for example with XRF *Kopczynski et al. (2017)*, various imaging techniques, and microscopy *Gasanova et al. (2018)* often used together. It can be successfully installed within a museum setting for example a painted reconstruction of the Prima Porta Augustus *Bradley (2009)*. Digital reconstruction can be automated *Woolfe et al. (1998)*, and carried out in simple programs such as Photoshop *Fieberg et al. (2017)*. Other notable examples include the wall paintings at Mogao Grottoes, N.W. China where the Dunhuang Academy utilises image processing and other tools to help with conservation efforts *Li et al. (2000a), (b)*. Investigations into the polychromatic pigmentation of Ancient statuary have led to a tour of fully coloured reconstructions *BBC (2019); Prisco (2017)*, though the public's reaction to them was mixed *Artforum (2019); Inglis-Arkell (2019)*. Concerns over “methodological rigour” lead to the creation of the London Charter in 2006 in order to aid the reliability and transparency of computer based visualisation *Denard (2009)*. In the context of the Shrine of Taharqa, the original pigmentation of the shrine should be investigated and a suitable means of displaying the results identified in order to enlighten and educate museum visitors about the original appearance of the shrine.

5.2.2 Identifying pigments on Ancient Egyptian art from the XXVth dynasty

The pigmentation of multiple artefacts from Ancient Egypt has already been studied, most commonly using microscopy and XRF/XRD, combined with other methods (Fourier transform infrared (FTIR), Fibre optic reflectance spectroscopy (FORS), imaging) *Abdrabou et al. (2017), (2018); Berry (1999); Bracci et al. (2015); Fulcher (2017); Hallmann (2015); Lau et al. (2008a); Lynch et al. (2007)*. Such studies usually involve micro-destructive sampling. Lau et al sought to characterise green copper phase pigments in Egyptian artefacts but were unable to use Raman spectroscopy as fluorescence was too problematic *Lau et al. (2008a)*. Fluorescence is a problem for all visible light techniques but is particularly problematic for Raman spectroscopy because the high intensity light source needed due to Raman scattering being a weak effect causes even minor contaminants to produce large fluorescent signals *Smith & Dent (2008)*. Furthermore fluorescence occurs at lower energies than excitation, interfering strongly with the area covered by Stokes Raman scattering *Smith & Dent (2008)*. Common pigments found were Egyptian blue, carbon black, and red and yellow iron oxides *Abdrabou et al. (2017), (2018); Ambers (2004); Berry (1999); Edwards et al. (2004); Fulcher (2017), (2018); Lau et al. (2008a); Lynch et al. (2007); Nicholson & Shaw (2000)*. Artefacts studied include coffins *Abdrabou et al. (2017); Bracci et al. (2015); Lau et al. (2008a); Lynch et al. (2007)*, shrines *Berry (1999); Fulcher (2017), (2018)*, wooden statues *Abdrabou et al. (2018)*, and stelae *Hallmann (2015)*.

In terms of the pigments expected on the Shrine of Taharqa Egyptian blue is perhaps the easiest to detect due to its fluorescence *Dyer & Sotiropoulou (2017)*. Raman spectroscopy can be used *Dyer & Sotiropoulou (2017); Janssens et al. (2016a)*, but

fluorescence can cause problems *Lau et al. (2008b)*. Scanning techniques are used if there is concern that sampling may not be representative *Janssens et al. (2016a)*. Generally speaking NDT (Non-destructive testing) is preferred *Dooley et al. (2014)*; *Janssens et al. (2016a)*; *Lau et al. (2008a)*; *Scott & Swartz Dodd (2002)*, but in some cases cannot provide the desired information *Dyer & Sotiropoulou (2017)*; *Moussa & Ali (2013)*.

During the investigation both VNIR HSI and pXRF were used to analyse the surface of the west wall, these techniques worked well together with each technique informing us about different pigmentation. A brief comparison of the techniques is given in *Table 5.1*.

	VNIR HSI	pXRF
Detection range	400 - 1000 nm (visible light with very small amounts of UV and IR)	Monitors the interaction of X-rays with matter
Data returned	Reflectance spectra for every pixel in the image (250 µm across)	Elemental composition of subject (Mg or heavier elements)

Table 5.1. A brief comparison of the main study methods.

It was hoped that the elemental analysis provided by pXRF would provide us with insight into the chemical composition of the pigmentation once applied to the stone. For example, Cu could imply the presence of Egyptian blue. This is standard practice for the application of pXRF to the evaluation of pigmentation *Chaplin et al. (2010)*; *Magkanas et al. (2021)*. Pigments in common use in Ancient Egypt *Edwards et*

al. (2004); Fulcher (2017); Scott (2016) and their molecular formulas are given in Table 5.2.

Pigment	Colour (if a pigment)	Molecular formula
Egyptian blue	Blue	$\text{CaCuSi}_4\text{O}_{16}$
Haematite	Red	Fe_2O_3
Kaolin	White	$\text{Al}_2\text{Si}_2\text{O}_5(\text{OH})_4$
Ground white	White	CaSO_4
Egyptian green	Green	CaSiO_3
Orpiment	Yellow	As_2S_3
Realgar	Orange	As_4S_4
Quartz	Not a pigment	SiO_2
Feldspars	Not a pigment	KAlSi_3O_8 - $\text{NaAlSi}_3\text{O}_8$ - $\text{CaAl}_2\text{Si}_2\text{O}_8$
Calcite	Not a pigment	CaCO_3
Matrix	Not a pigment	Si, Fe, CaCO_3
Clay	Not a pigment	FeO, MgO, AlO, kaolin, Mn, Mg, Ni, Fe
Desert varnish	Not a pigment	Mn/Fe oxides + clay

Table 5.2. Pigments from Ancient Egypt and their molecular formulas. Also included are some components of sandstone. Desert varnish thickens and darkens with age becoming black Dietzel et al. (2008); Macholdt et al. (2018); Wang et al. (2018), it is not an original component of sandstone.

5.2.3 Analytical methods

Analytical methods are nowadays frequently used to aid conservation work *Bacci (1995); Liang (2012)* and are used to characterise and identify components *Delaney et al. (2016a); Pallipurath et al. (2014); Ricciardi et al. (2009)*, monitor and report on the artefact (*Ricciardi et al. 2009; Clark 2002*), reveal hidden information *Delaney et al. (2016a); Ricciardi et al. (2009); Snijders et al. (2016)*, determine provenance *Burgio et al. (2005); Clark (2002); Delaney et al. (2016b); Douma n.d.; Liang et al. (2011); Pallipurath et al. (2014); Ricciardi et al. (2009)*, and provide information about the artist and their technology *Coupry et al. (1994); Douma n.d.; Royal Society of Chemistry (2020)*. This information is worthwhile to researchers and assists effective conservation strategies *Clark (2002); Zhao et al. (2008)*. Analytical methods can be classed as non-destructive testing (NDT) methods, which can be point based or full field methods, or sampling-based methods.

NDT methods offer a clear advantage for conservators whose primary concern is the maintenance of artwork *Creagh et al. (2017); Hum-Hartley (1978)*. NDT can be used with fewer restrictions because of this, thus more tests can be run and a more representative view can be given *Amat et al. (2013)*. Sampling methods are of course invasive, however, modern sampling techniques require so little material that the sampling can be done without visually impairing the artwork whilst still providing considerable data *Aceto et al. (2014)*. Their use is nonetheless restricted and may not provide an accurate representation of the full work of art *Ricciardi et al. (2009)* though it is worth mentioning that point based techniques would obviously share this concern to some extent. The obvious advantage of full field NDT methods, therefore, is the provision of a full representation of the inhomogeneity of works of art.

5.2.3.1 HSI

Hyperspectral imaging illuminates a subject with a white light source and for each pixel in an image detects the reflectance spectra produced *Liang (2012)*. This can be used to characterise and map the colours in the image *Delaney et al. (2016b); Janssens et al. (2016b); Moutsatsou & Alexopoulou (2014)* and is capable of detecting things outside the visible spectral range provided the right wavelength range is detected for the chemical that is being looked for *Cucci et al. (2015); Liang (2012)*. Originally a remote sensing technique *Cucci et al. (2015)* it has been developed over the years for many applications *Maybury et al. (2018)*, more recently for the non-destructive investigation of works of cultural heritage *Attas et al. (2003); Balas et al. (2003); Daniel et al. (2016); Delaney et al. (2010b), (2016b); Fischer & Kakoulli (2006); Moutsatsou & Alexopoulou (2014); Schlamm & Messinger (2010)* notably the Declaration of Independence *France (2011)* where alterations to text were revealed, and Edvard Munch's "The Scream" where pigments were characterised and mapped *Deborah et al. (2014)*.

HSI is often used in conjunction with other techniques such as Raman spectroscopy *Daniel et al. (2016); Mounier & Daniel (2015)*, XRF *Catelli et al. (2017); Rebollo et al. (2013)*, and FORS *Melo et al. (2016)* to give a more detailed analysis *Aceto et al. (2014); Clarke (2001); Ricciardi et al. (2013); Trumpy et al. (2015)*.

Working with a combination of techniques allows for the best results to be generated, for example FORS has been used to characterise colourants on illuminated manuscripts, and as a preliminary technique backed up by Raman spectroscopy and XRF *Aceto et al. (2014)*. It has been shown that VNIR HSI can aid with the mapping of pigments, however, techniques such as Raman spectroscopy are needed to definitively identify a pigment *Maybury et al. (2018)*, and K. Melessanaki et al used laser induced breakdown

spectroscopy (LIBS) to identify pigments that were then mapped by VNIR HSI *Melessanaki et al. (2001)*.

VNIR HSI data can be used to generate false colour images using data both inside and outside of the visual light range *Hayem-Ghez et al. (2015)*. These images help the user to see hidden details and can also be used to differentiate between colours that look the same in the visible range but have different spectral signatures in regions of the spectrum that VNIR HSI can detect *Mulholland et al. (2017)*.

The differentiation of two colourants which are similar visually but chemically distinct by HSI has been demonstrated (*Aceto et al. 2014; Balas et al. 2003; Montagner et al. 2016; Centeno 2015; Vitorino et al. 2014; Martinez et al. 2002*) and while VNIR HSI has been used for the detection of anachronistic pigments it was noted that the results would only become robust by inclusion of infrared reflectance spectra *Polak et al. (2017)*.

Doubts about the ability of VNIR HSI to identify a pigment definitively have been raised due to the complications of mixtures or degraded pigments *Liang (2012)* and the ability of the present algorithms to take advantage of increasing information *Liang (2012); Zhao et al. (2008)*. However, VNIR HSI has been shown to successfully differentiate between colourants that other techniques find difficult to separate *Vitorino et al. (2015)*. VNIR HSI has been used to discriminate between madder, cochineal, and brazilwood however the addition of binding media etc. made it more ambiguous *Vitorino et al. (2015)* and a more comprehensive database was needed *Vitorino et al. (2015)*.

In this study spectral angle mapping (SAM) is used to process the hyperspectral data. Briefly, SAM treats each spectrum as a vector and calculates the angle between two spectra, thus determining spectral similarity. Smaller angles represent better

matches and the technique is relatively insensitive to illumination effects *Harris Geospatial Solutions, Inc. (2020h); Kruse et al. (1993)*. SAM was developed for remote sensing data, but has also been used for the analysis of cultural heritage data *Catelli et al. (2017); Cucci et al. (2016); Maybury et al. (2018); Wu et al. (2017)*.

5.3 Materials and methods

5.3.1 Equipment (primary data collection)

5.3.1.1 HSI

The hyperspectral camera used was a Headwall Photonics VNIR 1003B – 10147 which detects 972 contiguous wavelengths from 400 nm to 1000 nm and has a spectral resolution of 0.64 nm. The lens used is a Schneider XNP 1.4/17 – 0303 with a headwall ACOBL – 380 – 49X, 075 filter. The light source is a halogen bulb controlled by a Techniquip 21DC, and cooled by a Minebea Motor Manufacturing Corporation 3110KL – 04W – B50 fan. The stepping motor (used to produce the motion of the stage in the equipment's line-scanning setup but in this instance to move the camera) is a Vexta PK264A2A – SG3.6 controlled by a Velmex VXM stepping motor controller. All aspects of the setup were supplied by Headwall Photonics, including the light source and stepping motor. The output of the light source is sufficient for scanning but is not expected to cause significant colour change in the subject. The light source of the HSI equipment will output power equivalent to 3.5 hours exposure under museum conditions (50 lux) during a typical scan.

As HSI gives values of reflectance, calibration is performed by giving the software an example of 100 % reflectance, and 0 % reflectance, these are the white and dark calibrations respectively. White calibration is carried out using a piece of Spectralon®, and dark calibration is performed by covering the lens with its lens cap. Equipment calibration (such as signal linearity and accuracy of the wavelength axis) are performed by Headwall prior to shipping. The room lights are off during calibration and scanning as the fluorescent lights produce unwanted lines in the scan. Ideally the room would be in darkness so that any fluctuations in light intensity and reflectance values

are eliminated. In this case overhead lighting was turned off but some light pollution was unavoidable due to physical constraints. See section 5.3.1.2 Light pollution

The spatial resolution depends on the distance between the detector and the subject which can be adjusted at the operator's discretion. For this investigation, the equipment was set up to scan an area roughly 30 x 70 cm, giving a pixel size of approx. 250 μm . It is a line scanning method, and there are 1600 pixels per line scanned.

The light source and detector are mounted perpendicular to the axis of movement of a stepping motor such that the stationary vertical object is within the field of view and illuminated. They move together relative to the object to ensure constant illumination, the light source and detector move in synchrony relative to the object as shown below in *Figure 5.1*.

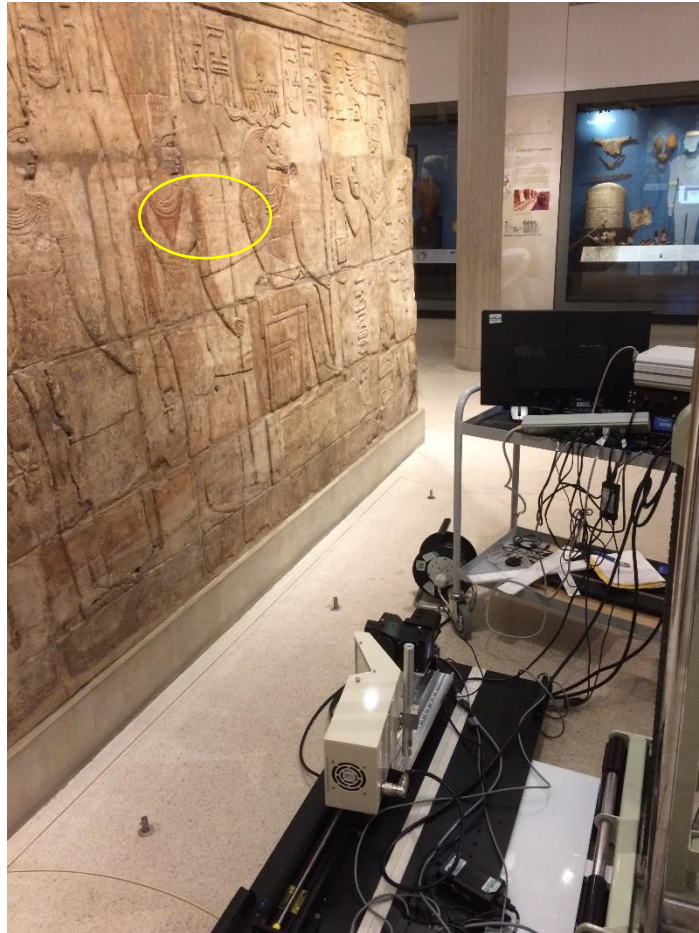


Figure 5.1 The HSI equipment during a scan of The Shrine of Taharqa in the Ashmolean Museum, University of Oxford. The equipment is mounted to a pedestrian stacker allowing for the adjustment of the height. For the purpose of taking this photo of the equipment the room lights were left on, during a scan the room lights are always off.

Note the red colouration on the chest of Anukis Nethy (circled).

The scan speed is calculated based on the distance between the object and the detector in order to ensure that the pixels produced represent square sections of the object. This is done by capturing a single line of pixels from a calibrated sheet on which there are lines separated by a known distance. This is also used to ensure that the area of interest is within the range of the scan.

For processing the Hyperspectral data cube (post-acquisition) the software ENVI (environment for visual imaging, originally designed for remote sensing) was used (version 5.3.1). 35 HSI images were used to create the final composite mapping the visible red pigments on the west wall of the Shrine. This number was chosen based on the desire to scan as much of the wall as possible in as short a time as possible whilst including an overlap of a couple of inches in each direction for the purposes of image registration. Scanning took place over four days and 1.31 TB of data was produced. A computational technique called spectral angle mapping (SAM) where the computer finds and displays all pixels where a colour of our choosing is detected (based on the reflectance spectra) was applied to the data and the results of this are shown in *Figure 5.5*. The output of each individual SAM calculation was saved as a JPEG in ENVI and these 35 JPEGs were then mosaicked using the panorama generation software PTGui Pro, version 11.6 *New House Internet Services B.V. (2021)*, in order to generate the final composite images.

5.3.1.2 Light pollution

The nature of the light pollution on the shrine of King Taharqa is variable both spatially and temporally. Whilst the majority of light illuminating the shrine is artificial, produced by interior lighting of the museum's design, it is not intended to light the shrine exclusively. The gallery in which the shrine is housed also houses other artefacts all with their own illumination requirements and thus light unevenly hits the shrine indirectly from the other exhibits as well as from lighting designed to illuminate the shrine. In addition, there is a small series of windows in the gallery, and the light from these reaches the shrine. This natural light source varies with the time of day, as well as from day to day. During scanning an attempt was made to reduce variation in the

ambient lighting as much as possible by turning off all unnecessary artificial lighting, however, not all of the lighting could be turned off (for health and safety reasons), and the windows could not be covered.

Figure 5.2 shows the location of all the hyperspectral scans taken of the shrine throughout the project. Two of the scans were chosen (at random) and the white calibration data, used here to approximate the spectral output of the light source, was used to demonstrate how, as a result of the changing lighting conditions in the gallery, the light falling on the shrine during scanning can vary.



Figure 5.2 The shrine of King Taharqa. Locations of scans taken are shown in alternating blue and pink rectangles across the surface of the shrine, the two highlighted in red are those scans for which the white calibration data has been reviewed to investigate the effect of light pollution on the spectra obtained. The left hand side scan was taken on Jan 30th 2017, and the right hand side scan was taken on Aug 16th 2017.

Figure 5.3 shows the white calibration data from August and January. The left hand side scan was taken on Jan 30th 2017 and the right hand one was taken on Aug 16th 2017. This data indicates that there is more light falling on the lower left hand side of the shrine, than fell on the lower right. This variation in illumination is taken into account during calibration.

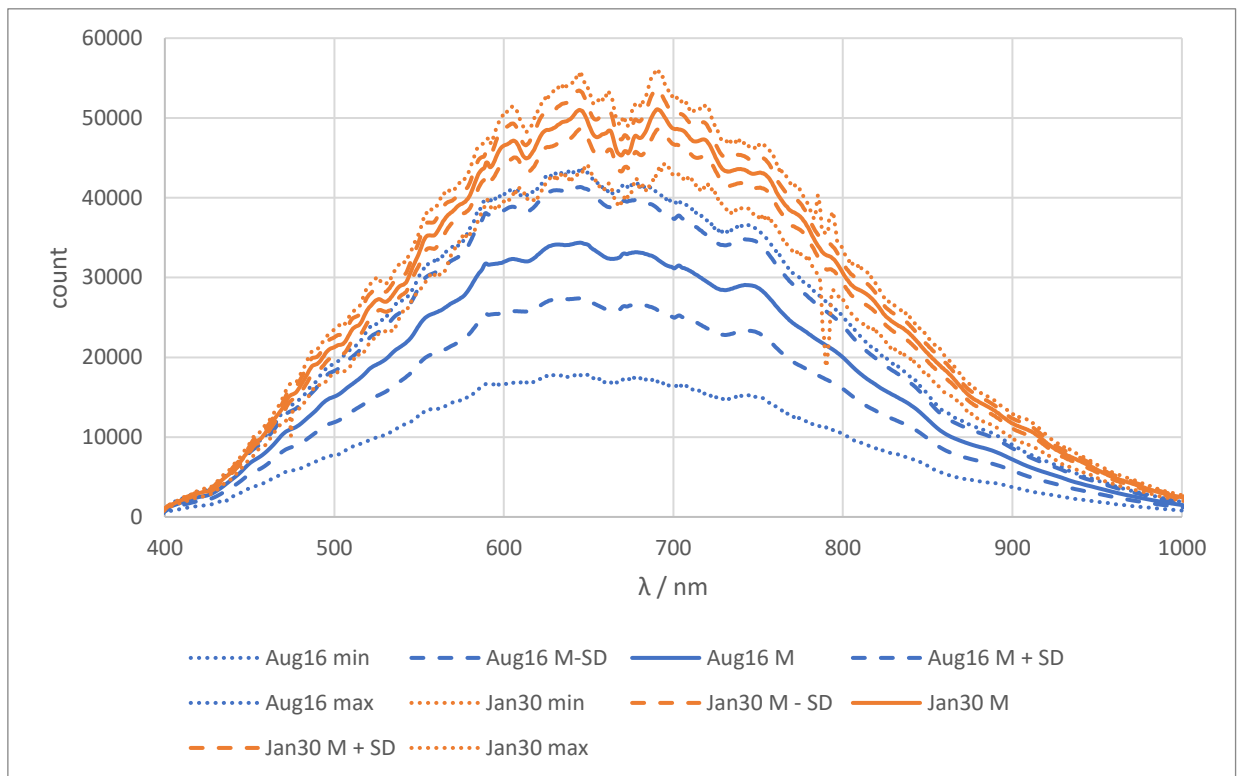


Figure 5.3 The white calibration data for two scans taken of different areas of the shrine of King Taharqa. Shown here are the mean spectra (averaged over all the pixels in the scan) as well as the minimum, maximum, mean – standard deviation ($M - SD$), and the mean + standard deviation ($M + SD$).

Figure 5.4 compares white calibration spectra taken during scanning of the shrine to data obtained in the laboratory where extraneous light sources can be more closely controlled (all lights can be turned off, and there is a blackout curtain for the window). The variation typical of spectra obtained in the laboratory is smaller than the

variation seen between the two spectra obtained in situ during the scanning of the shrine. The peak of both the spectra from the shrine have shifted to the blue end of the spectrum which could be due to the presence of some daylight (the peak intensity of natural daylight is between 400 and 600 nm *Iqbal (2012); Thuillier et al. (2004)*).

That the brightness (peak height) should be different is not unusual between one setup and another however this is accounted for during calibration. If the distance between the light source and the object is changed then the brightness will change as well. With the light source further away the object will appear dimmer to the detector. This accounts for the difference in brightness between the lab-acquired spectra and the in-situ spectra however the two in-situ spectra have different brightness levels from each other despite there having been a consistent distance between the light source and the shrine throughout the scanning. This is due either to light sources within the museum shining inconsistently across the surface, or due to the inconsistency in brightness of the daylight entering the gallery through the window.

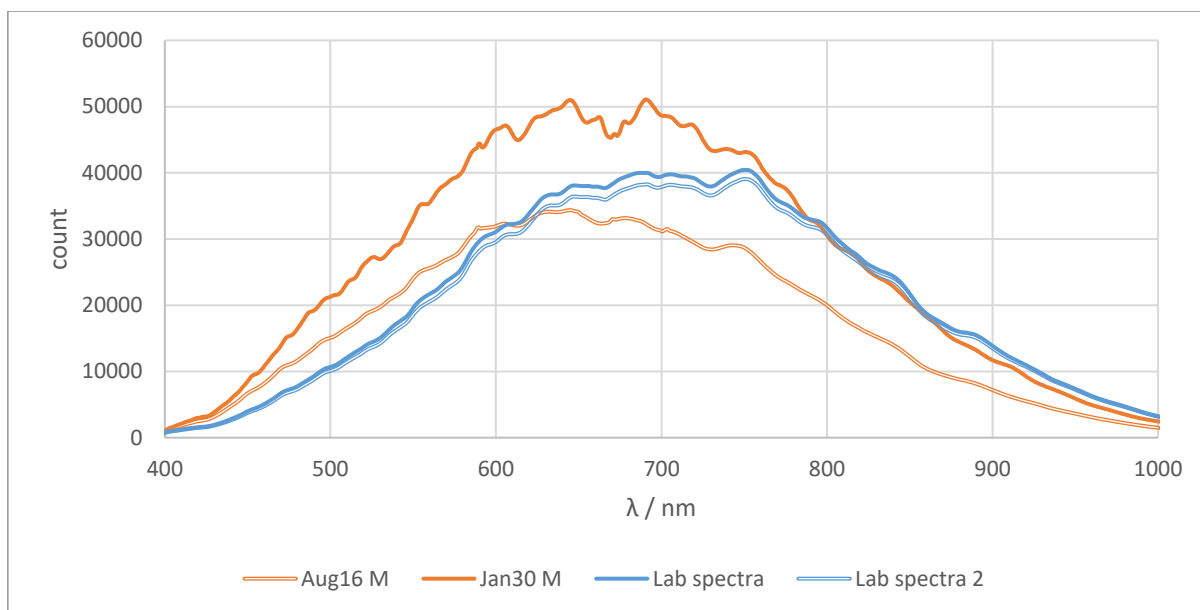


Figure 5.4 Showing how the two white calibration spectra taken “in the field” during image capture for the shrine of Taharqa differ from white calibration spectra taken in ideal laboratory conditions.

5.3.1.3 pXRF

The pXRF equipment used was an Oxford Instruments X-MET 8000 series light element handheld pXRF analyser, 5 mm spot size, in air. Calibration has been performed on an ongoing basis as per the manufacturers recommendations to ensure the equipment is up to standard. Thirty points were analysed using pXRF, areas were chosen based on what is known of the 1990 sample locations, some were chosen based on the results of the 2015 luminescence study, further locations were chosen based on their visual appearance to give a good subset of red, black, bare sandstone, and any other features of interest. Elements given in *Table 5.2* above were of particular interest. The software used to analyse the pXRF spectra was Bruker Spectra Artax Version 7.2.0.0.

5.3.2 Secondary data collection methods

5.3.2.1 Photo induced luminescence (PIL)

In 2015 PIL was used to identify areas where Egyptian blue was present *Armstrong (2015)*. Armstrong studied several objects in the Ashmolean museum, among them was the Shrine of Taharqa *Armstrong (2015)*. Due to its fluorescent properties Egyptian blue can be detected using photoinduced luminescence *Armstrong (2015)*. Armstrong used a modified digital camera and flash, taking photos at regular intervals, forming a grid across the surface, and registering the images in Photoshop to generate the “map” of Egyptian blue.

5.3.2.2 Microscopy

Nine small samples were taken by Howard from positions shown in *Figure 5.9* prior to the application of treatment to the west wall in 1990 *Hanna & Norman (1990)* to identify pigments using microscopy and SEM-EDX. It is interesting to note that draft lines and underpainting from the original craftsmen were found during the study and that traces of the cellulose nitrate could still be present. The study in 1990 served to identify a palette of pigments.

5.4 Results

5.4.1 VNIR HSI mapping



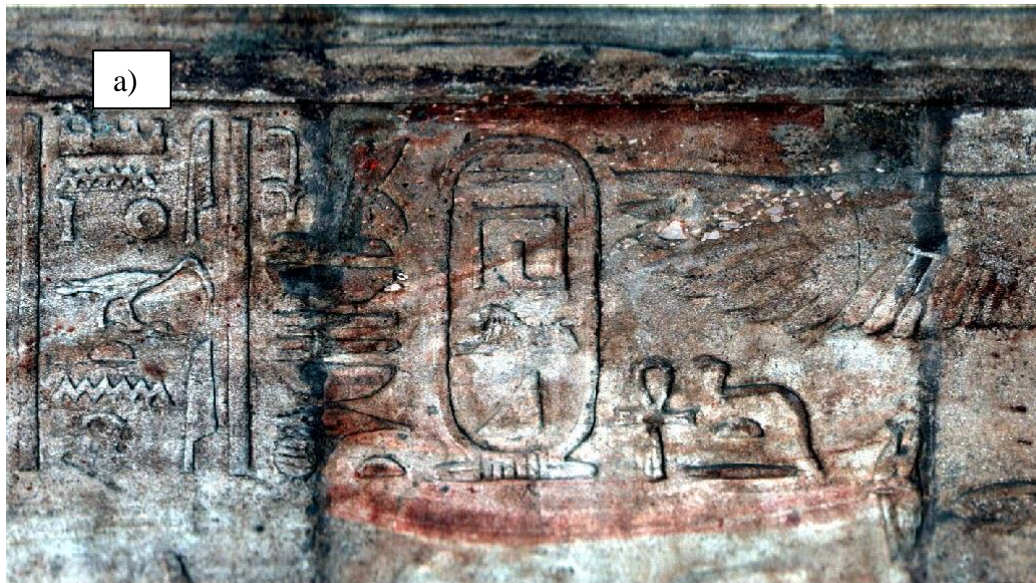
Figure 5.5. HSI map of red colouration on the west wall. Analysis performed on the HSI obtained data cube was able only to map red spectra, it could not discriminate between two or more reds in this instance thus this image cannot be used to differentiate between pigmentation intended by the architects or subsequent artists, and natural colouration of the stone. It is exclusively through comparison with other techniques and logical deduction from art historical sources (section 4.8) that the red from paint and red from the stone has been differentiated in the final figure.

It was believed that the VNIR HSI equipment would be able to assist in the mapping of pigmentation that, with the naked eye, would be difficult to see. Red colouration was the most simple to begin mapping, as some red pigmentation was easy to make out with the naked eye, which provided an excellent target for the SAM computational technique. An attempt was made to map Egyptian blue with this technique, target spectrum from the areas of the shrine identified as having traces of Egyptian blue by PIL were given to the SAM algorithm but this failed to produce any results that could be made sense of, and a weak correlation could be made between

these results, and those of PIL. It is likely that the SAM was mapping aspects of the stonework as opposed to Egyptian blue. Other colours, as identified by the sampling study of 1990, could not be identified visually with the VNIR HSI equipment and so no target spectra could be given to the SAM algorithm.

In the end, just the red pigmentation of the shrine was mapped using VNIR HSI as can be seen in *Figure 5.5*. All red pigmentation that could be seen with the naked eye was identified by SAM, and the technique helped reveal and confirm sections of red pigmentation that would have been difficult to identify otherwise. It is believed that VNIR HSI has been able to fully identify the red pigmentation remaining across the west wall. This technique does not distinguish between red pigmentation from the decoration and red pigmentation naturally found in the rock. However, the information was useful in determining the original colour scheme. Note for example the pattern found on the clothes and headdress of the third figure (Anukis Nethy) and the high concentration of red pigmentation on the clothes of Amun-Re and parts of King Taharqa's attire.

On the other hand, one can see that some of the red pigmentation is likely from the stone. This is seen clearly in *Figure 5.6* which details the red mapped near some hieroglyphics at the top of the Shrine.



← 50 cm →



Figure 5.6. a) A VNIR HSI RGB image taken of the upper band of hieroglyphics near the southwest corner and b) the map of the red spectra produced by SAM. The distribution appears to be caused by features of the stone and its environment, desert varnish for example is a mark upon the rock resulting from weathering and other effects Dietzel et al. (2008), rather than corresponding to particular features of the relief decoration.

A direct comparison of the photo-induced luminescence results to the HSI results show that the pattern on the dress of Anukis Nethy must have once been a blue and red repeating pattern. This is discussed further in section 3.2.1.

5.4.2 XRF

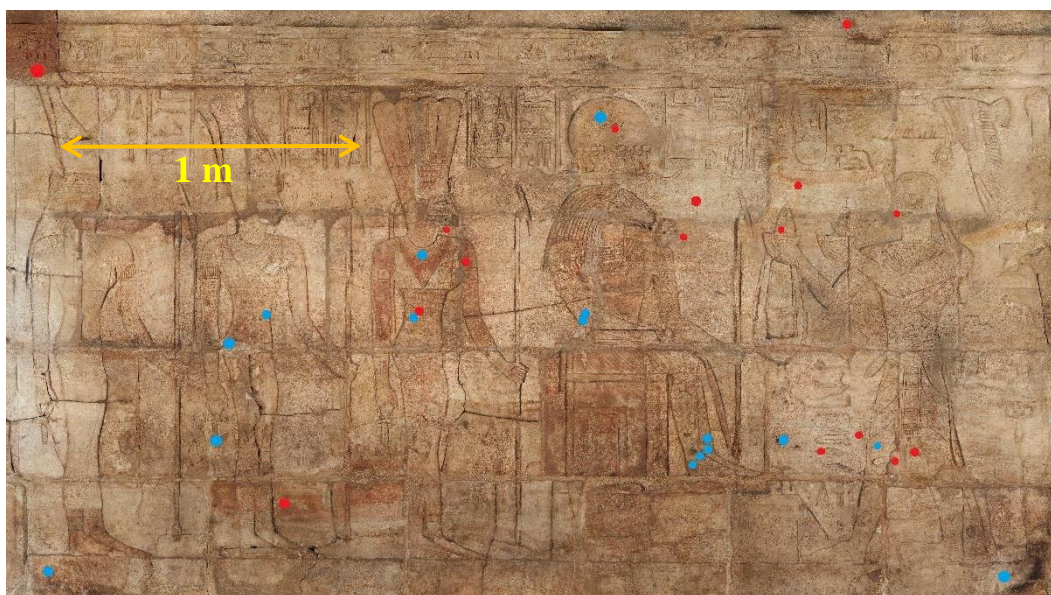


Figure 5.7. XRF showing Cu found on the west wall. 30 points of approx. 30 μ m diameter were analysed. The spectra were analysed by software and the points above have been differentiated into either having a Cu peak (blue) or having no detectable Cu peak (red). For example we therefore assume from this that the skin of Amun-Re is blue, as are the dresses of Anukis Nethy and Satis, as well as other details in the frieze.

Figure 5.7 illustrates where blue pigment is inferred to be present, from Cu peaks identified by pXRF. 16 out of 30 spots sampled were found to have evidence of Cu (shown as blue on figure 5). The remaining areas (shown as red in Figure 5.7) had no detectable Cu. A representative pXRF spectra showing a large Cu peak is shown in Figure 5.8.

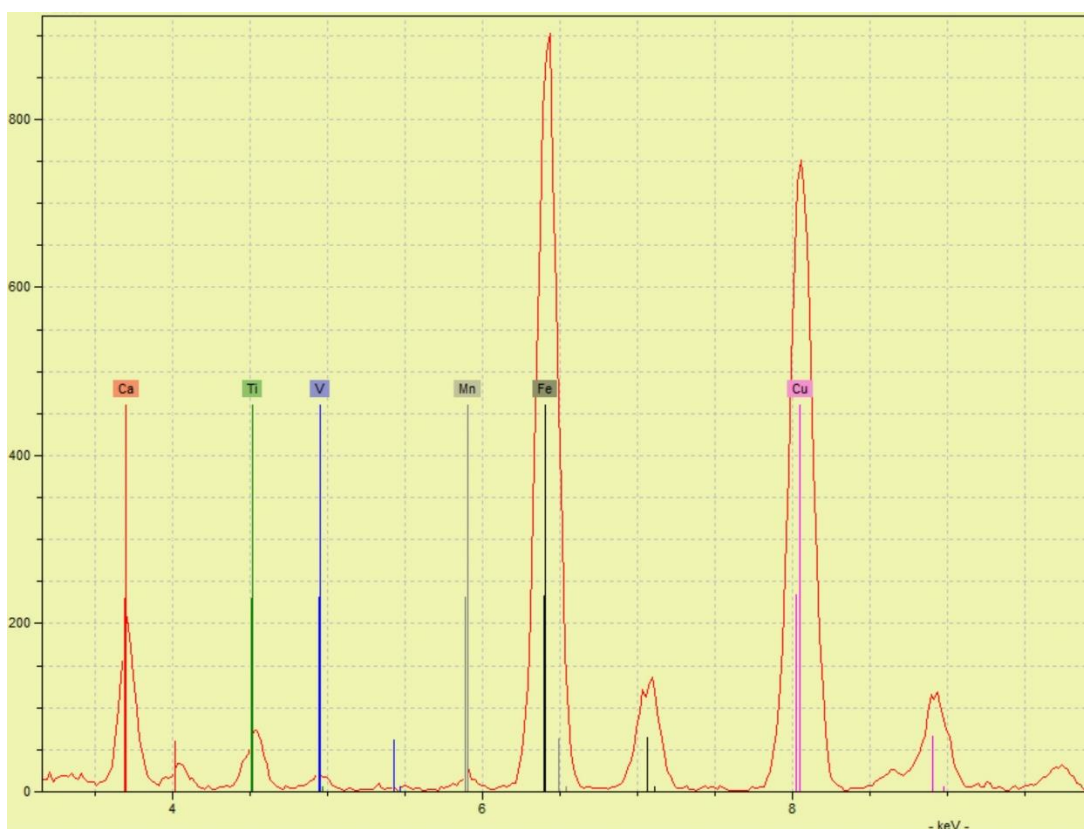


Figure 5.8. A representative spectra from the pXRF experiment showing the presence of Cu, and Fe.

It is interesting to compare these results to those of the photoinduced luminescence (*Figure 5.10*) conducted by Armstrong in 2015, prior to this study. There are areas analysed by XRF which were identified as containing Cu which were not identified by luminescence as having Egyptian blue. It is interesting that these are XRF areas with a lower Cu peak height, and that other XRF areas with a lower Cu peak correspond to areas of a lower luminescence. This would suggest that XRF has identified additional areas of Egyptian blue on the west wall, that may have been faded to such an extent that the trace amount left was insufficient to be detected by luminescence. It is suggested therefore, that in this case the pXRF results were able to add information to the PIL survey results shown in *Figure 5.10*.

Bearing in mind that XRF is slightly penetrative it is expected that the signal will comprise elements from both the pigmentation and stone structure. The iron detected is therefore not conclusive proof of the use of iron oxide pigments by the Ancient Egyptian artist(s) because many components of sandstone also contain Fe, as can be seen in *Table 5.2*. Other elements that can be accounted for in this manner are Ca which can be found in feldspars and calcite, and Mn which can be found in clay and desert varnish.

Elements not explained by common components of sandstone are Ti, V, Zn, As, Br, and Sr. Of these As stands out as an element found in orpiment. As was found in eight areas, this could indicate that the reddish hue of the sandstone is due to As containing sandstone.

5.4.3 Microscopy

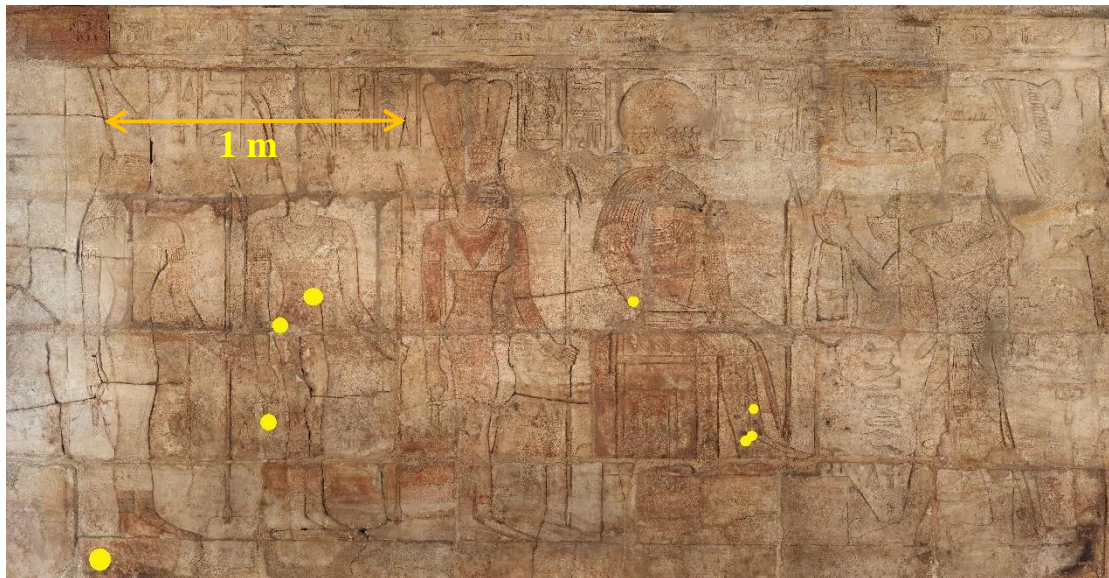


Figure 5.9. The approximate locations of the samples used for microscopy. As you can see the position of only eight samples is known.

The study concluded that the pigments used were Egyptian blue, haematite (red), haematite and kaolin mix (pink), yellow iron oxide, and most likely lamp black. Howard noted that the use of Kaolin is inconsistent with literature reports and that it would be desirable to use XRD to confirm the analysis.

5.4.4 Photo-induced Luminescence (PIL)

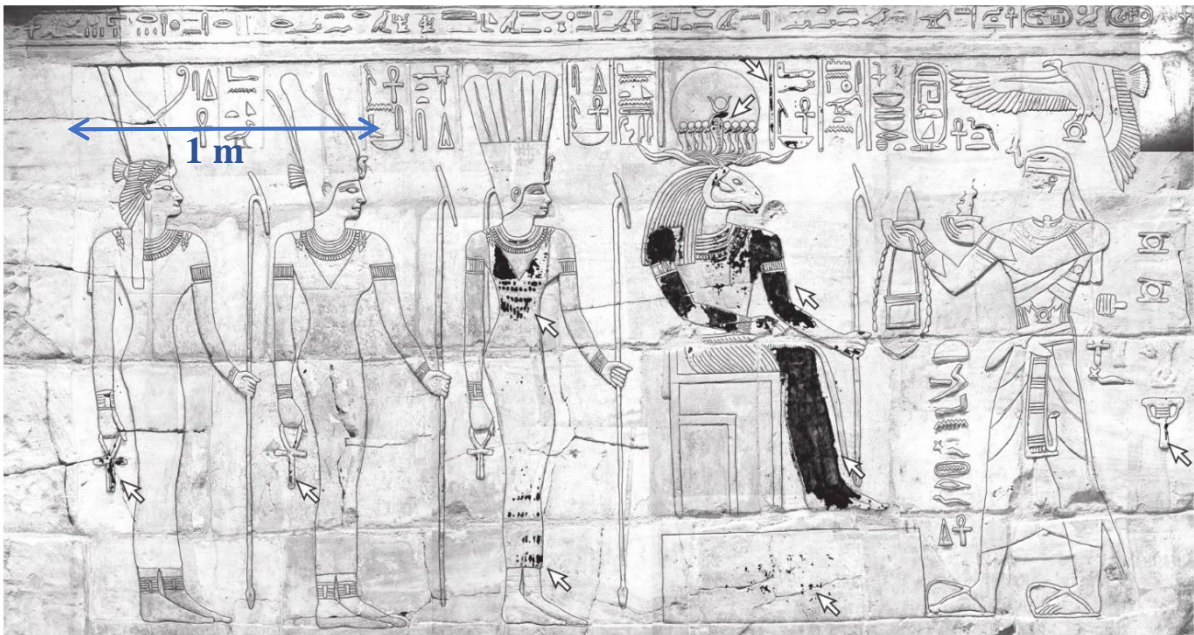


Figure 5.10. Armstrong's photoinduced luminescence results showing the location of Egyptian blue pigment on the west wall of The Shrine of Taharqa Armstrong (2015) (Figure 8, page 184). The shaded areas show where the equipment used was able to detect fluorescence indicative of the presence of Egyptian blue. It is interesting that the hieroglyphs could have been painted with Egyptian blue as indicated by the fluorescence, right of Amun-Re's headdress.

Figure 5.10 shows the PIL results. There is some evidence that the hieroglyphs and other decorative features were once painted with Egyptian blue but that the

pigmentation on these parts must have faded more than the blue on Amun-Re, given that there is a lower concentration of luminescence in these parts.

5.4.5 Creating an amalgamated map of pigments on the west wall of the Shrine of Taharqa

Once data from each technique had been fully examined independently, they were directly compared visually, so that an artist's reconstruction could be made using Photoshop for each area of the shrine's decoration. For some areas this was simple, as only one colour presented itself based on the scientific evidence, for example the skin of Amun-Re was shown to be blue by pXRF and PIL, and VNIR HSI did not provide strong enough evidence to dispute this. The skin of Amun-Re was therefore coloured blue.

In this way many of the colours were safely assumed based on the scientific observations made, for example most of the clothing, and the hieroglyphs. Remaining coloration was inferred from that first set of colours rather than from direct scientific observation, the yellow coloration shown in *Figure 5.12* is an example of this. In some cases it is clear that HSI and luminescence disagreed for example in the case of the dress of Satis a blue was chosen because the red identified by HSI was not limited to the area of the dress and could therefore be argued to be a feature of the stone.

Figure 5.11 shows the reconstruction but sections that are not based directly on analytical evidence have been greyed out. *Figure 5.11* (a) shows the results of the combination of scientific techniques. While microscopy detected a more extended palette than the blue and red shown in *Figure 5.11* (a), these other pigments could not be mapped because of lack of sample points.

The microscopy results could however be used to aid in the determination of the colour palette applied based on art historical knowledge. *Figure 5.11* (b) shows coloration that could be extrapolated from scientific evidence, and is consistent with the colour palette derived from microscopy, though it is to be noted that the scientific means used could not directly identify colours for these areas.

Figure 5.12 was generated using an artistic interpretation of the combined results of these scientific investigations and further inference. Gaps in colour were filled following logical deduction by looking at nearby parts of the colour scheme, and in consultation with the curator regarding what would be normal for Egyptian art during this period (this interpretative measure always being part of digital reconstruction *Denard (2009)*). Some remaining colours were easily inferred from historical sources for example the colours of headdresses and hair are rather consistent across observed artwork from the period and region. Few colours remained to be filled in after this second stage.

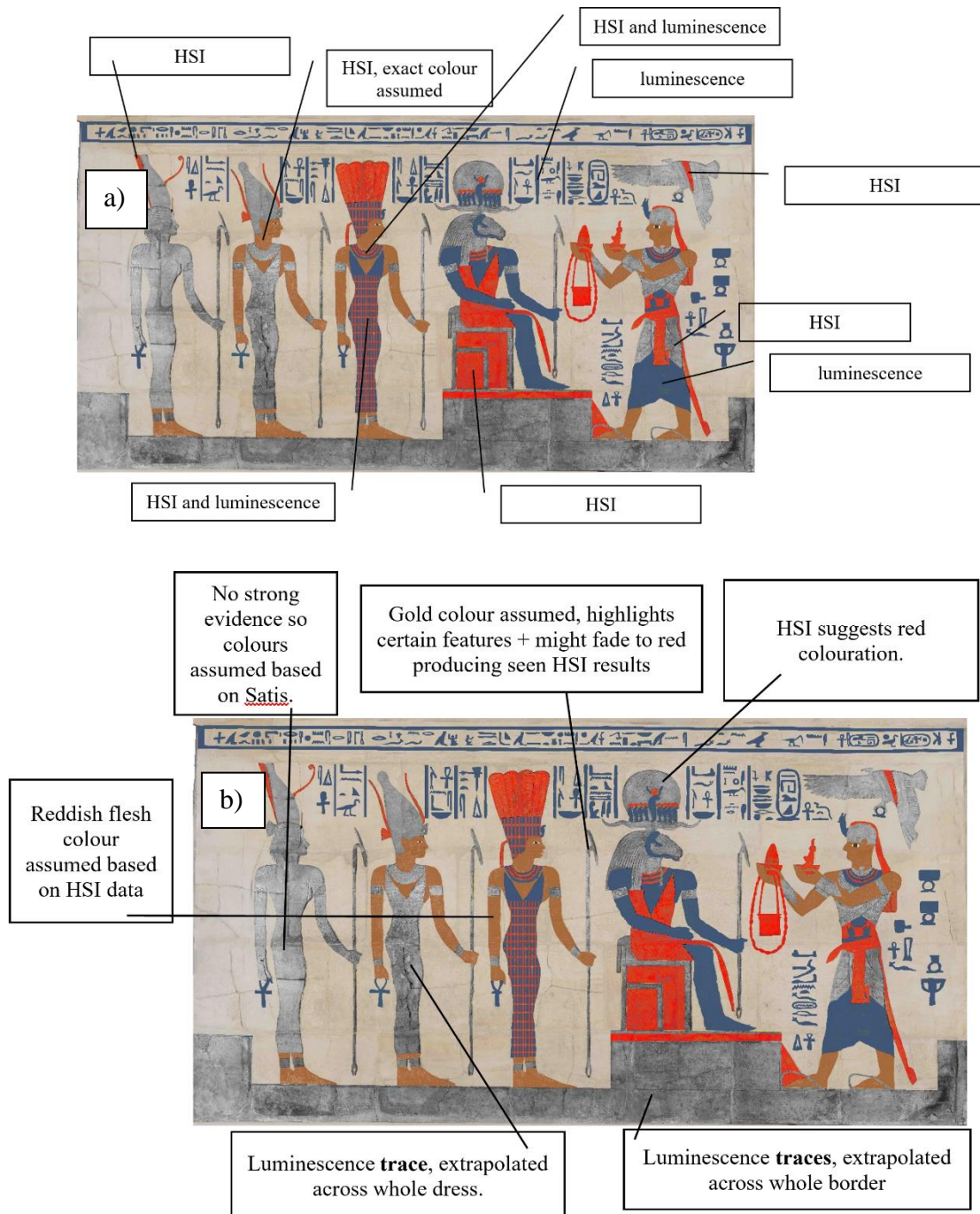


Figure 5.11. Showing the choices made to turn the scientific data into the finished figure. Colours not directly based on scientific data have been greyed out and some of the reasoning behind the choices has been given. a) Colours based on scientific data, the technique used has been given, b) colours not based on scientific evidence are explained.



Figure 5.12. An artistic extrapolation of the scientific results of the investigation. Some colours shown here were determined by analysis, others have been extrapolated based on the results. The west wall depicts (from left to right) Anukis Ba, Satis, Anukis Nethy, Amun-Re, and King Taharqa.

5.5 Discussion and conclusions

As an exercise to demonstrate the utility of VNIR HSI this study has shown that the equipment can aid the understanding and digital restoration of the coloration on an Ancient Egyptian shrine. We have also demonstrated its limitations - it cannot generate a map for pigments that it cannot detect. There are additional NDT methods that provide a wealth of data, and in this case the combination of VNIR HSI with pXRF enabled increased understanding of the coloration on the shrine. VNIR HSI was found to provide good mapping of red pigment, whilst XRF and luminescence were most fruitful techniques to infer the location of Egyptian blue across the west wall. In combination VNIR HSI, pXRF and luminescence provided good mapping of red and blue pigments.

As a comparison between data obtained from destructive and non-destructive testing it is important to note that very little sample was taken in 1990 and it is therefore a good example of how much information can be obtained from micro-destructive analysis. In this instance the microscopy revealed the palette, and identified the pigments. It is, however, a demonstrable advantage of the NDT techniques used here that the general mapping of pigments could be undertaken without harm to the shrine.

The more visual, imaging methods provide excellent reference points for analysis and quickly allowed the characterisation of Egyptian blue (luminescence) and red pigmentation (HSI). Hyperspectral imaging provides data which can be used to make useful inferences, even in a limited detection range (400– 1000 nm). As discussed in section 2.3.2 XRF is a popular method and it proved useful here for tracking elements across the surface quickly and easily.

In terms of imaging techniques utilised for the study of Ancient pigmentation, it is useful to compare this study to two similar studies (one of Ancient Egyptian polychrome wood, and one of an Egyptian coffin), to place this work in context *Abdrabou et al. (2017)*; *Bracci et al. (2015)*. Both studies used, and were able to use it to infer the location of various pigments. More interesting is the use of FORS with a detection range of 350 – 900 nm in the study of an Egyptian coffin which was always used in tandem with another technique, and was shown not to be able to differentiate between some pigments *Bracci et al. (2015)*, as has also been found in this study.

VNIR HSI can indeed be used to provide analyses that assist conservators and art historians as part of a suite of scientific methods. In the case of an investigation into the palette the equipment is of limited use as it lacks the characteristic peaks needed for analysis, and spectra are further complicated because the spectra in the VNIR range will vary depending on all past conservation treatments and other exposure caused by events

in the object's history which may not be well known, SWIR reflectance data would provide these characteristic peaks. Multispectral imaging, which gives a higher quality end result in terms of spatial resolution, but involves the use of different light sources, is another useful technique for this type of investigation *Bracci et al. (2015)*. The best use of VNIR HSI in the case of an investigation into the previous state of surface pigmentation, as demonstrated in this study, is to aid in the assessment of pigmentation visible upon the surface of interest at present and to combine these results to extrapolate the previous colouration of the object.

Chapter 6 Experiment 3: Visible and near infrared hyperspectral imaging for the analysis of colour change in cultural heritage artefacts.

Ian Maybury

6.0 Abstract

The light induced colour change of collections items is of real concern. Various tools are used to monitor it presently, however, VNIR HSI may afford some advantages over present systems. The efficacy of visible/near infrared hyperspectral imaging (VNIR HSI, 400 – 1000 nm) for the purpose of monitoring, and assessing colour change (ΔE) of collection items is examined in order to determine if the technique is valuable for such monitoring. Values for ΔE are calculated according to CIELAB (1976) and the scans are additionally evaluated for material diversity by principal components analysis (PCA). The hyperspectral analysis of a faded silk robe from the Ashmolean Museum, University of Oxford, indicates that VNIR HSI is able to provide quantitative analysis of fading in heritage items after long periods of display. However, analysis of an illuminated manuscript from the Bodleian Libraries, University of Oxford, before and after a period of 111 days on display in museum conditions illustrates some challenges for using VNIR HSI to discriminate minor fading after short term display. After initial values for ΔE were greater than expected radiometric calibration was applied to the data to account for discrepancies in the two different scans. The ΔE value now indicates a change not visible by the human eye. PCA was successful at grouping spectra from the robe into regions comparable to the fading seen by the human eye, however, PCA groups from the scan of the illuminated manuscript after having been on display for a period of 111 days were dissimilar to those from prior to display. VNIR HSI was found to be advantageous because it is non-contact, able to scan the entire surface relatively

quickly, and generates an RGB digital image which can be used for digital conservation methods.

6.1 Introduction

6.1.1 Light induced fading of pigmentation

Museum curators are aware of the problem of light-induced fading *Mignani et al. (2003)*, and the trade-off required between display and conservation *Cuttle (1996)*. Current methods for dealing with these issues include the utilisation of appropriate lighting, and rotation of displays *Artioli (2010)*. To gauge the lightfastness of items prior to display the microfadometer (a microdestructive testing method) *Whitmore (2002)* can be used, and diffuse reflectance spectrophotometry (DRSP) is often used in experiments investigating the characteristics of fading materials *Grosjean et al. (1994)*; *Yoshizumi & Crews (2003)*. DRSP is a non-destructive technique, but it is a contact method, and can analyse only a single point at a time. A full-field, non-destructive methodology such as VNIR HSI could have many advantages such as rapid non-contact scanning *Liang (2012)*. VNIR HSI has not yet been used for this purpose.

It can be argued that painters have known of the fugitive state of their medium for many years. Certainly Van Gogh was aware of the problem when he wrote to his brother in the late 19th century *Burnstock et al. (2005)*. Similarly, the Russel and Abney report in 1888 evaluated the lightfastness of watercolours on display, as a response to a public debate at the time over extended museum opening hours *Brommelle (1964)*. The report was an extremely systematic and extensive investigation for its time and led to the first attempt by an institution to use glass screens to reduce the effect of sunlight on their exhibits. These and other studies such as *Barat et al. (2021)*; *Gawade et al. (2021)*; *Padoan et al. (2021)* demonstrate that the fading of artefacts due to light exposure and the need to monitor them is of importance to museums, art galleries and other similar institutions.

6.1.2 Monitoring of collections

Early attempts at monitoring fading in collections involved the use of blue wool standards *Giles (1965)*, but more recently monitoring has been carried out by handheld DRSPs such as the Konica Minolta CM-600d which give results in the form of reflectance spectra or as tristimulus values. For example, Ford used tristimulus values to monitor colour change in textiles over three months and noted the continuing need to monitor collections rather than hypothesise on potential light fastness, due to great variability in behaviour between different examples *Ford (1992)*. Ford also highlighted some negatives of the presently used system, namely that the head of the equipment (which is a contact method) is difficult to place exactly in the same spot as before which is necessary for the monitoring, that this problem is amplified by uneven surfaces, and that the equipment does not have a high enough spatial resolution to properly analyse objects with considerable spatial inhomogeneity in terms of the dyes or pigments used *Ford (1992)*.

The VNIR HSI equipment held at the Bodleian Libraries, University of Oxford offers the following benefits compared to DRSP. Firstly the spatial resolution is much higher. Instead of one reflectance spectrum per 3 mm radius (as the best DRSPs can produce) the VNIR HSI equipment used in this study gives one reflectance spectrum per pixel. Although pixel size varies from case to case, as an example the equipment setup for this experiment had a pixel size of < 0.2 mm. Thus the VNIR HSI equipment used in this study can monitor, over time, the spectrum of a single square of roughly 0.2×0.2 mm which is advantageous for collections with intricate detail. Secondly, VNIR HSI equipment is entirely non-contact, and can be used on uneven surfaces of collections, to which it is relatively insensitive. This also allows the user to monitor the same location more consistently. Finally, VNIR HSI data, like DRSP data, can be expressed as

reflectance spectra and used to provide tristimulus values. The spectral range of the VNIR HSI equipment used in this study is greater than that of the DRSP, 400 – 1000 nm compared to 400 – 740 nm, and the spectral resolution of the VNIR HSI equipment used in this study (0.6 nm) is greater than that of the DRSP (10 nm). Finally the VNIR HSI equipment used in this study is a scanning-based method, making it able to more quickly analyse larger surfaces than the point-based DRSP.

6.2 Aim & research questions

Aim: To determine the efficacy of VNIR HSI for the monitoring of light-induced change in heritage collections.

Research questions:

- Can VNIR HSI be used to determine accurate values for CIELAB colour change (ΔE) in heritage items that have visible damage for purposes of condition assessment?
- Can VNIR HSI be used to determine accurate values for CIELAB colour change (ΔE) in heritage items that have been placed in a short term display (weeks to months), for the purposes of condition monitoring?
- Is principal components analysis (PCA) a useful tool for the recording, and monitoring of the material diversity of heritage items?

To address this overall aim a set of experiments has been carried out based on research questions posed by staff at the Bodleian Libraries, and the Ashmolean Museum, University of Oxford, involving the monitoring of an illuminated manuscript on display in the Bodleian Libraries, and the evaluation of a silk robe in the collection of the Ashmolean Museum. Accuracy in this context refers to the closeness of the given value to the true value.

6.3 Materials and methods

6.3.1 Materials

6.3.1.1 VNIR HSI

The visible-near infrared hyperspectral imaging equipment used is a Headwall photonics VNIR 1003B – 10147 camera with a detection range of 400 – 1000 nm (spectral resolution 0.64 nm), a Schneider XNO 1.4/1.7-0303 lens with a Headwall ACOBL – 380 – 49X, 075 filter. The light source is a broad spectrum QTH lamp supplied by Headwall. The system records 1600 pixels in each scan line, giving a spatial resolution of < 1 mm. Calibration is carried out with a white calibration using Spectralon, and dark calibration is done with the lens cap on. Samples are scanned without room lighting to reduce noise. ENVI 5.3.1 was used to produce the average reflectance spectra from the data. The setup is described in more detail in a previous publication *Maybury et al. (2018)*.

6.3.1.2 DRSP

For comparison diffuse reflectance spectrophotometry was performed on EAX 3873 using a Konica Minolta CM 600 d connected to a laptop (Windows 10 pro 1903) running SpectraMagic NX. White and black calibrations were performed at the beginning of use using the provided reference samples. The software guided the user through setup and when prompted for reference samples they were presented to the machine. Reflectance spectra are in the range of 360 – 740 nm, spectral resolution 10 nm, spatial resolution diameter 3 mm.



Figure 6.1 The DRSP equipment in use, analysing the robe EAX 7873.

6.3.1.3 EAX 3873 Faded silk robe

In order to investigate the utility of VNIR HSI in discriminating fading after display, EAX 3873, a dyed silk robe in the collection of the Ashmolean Museum, University of Oxford was investigated. The robe had become visibly faded whilst on display at an earlier institution (details of the display conditions have now been lost). It was decided to examine the robe with VNIR HSI and DRSP in comparison with visual assessments of fading.

The robe appears to have been folded whilst on display, protecting some areas from exposure to light, while other areas have faded. It also appears to have been rearranged in the display case at some point, producing three areas of fading, area X, which has been severely faded, area Y, which has been moderately faded, and area Z, which is the least faded (*Figure 6.2*).



Figure 6.2. Ashmolean accession number EAX 3873. Faded sections have been outlined in dotted lines on this image for ease of viewing. Note that there is a region in the centre (marked with the letter X in this photo) that has received a greater light dose than the other areas. This is because area X was on display during both periods of exposure that lead to fading. Area Z is the least faded section, and area Y is between the two.

6.3.1.4 Bodl. 394

In order to evaluate the utility of VNIR HSI to discriminate any fading from short-term display, an experiment was carried out at the Bodleian Libraries, University of Oxford to examine a manuscript before and after 111 days on display. This was intended to represent the shortest display length expected in most museum environments. As part of the exhibition “Thinking 3D” the 12th century CE manuscript (Bodl. 394, shown in *Figure 6.3*) was placed on display in the Weston Library, Oxford. The manuscript is historically interesting because it is one of the first realistic architectural drawings, hence its inclusion in the exhibition which explored three-dimensional representation in art from medieval times to the present day. The use of red, blue, and yellow on the same illumination made it a good candidate for this study.

The illumination of interest, ‘In visionem Ezekeielis’, was scanned by VNIR HSI before going on display, and after 111 days on display.

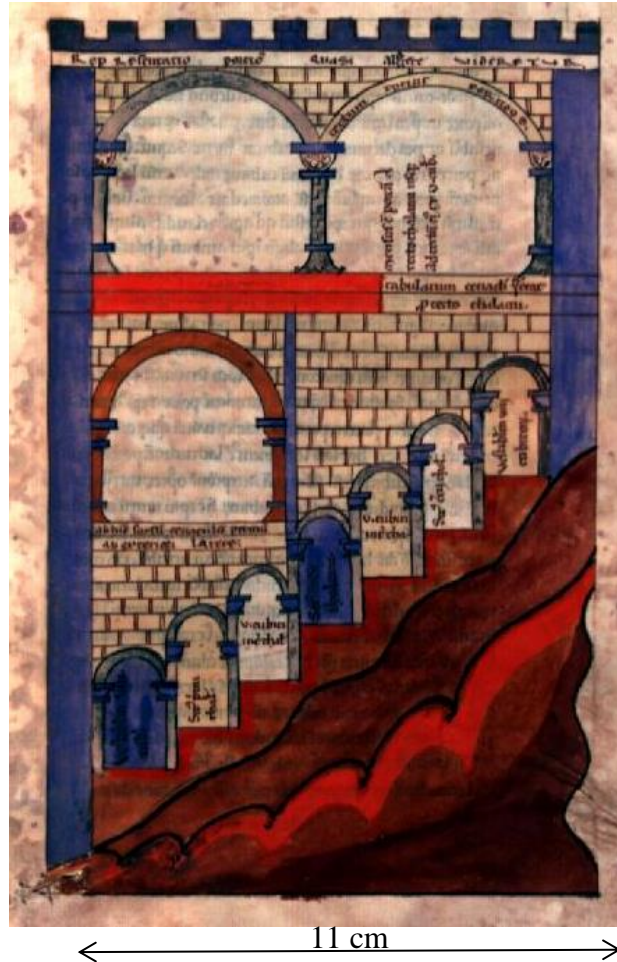


Figure 6.3. MS Bodl. 394, 12th c. Richard of St. Victor, *In visionem Ezekeielis*.

6.3.2 Methodology

Hyperspectral scans of EAX 3873, and Bodl. 394 were spectrally binned (the reduction of bands by the combination of adjacent bands leading to a reduction of noise and processing time), and processed with the ENVI spectral hourglass wizard (PCA, PPI, SAM). In the case of Bodl. 394, the scan from day 111 was corrected using the ENVI IDL Radiometric normalisation task to allow comparison with the scan from day

0. The Eigenvalues from the spectral hourglass wizard were used to determine the number of useful bands, and the pixel count from the SAM metadata was used to determine which bands were the most useful bands. The spectra of these bands were selected from the endmembers, and the pixels related to these endmembers were plotted using the SAM data giving an indication of material diversity. In the context of these experiments material diversity refers to the number of different spectra contributing to final image. The more endmembers representing a significant proportion of the image, the greater the material diversity. A change in material diversity could be due to a change in the condition of the artefact.

CIELAB values were calculated from representative regions of interest in order to determine a value for ΔE .

6.3.3 Data processing for hyperspectral data

Various processing methods were performed on the hyperspectral data cubes obtained for this experiment. Some processing was applied at point of capture by the capture software (binning, some noise reduction methods), but the bulk involved manipulation of data in ENVI in order to reduce the large quantities of data into the most meaningful and relevant spectra. The methods used are outlined below.

6.3.3.1 Pre-processing

The raw data from the CCD is transformed into reflectance data (this transformation is a form of correction, and allows the data to be compared) according to *Equation 6.1*

Bonifazi et al. (2019)

$$R = 100 \left(\frac{R_0 - B}{W - B} \right)$$

Equation 6.1. The transformation of raw data into reflectance data for each pixel in a hyperspectral image. Where R is the reflectance, R_0 is the raw data, B is the dark calibration spectrum, and W is the white calibration spectrum.

Spectral binning was also performed on the data at the point of acquisition, with 972 wavelengths binned to 248 as a means of data reduction (which improves processing time) that also improves the signal to noise ratio *Bai et al. (2019)*.

6.3.3.2 Principal components analysis (PCA)

Principal components analysis is a statistical analysis method, the purpose of which is primarily data reduction through dimensionality reduction *Bai et al. (2019)*; *Harris Geospatial Solutions, Inc. (2020f)*, defined as the creation of a smaller subset of data whilst retaining as much of the spectral information as possible. It is possible to do this because much of the data can be wasted (noise for example) *Harris Geospatial Solutions, Inc. (2020f)*. Through the removal of redundant data PCA will also reveal relationships among spectral features, and identify the most (and least) prevalent spectral characteristics *Harris Geospatial Solutions, Inc. (2020f)*.

6.3.3.3 Spectral angle mapping (SAM)

SAM is a form of image segmentation, or classification *Bai et al. (2019)*. SAM transforms all spectra into a vector and compares each vector to a reference by directly comparing the angle between the two vectors. If the angle is within parameters set by the user, the two spectra are said to be similar. An image is then produced based on a user-specified angle. Lower angles result in fewer (but closer) matches to the reference

spectrum, larger angles result in greater numbers of matches to the reference spectrum (and thus a more coherent image), but the matches will not be as close *Coren et al. (2005); Harris Geospatial Solutions, Inc. (2020d)*.

6.3.3.4 Radiometric normalisation

In the case of the analysis of Bodl. 394 radiometric normalisation was performed as a further pre-processing step. It is similar to sphering, a popular pre-processing step prior to the comparison or registration of hyperspectral data cubes *Bai et al. (2019)* whereby each pixel is normalised to a unit magnitude to eliminate brightness differences between HSI scans *Bai et al. (2019)*. Radiometric normalization reduces erroneous discrepancies between two images caused by inconsistencies in the acquisition conditions, for example changes in geometric and illumination conditions *Canty & Nielsen (2008); Harris Geospatial Solutions, Inc. (2020b); Q. Du et al. (2007)*.

Radiometric calibration, or an equivalent, is not normally applied to HSI for heritage as two scans are not often compared *Pillay et al. (2019)*. In the case of multiple scans requiring registration, however, examples do exist such as the analysis of the Gough map which used PCA, binning, and sphering as part of the research into the material diversity *Bai et al. (2019)*.

6.3.3.5 The calculation of CIELAB values from reflectance spectra, and the calculation of colour difference from CIELAB values

The CIELAB system was used in this experiment as it is a widely-used colour space. In terms of the experimental limitations, it is worth considering that more accurate versions of the CIELAB 1976 formulae used here have since been released based on more up to date experimental data. It is generally believed that these new formulae will

more accurately represent colour change for small values of colour difference, as they are more accurately corrected for brightness, hue, and chromaticity. The 1976 formulae were used here though, as the a,b plots are widely used due to their ability to relate perceived colours to plots on the graphs. Similarly the ΔE value is directly relatable to these graphs (a length on these graphs is directly proportionate to a change in colour difference value), indeed this version of CIELAB is the only one with an associated colour space making it ideal for the comparisons desirable for this experiment.

The workflow is visualised in *Figure 6.4*. VNIR HSI required steps 1-4 but DRSP provided the L*a*b values alongside the reflectance spectra, and so only step 4 was necessary for this data.

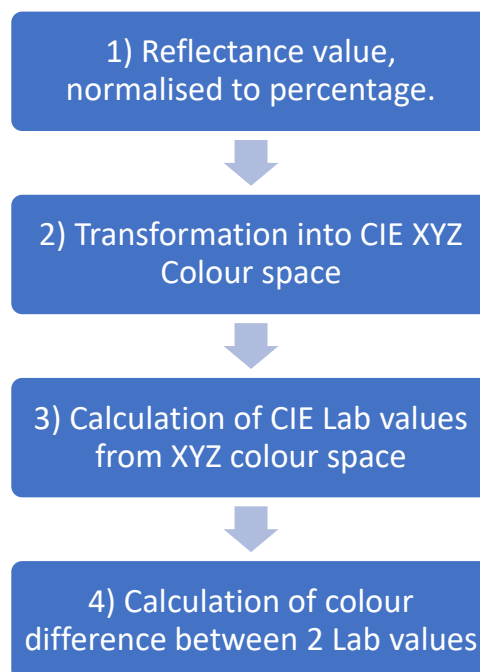


Figure 6.4. Workflow to obtain CIELAB values and colour difference values.

Step1: VNIR HSI data is normally given as a value between 0 and 1, thus the reflectance values must be multiplied by 100. CIELAB is designed for visible spectra and so only the reflectance data for between 400 and 740 nm were converted.

Step 2: The formula for this transformation *Luo (2002)* is as follows:

$$[XYZcs] = [spdD65] \times [sof10^0]$$

Equation 6.2: The transformation of reflectance values into CIE XYZ colour space.

Where XYZcs is the CIE XYZ colour space, spdD65 is the reflectance illuminant spectral power distribution (D65), and sof10° is the standard observer function for a 10° observer.

More properly this becomes:

$$X = k \sum P(\lambda)\bar{x}(\lambda)R(\lambda)$$

$$Y = k \sum P(\lambda)\bar{y}(\lambda)R(\lambda)$$

$$Z = k \sum P(\lambda)\bar{z}(\lambda)R(\lambda)$$

Where

$$k = \frac{100}{\sum P(\lambda)\bar{y}(\lambda)}$$

Equation 6.3. $R(\lambda)$ is the spectral reflectance of the sample at the wavelength λ (the result of the VNIR HSI analysis), $P(\lambda)$ is the spectral power distribution of the reference illuminant at the wavelength λ , (a standard from CIE), and $\bar{x}(\lambda)$, $\bar{y}(\lambda)$, and $\bar{z}(\lambda)$ are the CIE standard observer functions at the wavelength λ . The equations calculate a value for each wavelength and give the sum of those values as X , Y , Z , or k . k is a factor which normalises X , Y , and Z so that Y will have a value of 100. This is the value of a theoretical material that reflects or transmits 100 % of the incident light. The values calculated are tristimulus values where Y is the luminance, Z relates to blue light, and X is a mixture of response curves chosen to be non-negative Marcus (1998).

Step 3: The formulae to transform CIE XYZ values to CIELAB values *Luo (2002)* (so that the results can be displayed in a colour space) are as follows:

$$L = 116 \left(\frac{Y}{Y_n} \right)^{1/3} - 16$$

$$a = 500 \left(\left(\frac{X}{X_n} \right)^{1/3} - \left(\frac{Y}{Y_n} \right)^{1/3} \right)$$

$$b = 200 \left(\left(\frac{Y}{Y_n} \right)^{1/3} - \left(\frac{Z}{Z_n} \right)^{1/3} \right)$$

Equation 6.4. Where X_n , Y_n , and Z_n are the tristimulus values for the reference illuminant, in this case for the 10° observer: $X_n = 94.811$, $Y_n = 100$, and $Z_n = 107.304$.

L values give the brightness of the spectra, white is 100, black is 0, a values give the redness of the spectra, green colours are - a, red colours are + a, and b values give the blueness of the spectra, blue colours are - b, yellow colours are + b. This system allows any colour within the human visual spectrum to be plotted in a 3D colour space. More typically only the a and b values are plotted, as it is easy to relate perceived colours to points on an a, b plot.

Step 4: To compare two L*a*b values, the CIE76 formula for colour difference (ΔE) Luo (2002) is used. $\Delta E < 2.3$ is considered not noticeable Amanatiadis et al. (2021).

$$\Delta E = \sqrt{\Delta L^2 + \Delta a^2 + \Delta b^2}$$

Equation 6.5. The calculation of a value for colour difference from values of brightness, chromaticity, and hue.

6.3.3.6 Spectral hourglass wizard

Spectral hourglass wizard is a tool within the ENVI software Harris Geospatial Solutions, Inc. (2020j) designed to determine the most “spectrally pure” or unique pixels, termed endmembers. These are then mapped using a SAM comparison algorithm. The workflow of the spectral hourglass wizard can be described as having 3 steps.

Step 1: The minimum noise fraction (MNF) transform (the algorithm in ENVI for carrying out PCA) determines the dimensionality, segregates and equalises noise, and reduces computational requirements for subsequent processing Boardman & Kruse (1994); Harris Geospatial Solutions, Inc. (2020c). It is a modified form of the PCA transform developed by Green et al. (1988). It is linear and performs PCA twice, the first ‘rotation’ for the purpose of noise whitening, and the second to determine the inherent dimensionality of the data by using the principal components derived from the first. Inherent dimensionality is determined by a property termed eigenvalues. Following the MNF transform the data cube is divided into two parts, the first has large Eigenvalues associated with coherent images, and the second has near-unity Eigenvalues and is mostly dominated by noise. Only the first part need be carried forward through to the next step of the spectral hourglass wizard.

Eigenvalues indicate the length of a principal component (which equates to the proportion of original information that each component contains) therefore the Eigenvalue plot is used to determine which of the principal components (bands) will be most useful.

The data's dimensionality is the quantity of endmembers that the data cube contains. For each new component another dimension is added through spectral mixing. Dimensionality is determined from a plot of Eigenvalues vs bands. At the point where the slope of the curve approaches 1 the number of bands is the number of endmembers.

Step 2: Endmembers (a representation of the "most pure" spectra in the scan) are determined from the image by calculating the pixel purity index *Harris Geospatial Solutions, Inc. (2020e)* the PPI algorithm runs multiple (5000) iterations of a projection in spectral space (where image bands are plot axis) and classes the most pure spectra as those that appear in the extremes of this space more often. The n-D visualiser *Harris Geospatial Solutions, Inc. (2020k)*, as shown in *Figure 6.5*, is a representation of the spectral space, plotting only the purest of pixels. Step 2 ends by grouping these pixels based on their endmembers.

Step 3: The software a classification (using SAM) of all pixels in the image based on each pixels similarity to the endmembers. It is possible that not all pixels will be classified.

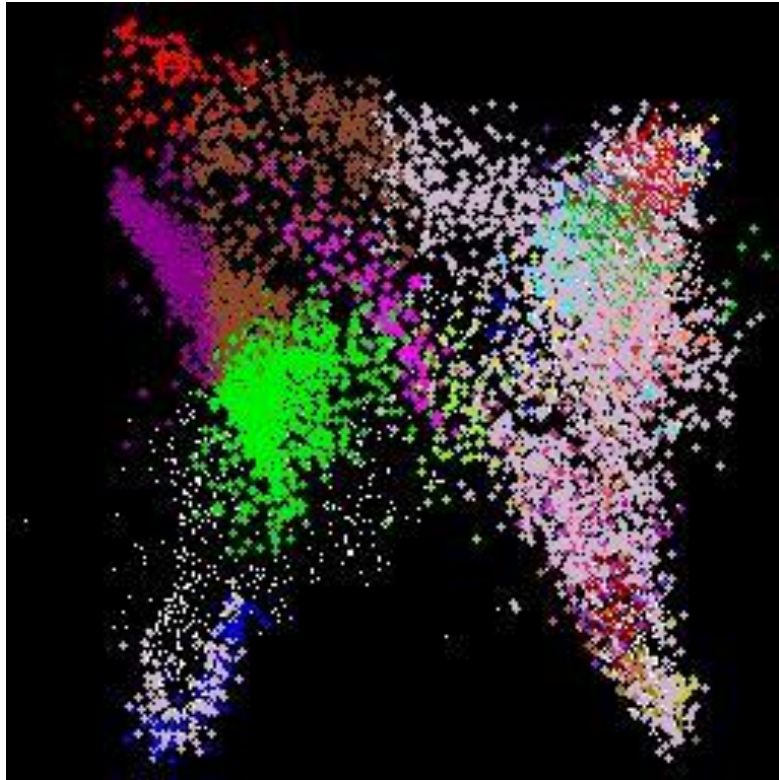


Figure 6.5. The PCA plot for Bodl. 394: Day 111 corrected. In 3D space this resembles a saddle. This representation of the data cloud resulting from plotting image data in spectral space is meant to aid in visualising which pixels are similar.

6.4 Results

6.4.1 Analysis of EAX 3873: Faded silk robe

For the robe the spectral hourglass wizard determined that there were 48 endmembers, which indicates that there were 48 different components making a significant contribution to the final data cube. These 48 endmembers are plotted in *Figure 6.6*. In the case of the robe 13 % of pixels remained unclassified.

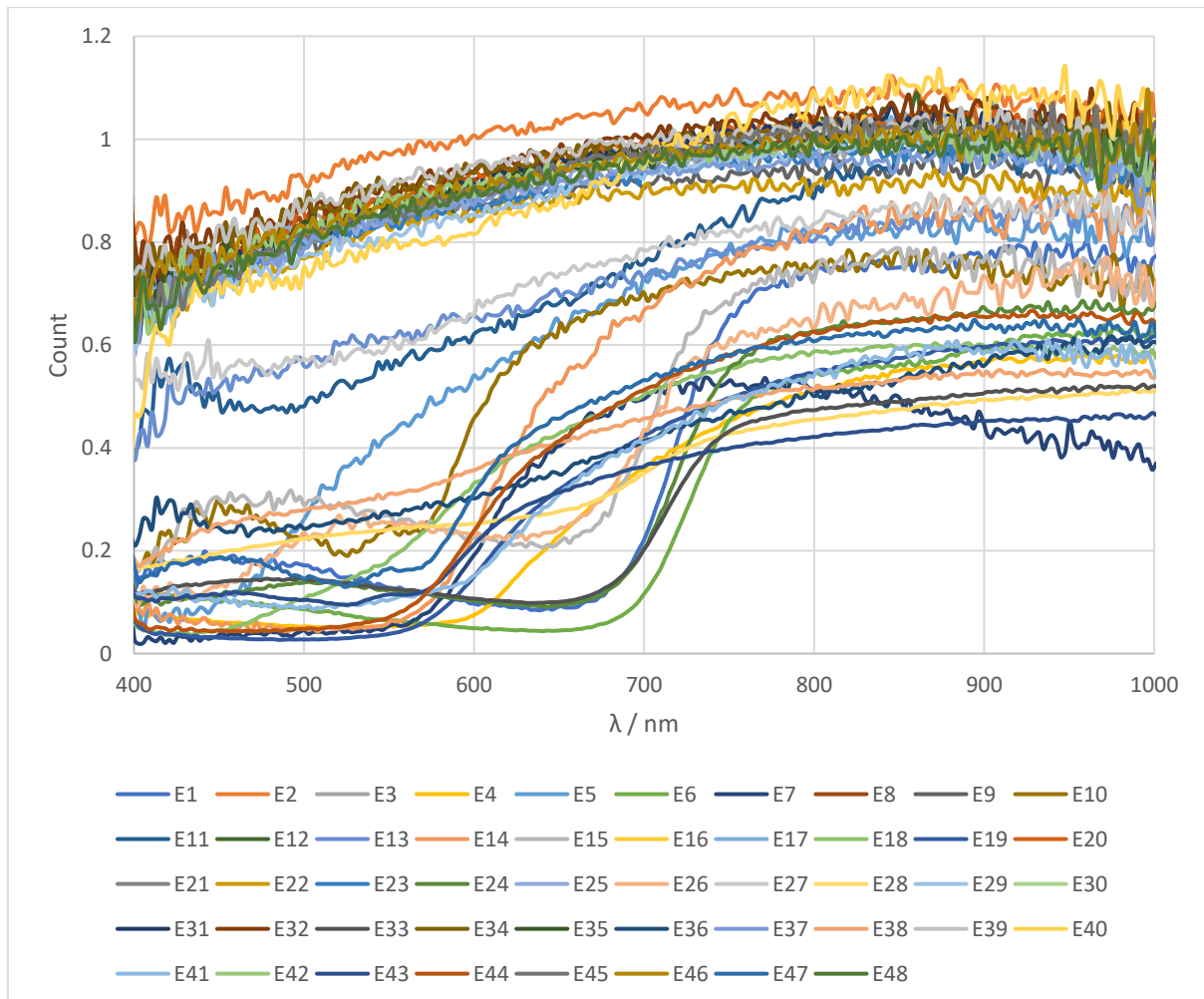


Figure 6.6. All 48 endmembers identified by the ENVI processing software

To reduce this further the quantity of pixels represented by each endmember, and their Eigenvalues, were analysed. *Figure 6.7* shows the plot of Eigenvalues vs principal components. Though it may appear to reduce to unity within the first 10 bands it does not. *Table 6.1* lists the Eigenvalue of each principal component. In this data cube the Eigenvalues never reach unity (the dataset is not “ideal”) however, the amount of useable data given by each new principal component (indicated by the Eigenvalue) does reduce significantly after the 9th band. The table also reveals that 78 % of the data is in the first 10 bands with each subsequent band providing < 0.3 % of the data per band.

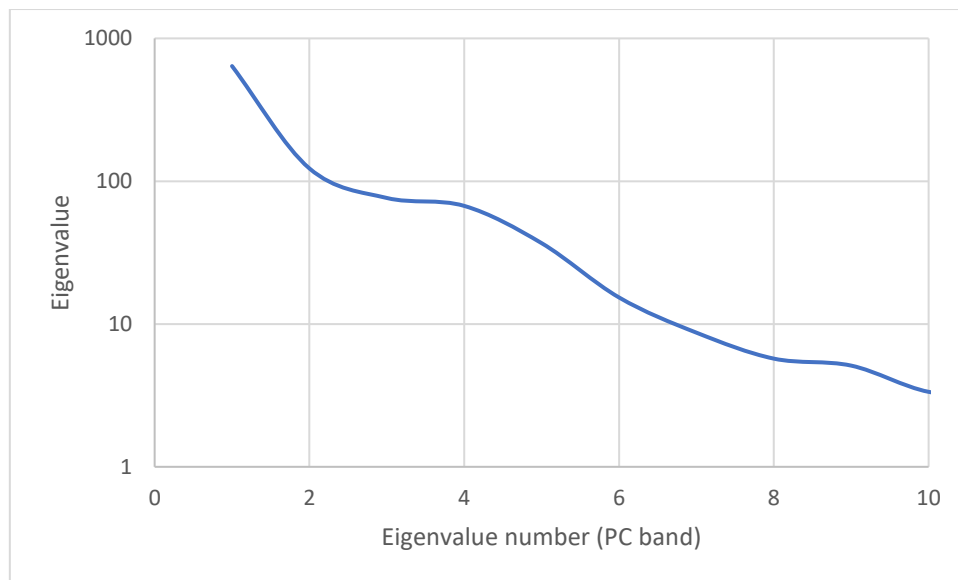


Figure 6.7. Plot of eigenvalues as used in the spectral hourglass wizard to determine the data dimensionality.

Eigenvalue number (PC band)	Eigenvalue (SUM = 1250.476)	% total variance	Cumulative % variance
1	640.010631	51.18	51.18
2	122.825017	9.82	61.00
3	76.300495	6.10	67.11
4	67.143461	5.37	72.47
5	36.821586	2.94	75.42
6	15.342697	1.23	76.65
7	8.697883	0.70	77.34
8	5.72366	0.46	77.80
9	5.112524	0.41	78.21
10	3.350642	0.27	78.48
240	1.031434	0.08	99.34
241	1.030913	0.08	99.42
242	1.030663	0.08	99.51
243	1.030107	0.08	99.59
244	1.029839	0.08	99.67
245	1.029636	0.08	99.75
246	1.028871	0.08	99.84
247	1.027812	0.08	99.92
248	1.027181	0.08	100.00

Table 6.1. Analysis of Eigenvalues for EAX 3873.

Table 6.2 shows the pixel count of each of the endmembers identified by the spectral hourglass wizard. This was used to determine which of the endmembers were the 10 most significant principal components. The third most significant band was comprised of the pixels that could not be classified by SAM. Pixels matched with endmembers not considered to be significant contributed less than one percent each to the final image. The most significant SAM classes (endmembers) are 4, 19, 24, 28, 33, 38, 41, 43 and these are plotted in *Figure 6.8*.

E#	Pixel count	Percentage		E#	Pixel count	Percentage
#4	2758624	44.18606		#16	17436	0.27928
#41	1017420	16.29645		#34	17431	0.2792
Unclassified	804683	12.88895		#20	17139	0.274523
#43	352617	5.648017		#46	16700	0.267491
#19	151946	2.433784		#13	15689	0.251297
#38	100524	1.610136		#21	13910	0.222802
#24	91731	1.469295		#32	12605	0.2019
#28	87706	1.404824		#17	12273	0.196582
#18	84938	1.360488		#9	11793	0.188894
#33	73303	1.174125		#11	11544	0.184905
#44	61391	0.983326		#42	9994	0.160078
#26	61206	0.980363		#14	9490	0.152005
#5	50995	0.816809		#48	8129	0.130206
#39	44957	0.720095		#1	7684	0.123078
#6	41553	0.665572		#29	6448	0.10328
#15	40897	0.655065		#10	6099	0.09769
#31	31014	0.496764		#40	6030	0.096585
#3	27187	0.435466		#8	5371	0.08603
#22	25204	0.403703		#12	2438	0.03905
#45	23884	0.38256		#2	2069	0.03314
#36	20358	0.326083		#27	2065	0.033076
#35	19774	0.316729		#30	1596	0.025564
#47	19055	0.305212		#37	1161	0.018596
#25	19009	0.304475		#7	47	0.000753
#23	18083	0.289643		Total pixel count: 6243200		

Table 6.2. The pixel count of the endmembers and the percentage of total pixels that each endmember contributes to the final picture. Shown in green are the endmembers whose contribution was significant enough for inclusion into Figure 6.9.

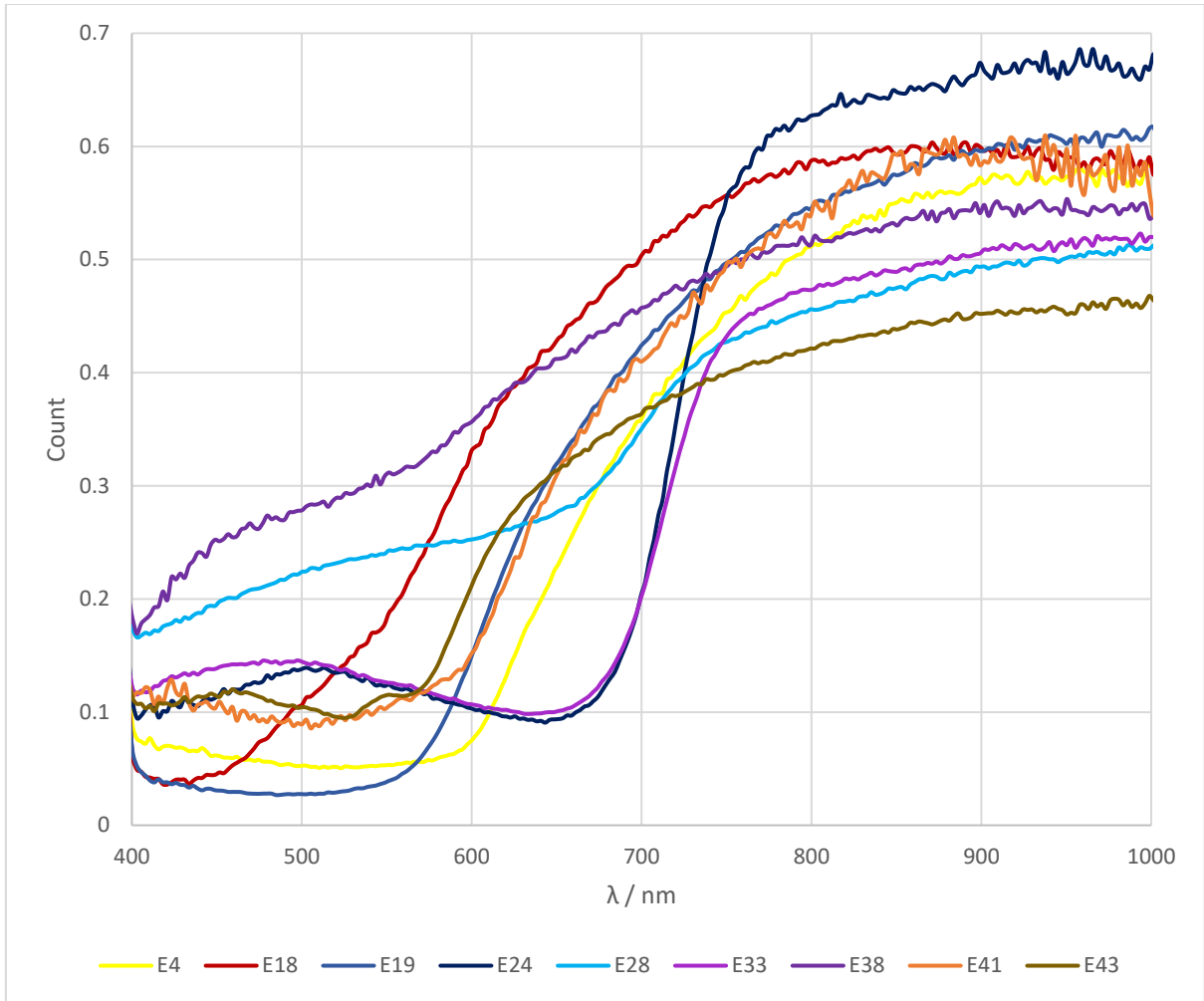


Figure 6.8. The most significant Endmembers. Figure 6.9 a) shows an image of the robe made exclusively of pixels whose spectra matches that of one of these 9 endmembers.

The final image is given in Figure 6.9. The spectral hourglass wizard (PCA, PPI, SAM) has successfully grouped the pixels into endmembers representing the extent of the fading that is seen visibly. These groupings could be used by conservation teams to monitor change over time, or analyse the extent of damage. In this instance the analysis of the data has complemented the fading seen by the human eye and provided the analyst with additional data derived mathematically to aid conservation.

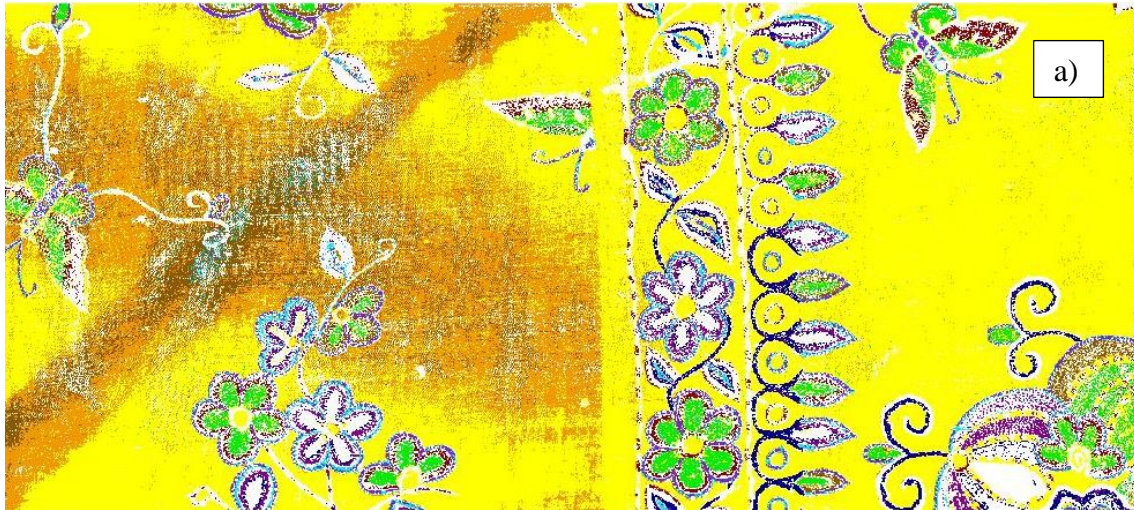


Figure 6.9. a) A false colour image of the robe where each coloured pixel corresponds to the endmember (Figure 6.8) of the same colour, b) RGB image of the robe for comparison.

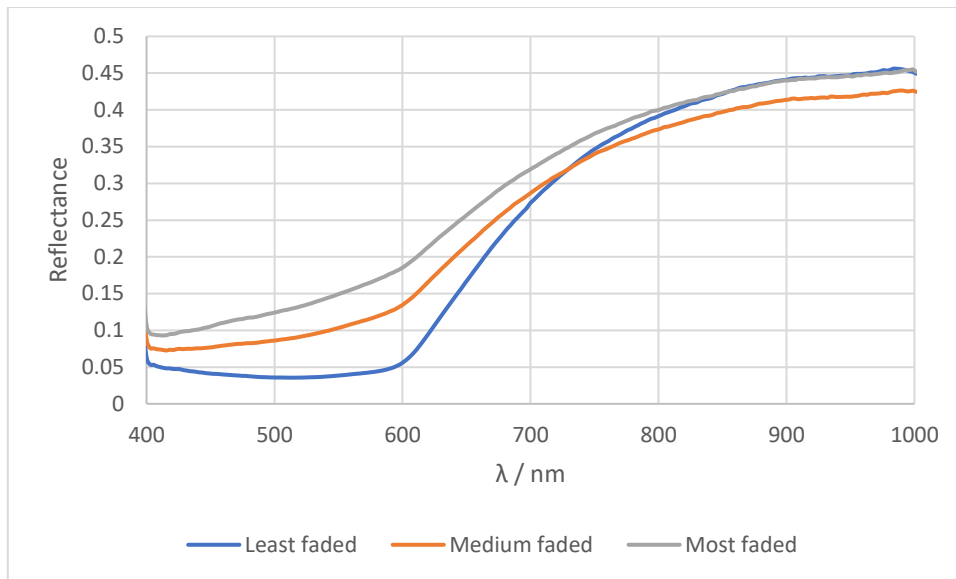


Figure 6.10. Spectra taken from areas x, y, and z (Figure 6.2)

Spectra were taken from the 3 regions of interest for the robe (*Figure 6.10*) in order to calculate a ΔE value for the fading. ΔE between the most and least faded sections of the robe was calculated to be 23.68, similarly the DRSP equipment found a ΔE of 26.90.

6.4.2 Analysis of Bodl. 394: Illuminated manuscript

In order to evaluate the utility of VNIR HSI in monitoring fading over a short-term display, ENVI was used to compute average spectra for three regions of interest on the illumination (areas of red, blue and yellow pigments as shown in *Figure 6.11*). The reflectance spectra from these areas are given in *Figure 6.12*.

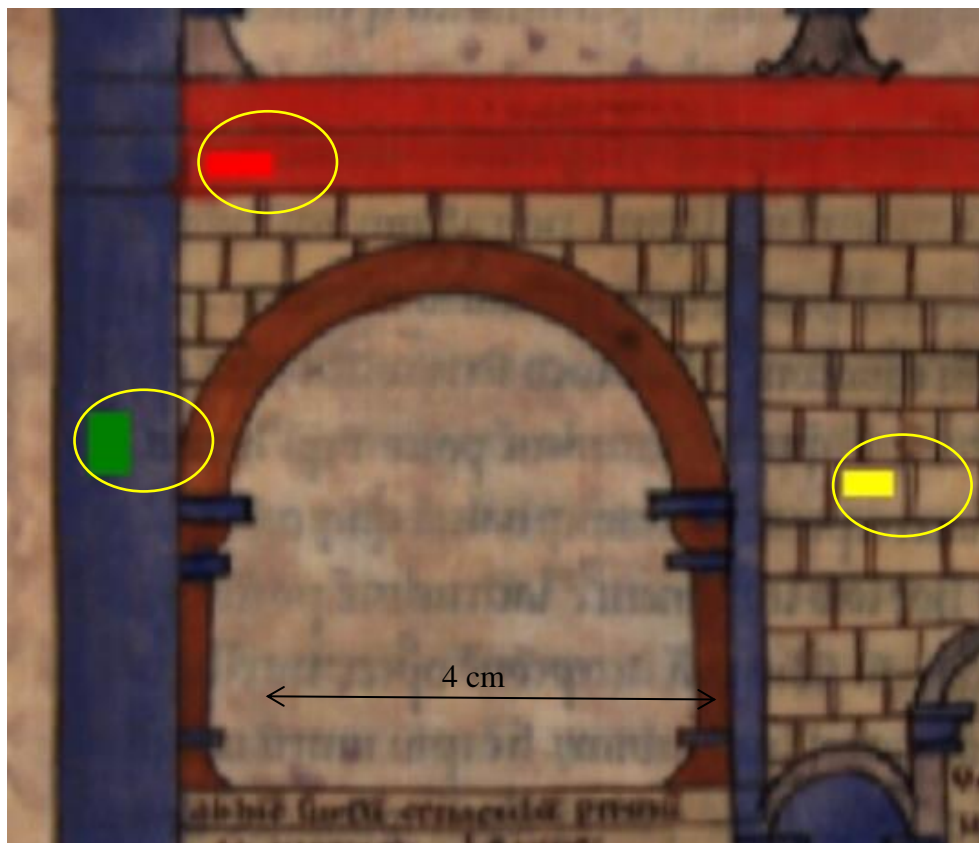


Figure 6.11. The rectangles marked on this Jpeg image of a section of Bodl 394 represent the regions of interest from which average spectra were taken on day 0, and day 111 of the “Thinking in 3D” display. These rectangles have been circled on this jpeg for ease of viewing.

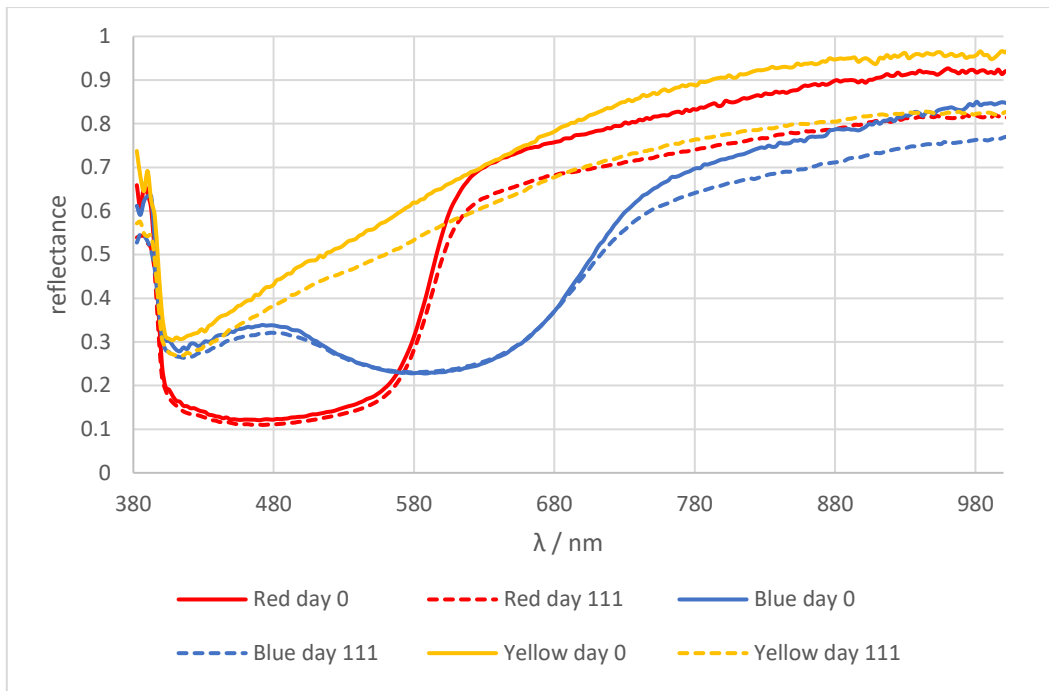


Figure 6.12. Six reflectance spectra taken from Bodl. 394. Day 0 spectra were taken before the manuscript was placed in its current display. Day 111 spectra were taken after the manuscript had been on display for 111 days.

The average spectra of all the pixels in each area produced the spectra given in *Figure 6.12*. There is clearly a difference between all day 0 spectra and their day 111 counterparts, indicative of a colour change. Changes in the red and blue pigments are mainly confined to the red end of the spectrum. Changes in the yellow pigment affect a greater range of wavelengths.

Area of analysis	ROI pixel count day 0	ROI pixel count day 111	$\Delta E_{0-111\text{days}}$ (44.4 Klux hours)
Red	260	264	3.28
Blue	400	408	2.57
Yellow	200	220	4.55

Table 6.3. Colour change values calculated from VNIR HSI reflectance spectra data for select Bodl. 394 pigments. These are the colour differences between two sets of VNIR HSI reflectance spectra, ones taken before and after a period of 111 days on display.

Spectra are averages from the regions of interest (ROIs) shown in Figure 6.11.

This trend can be quantified for the 3 pigments using CIELAB colour difference values (Table 6.3). Such colour change values are unexpectedly large for a display period of 111 days. Colour change values of < 2.3 are considered not noticeable by the eye as would be expected of short display items under controlled, museum conditions. As all the ΔE values for Bodl. 394 were calculated to be above the expected range, radiometric normalisation was performed on the data cubes. ENVI includes a programming package that can be used to initialise data processing not included in the standard software package *C. Li & H. Xu (2009)*. Radiometric normalisation must be initialised in this manner, and the code used for doing so here is shown below.

```

; Start the application
e=ENVI()

; Open two input files
File1=Filepath('dayz.tif', $

```

```

Root_Dir=e.Root_Dir)

Raster1 = e.OpenRaster(File1)

File2=Filepath('dayo.tif', $
Root_Dir=e.Root_Dir)

Raster2 = e.OpenRaster(File2)

; Get the task from the catalogue of ENVI tasks
Task=ENVITask('ImageIntersection')

;Define inputs
Task.INPUT_RASTER1=Raster1
Task.INPUT_RASTER2=Raster2

; Run the task
Task.Execute

; Get the task from the catalogue of ENVI tasks
RadNormTask = ENVITask('RadiometricNormalization')

; Define the inputs
RadNormTask.INPUT_RASTER1=Task.OUTPUT_RASTER1
RadNormTask.INPUT_RASTER2=Task.OUTPUT_RASTER2

; Run the task

```

RadNormTask.**Execute**

; Get the collection of data objects currently available in the Data

Manager

DataColl = e.Data

; Add the output to the data manager

DataColl.**Add**, RadNormTask.OUTPUT_RASTER

; Display the result

View = e.**GetView**()

Layer = View.**CreateLayer**(RadNormTask.OUTPUT_RASTER)

This code produces a corrected version of the data cube taken on day 111 taking into account differences in the equipment at the time of acquisition compared to day 0. It follows the two-step method of *Chander & Markham (2003)* by first converting the digital number of the raw imagery into the at-satellite spectral radiance value, then converting the spectral radiance values to reflectance values. This is known as illumination correction model (ICM) normalisation C. Li & H. Xu (2009).

To demonstrate the effect of this procedure, spectra were taken from all 3 data cubes (the two original scans and the corrected one). The spectra (taken from the region shown in *Figure 6.14*) are shown in *Figure 6.13*. The decision was made to take the spectra from a region of interest that had not previously been examined so as to clearly differentiate this experiment from others. The concept explored here, that radiometric

normalisation can account for the unexpectedly large colour change values, is viewed as a separate issue more clearly demonstrated by focussing on only one region of interest.

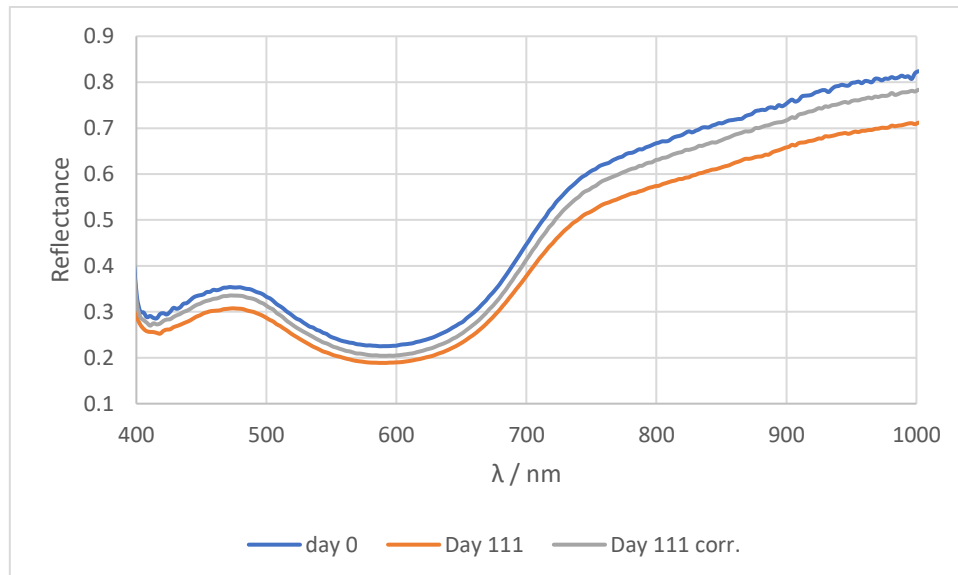


Figure 6.13. Reflectance spectra from the area of Bodl. 394 highlighted in Figure 6.14. Day 0 scans were taken prior to display, Day 111 was taken on the 111th day using the same equipment setup. After correction for unavoidable variation in the illumination the spectrum from Day 111 corr. more closely matches that of the spectrum from Day 0.

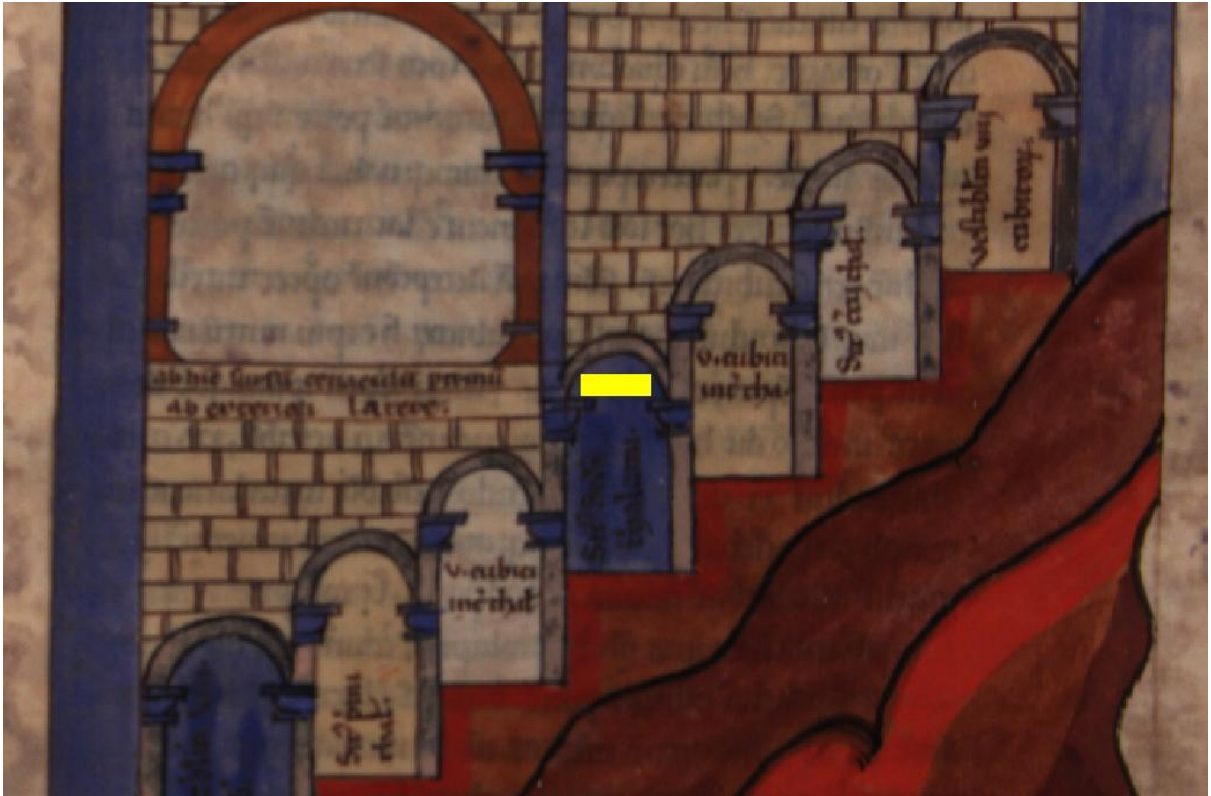


Figure 6.14 The area of Bodl. 394 that was used to demonstrate the effect of the Radiometric Normalisation process.

The corrected day 111 spectrum, and the day 0 spectrum are more similar than the day 0, and day 111 (uncorrected). This is reflected in the CIELAB colour change values, shown in *Table 6.4*. Notably ΔE for the region of interest has now been reduced to beneath 2.3 as expected for this display period.

Colour space values	L	a	b	
Day 0	58.49	-2.96	-10.07	
Day 111	54.55	-3.00	-10.62	
Day 111 corr.	56.53	-3.31	-10.92	
Colour change values	ΔE	ΔL	Δa	Δb
Day 0 & Day 111	3.98	-3.94	-0.04	-0.55
Day 0 & Day 111 corr.	2.17	-1.96	-0.34	-0.86
Day 111 & Day 111 corr.	2.03	1.98	-0.30	-0.30
	Standard deviation	Uncertainty		
Day 0 reflectance values	0.01	0.42 %		
Day 111 reflectance values	0.01	0.47 %		
Day 111 (corrected) reflectance values	0.01	0.43 %		

Table 6.4. Showing the effect of radiometric normalisation on the CIELAB values as calculated for the 3 data cubes for Bodl. 394.

For Table 6.4 standard deviation values were given for the reflectance values at each wavelength by the ENVI software and were combined to give a final standard deviation value for each dataset by summation in quadrature. Percentage uncertainty values were calculated according to

Equation 6.6 for the reflectance value at each wavelength, and final values were calculated by summation in quadrature.

$$\% \text{ Uncertainty} = \frac{\text{Smallest increment measured by equipment} \times n}{\text{Reading}} \times 100$$

Equation 6.6: Percentage uncertainty. Where n is the number of readings, in this case the number of pixels in the region of interest.

The spectral hourglass wizard was also applied to the data cubes for day 0, and day 111 (corrected) to determine the material diversity. Figure 6.15 and Table 6.5

provide the Eigenvalue data for day 0. Once again the decision was made to display only the 10 most significant bands.

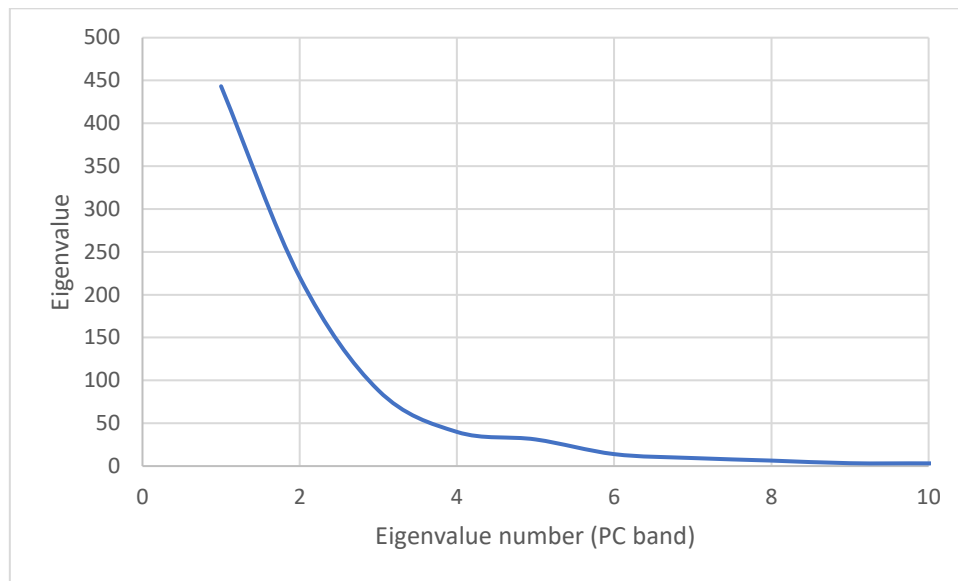


Figure 6.15. Plot of eigenvalues vs principal components used to determine the data dimensionality of the data cube for Day 0: Bodl. 394.

Eigenvalue number (PC band)	Eigenvalue (SUM = 1189.353)	% total variance	Cumulative % variance
1	443.278406	37.27	37.27
2	220.421855	18.53	55.80
3	88.414422	7.43	63.24
4	39.890185	3.35	66.59
5	31.101603	2.62	69.21
6	13.965186	1.17	70.38
7	9.390176	0.79	71.17
8	6.42803	0.54	71.71
9	3.359664	0.28	71.99
10	3.169943	0.27	72.26

Table 6.5. Eigenvalue data for Day 0: Bodl. 394 showing that the first 10 principle components contain 72 % of the data.

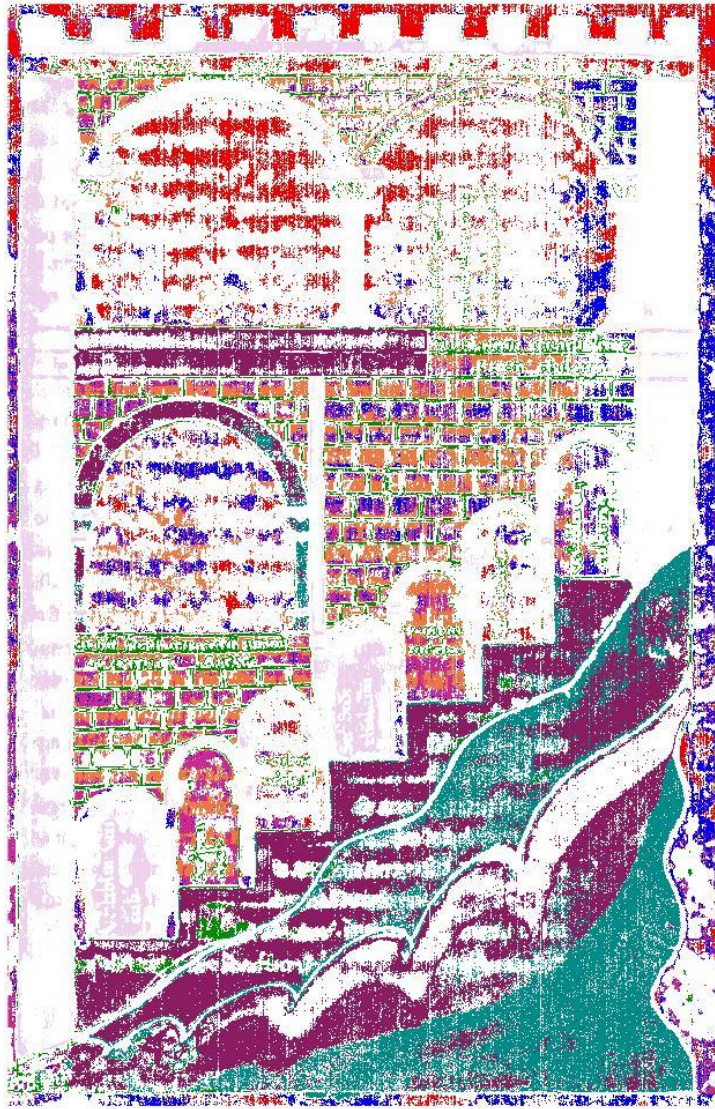


Figure 6.16. Pixels of the endmembers for Day 0: Bodl 394, the spectra for which are shown in Figure 6.17.

Figure 6.16 gives the product of the SAM classification, showing only the 10 most significant endmembers (plotted in *Figure 6.17*). *Figure 6.18* shows the spectra used to generate the plot of day 111 corrected, shown in *Figure 6.19*. The Eigenvalue data for the scans shows that the number of unclassified pixels dropped from 8 – 5 % between day 0, and day 111, and that for day 111 the top ten bands accounted for 79 % of the data. For day 0, the top 10 bands accounted for 72 % of the data whereas the top 4

bands alone accounted for 73 % of the data for day 111. More experimentation would be required before relating this to any loss in material diversity. Comparison of the false colour images certainly demonstrates a change though given the low ΔE value it is unlikely that this is attributable to any alteration in pigmentation owing to the display conditions, rather it is likely that differences in the acquisition conditions have caused the spectral hourglass wizard to group the pixels in a different manner.

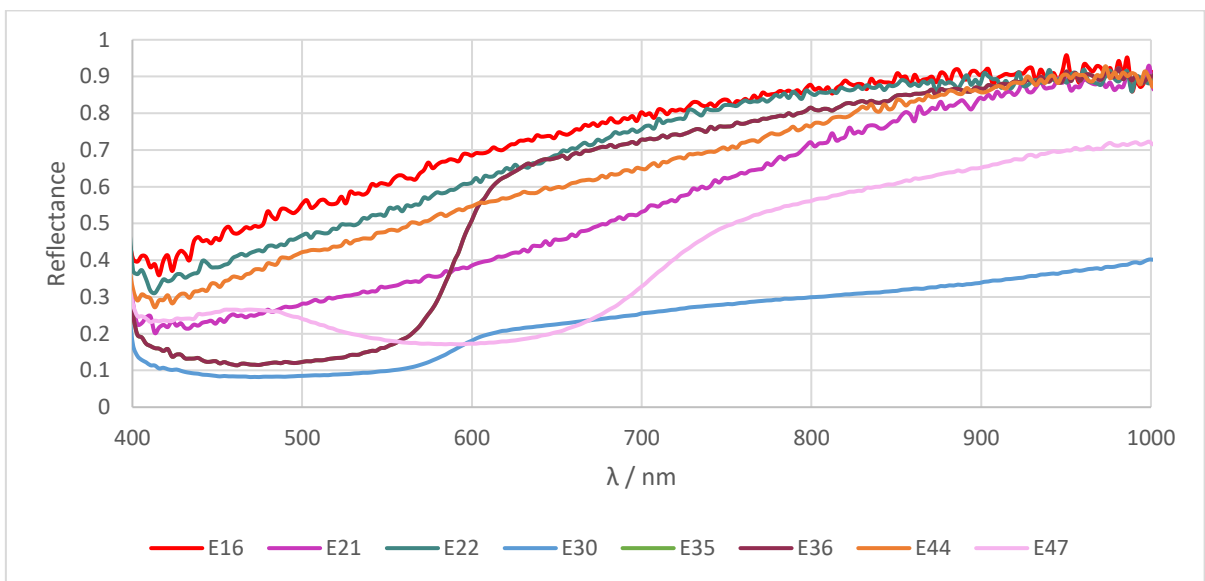


Figure 6.17. The spectra of the most significant endmembers for the hyperspectral scan of Day 0: Bodl.394.

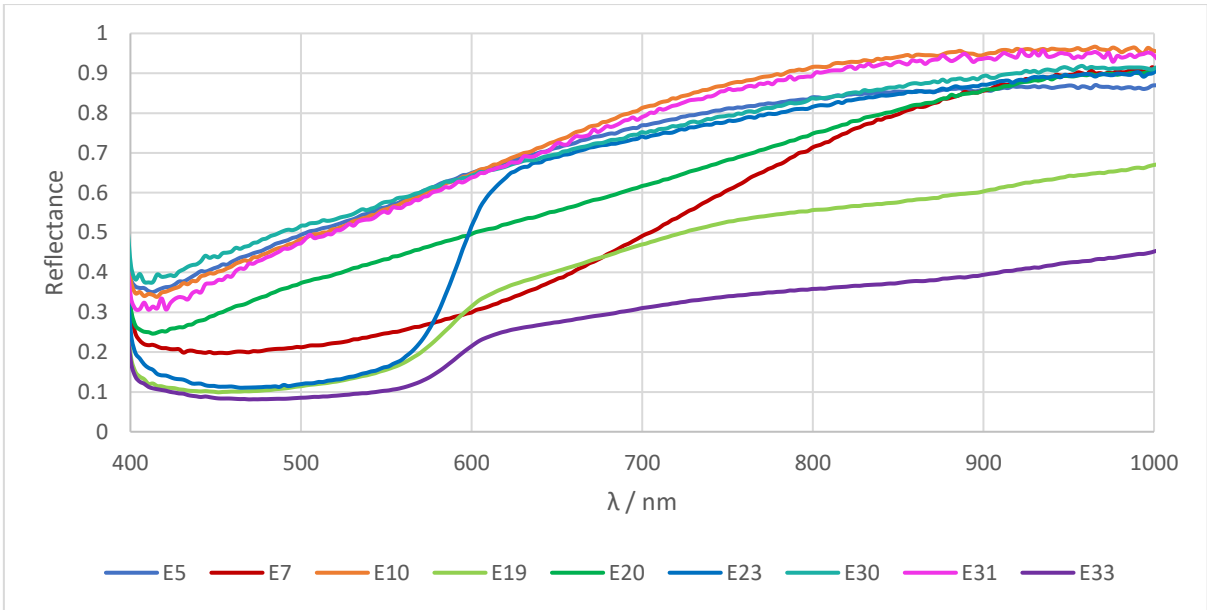


Figure 6.18. The Spectra of the most significant endmembers for Bodl. 394: Day 111 corrected.

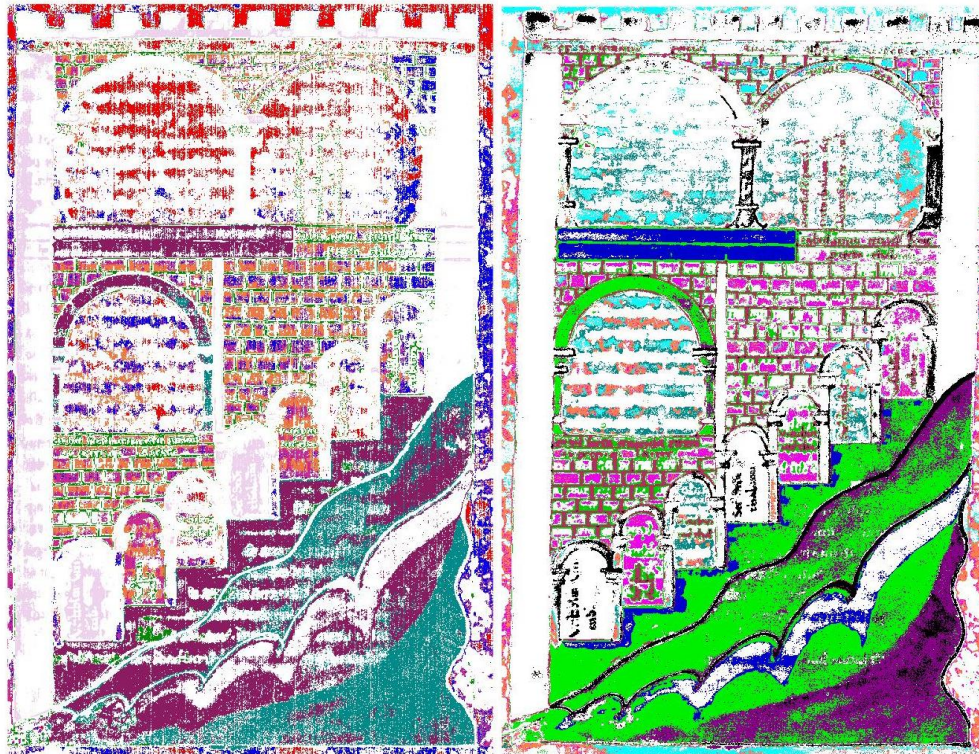


Figure 6.19. False colour images showing the pixels relating to the most relevant endmembers' spectra for Bodl. 394. Left is Day 0, right is Day 111 corrected. There are fewer unclassified pixels for Day 111 corrected, and a greater percentage of data can be found in a fewer number of endmembers but this is not necessarily attributable to loss in material diversity. A low ΔE value supports this interpretation.

6.5 Discussion and conclusion

VNIR HSI was used for the analysis of pigmentation of heritage items that have been on display assessing the fading of a silk robe with an unknown display history. A colour change value was determined within the scan, and principal components analysis used to give a representation of the material diversity in the item. The colour change value obtained by VNIR HSI was similar to the colour change value obtained by DRSP.

Additionally, VNIR HSI was used to assess the effect of a short display period on the pigmentation in an illuminated manuscript, a colour change value was determined for the difference between two scans, and principal components analysis was applied to

assess the change in material diversity between two scans. Radiometric normalisation was applied to the data for the illuminated manuscript in order to provide a better quantitative comparison.

VNIR HSI has been shown to be advantageous for the monitoring of colour change in heritage collection items either as an initial assessment of damage or as a tool for the active monitoring of collection items. Further work could focus on producing an optimal setup for suitable equipment that would enable more consistency in the acquisition of data leading to more accurate measurements.

The data collected in this experiment can be compared with data from a range of other studies. For example, *Amanatiadis et al. (2021)* have carried out a comparable study, using similar equipment. Using a control sheet of pigments representing those common to illuminated manuscripts, they simulated ageing over 150 years in 3 steps of 50 years. They obtained ΔE values of between 1.2 and 11.3 for the first 50 year cycle. Note that these values are not comparable to the ΔE value obtained for the silk robe EAX 3873, as the robe is coloured with dyes, not pigments, and the silk itself provides a different substrate to the one tested by *Amanatiadis et al. (2021)*.

Berns et al. (2005) carried out a comparison between small aperture and image based spectrophotometry for the purposes of monitoring colour change. They found that the difference in spectra from the two techniques was between 2 and 3.2 ΔE_{00} . This is similar to the difference between VNIR HSI and DRSP results from EAX 3873. Note that *Berns et al. (2005)* compared two different methods for identifying colour change and that therefore the ΔE values they give represent the difference between their two competing methodologies not the difference between two colours separated either spatially (as in the case of EAX 3873) or temporally (as in the case of Bodl. 394) however, they do draw some useful conclusions firstly their system had high uncertainty

at shorter wavelengths, something that this VNIR HSI equipment can suffer from, and secondly their spectral matches for flat spectra were worse than for other samples but that their equipment could be used for mapping and identification nonetheless.

Delaney et al. (2010a) used the N-d visualiser in ENVI to find endmember spectra and used SAM to classify the pigments identified as has been done here, however, their setup allowed scanning up to 1680 nm offering an advantage over the equipment used here and the monitoring of a subject over time was not attempted. *Bai et al. (2019)* used gram matrix and endmember analysis to estimate pigment diversity within colours i.e. the separation of the data cube not just into different colours, but into differences within each class. *Bai et al. (2019)* found that compared to SAM, the Mahalanobis distance classifier in ENVI provided the most visually accurate mask.

Kaew-On et al. (2020) used a VSC 8000 (a document examination system developed for forensics applications) in order to investigate colour change. They utilised MSI and HSI to investigate degradation that has already been analysed with invasive techniques in order to investigate how the non-invasive techniques handle the same thing. Transforming their data into CIELAB to calculate ΔE , they found ΔE values comparable to those generated in this experiment. They further analyse the CIELAB data to raise an interesting point that the ΔL are greater than Δa and Δb for their sample which meant that the lightness changed more than the chroma and hue which is also replicated in this experiment.

Similar to *Berns et al. (2005)*, *Kaew-On et al. (2020)* found that the VNIR HSI range was insufficient to provide perceptible differences for shorter exposure times (up to 50 hours accelerated fading, arguing that the NIR functionality of the VSC (900 – 1700 nm) would be more appropriate. This shows the advantage of the VSC over stand-

alone HSI for document examination, they were able to use the VSC for IR fluorescence when the 400 – 1000 nm range proved insufficient.

In a direct comparison with DRSP equipment, VNIR HSI was able to provide a satisfactory value for ΔE with the two techniques giving values within $\Delta E = 3$ of each other demonstrating that within a single scan VNIR HSI could be used to assess the condition of collection items.

VNIR HSI was capable of providing a satisfactory value of ΔE for a comparison between two data cubes however it did require the data to be corrected, indicative of the difficulties faced by the equipment for the discrimination of minor fading, findings which were mirrored in the literature.

Similarly the PCA output for the EAX 3873 was satisfactory, giving a good representation of the material diversity for the given data cube which could be utilised by conservators for collection management. PCA analysis and subsequent comparison of the data for Bodl. 394 however demonstrated that even after correction of the data cube the two PCA outputs were dissimilar and results could not be related to any data driven explanation. It is therefore difficult to recommend PCA analysis of VNIR HSI data for the comparison of two data cubes, but it can be of use for the analysis of a single data cube, once again mirroring findings in the literature.

VNIR HSI can be utilised as one part of a more comprehensive evaluation of the conditions of collection items. It offers advantageous scanning, analytical, and digitisation capabilities but can suffer from high uncertainty in the results, access to equipment, and analysis time.

Section 3: Concluding section

Chapter 7 Overall thesis discussion and conclusions

This thesis aimed to investigate how well hyperspectral imaging in the range of 400 – 1000 nm worked with regards to three applications of importance to library and museum conservation teams, namely the characterisation, location, and monitoring of colourants in their collections. Three experiments were carried out in order to determine the best use of the VNIR HSI equipment held at the Bodleian Libraries for the three purposes. These involved case studies from the collections of the Bodleian Libraries and the Ashmolean Museum in order to demonstrate the utility of the equipment.

The conclusions of the individual experiments, in response to the research questions, can be found within each paper and so this section of the thesis will discuss the broader ramifications of the experiments taken as a whole with regards to the aim of the thesis.

7.1 Experimental decisions

Experimental design was simple, the VNIR HSI equipment was tested against a tried and tested technique, or range of techniques, for one specific purpose in each experiment. When possible the techniques were used on collection items, to demonstrate real world applications.

For Research Question 1 the choice of Raman spectroscopy as the complementary method was a strong choice as it gives unequivocal identification of certain pigments. This fact allowed for a percentage accuracy to be given to the VNIR HSI equipment for the range of pigments in the study because of the certainty of the Raman spectroscopy identification. On the other hand this has the effect of limiting the study to those pigments which Raman spectroscopy could identify.

For Research Question 2 additional data, from previous studies, was available as well as data obtained throughout the course of the investigation, the most promising of which in terms of mapping the colouration was the photoinduced luminescence study which had been used to map the Egyptian blue pigment. This made a good contrast with the XRF spectroscopy study, performed as part of this thesis, which could identify potential areas of Egyptian blue by way of detecting a Cu signal. Unfortunately there was no data that could be used as a good comparison to VNIR HSI in this instance. Raman spectroscopy was attempted but the fluorescence experienced caused problems, and while the HSI equipment proved useful for identifying the red colouration across the surface of the shrine, other pigments could not be located. Thus for Research Question 2, while it was not possible to assess the accuracy of HSI in the same way as for Research Question 1, advice on the best use of the equipment in this situation should prove useful for others.

For Research Question 3 the choice was made to compare the HSI equipment to DRSP instead of microfideometry, another common technique, because the microfideometer predicts lightfastness based on a micro-destructive test, which is fundamentally different from the desired application of the hyperspectral imager. It was fortuitous for the investigation that the conservation team at the Bodleian had been experiencing issues with their current methodology. The DRSP they currently use is a contact method which is undesirable for their collections and makes the application of the technique to their collections difficult. It was possible to scan an illumination as part of a manuscript that was on a short display in the Weston Library and The Ashmolean Museum provided an article which had an uncertain history regarding the fading seen across it.

7.2 Review of the aim and research questions

Aim: What is the efficacy of VNIR HSI for the evaluation of the colouration of items of cultural significance in museum and archive collections?

7.2.1 Research question 1

What is the efficacy of the equipment in terms of chemical characterisation?

The VNIR HSI equipment used was given a percentage accuracy of 93 % at best, however this was achievable only through the manipulation of the methodology whilst in full possession of the knowledge of the identity of the colourant being scanned. Had the methodology been left as is, and VNIR HSI were asked to identify a colourant without assistance from the operator, the percentage accuracy could be as low as 9 %.

To what extent can reflectance spectra produced by VNIR HSI be differentiated so that different chemicals may be identified?

It became clear that the VNIR wavelength range was insufficient for the absolute identification of colourants in works of cultural heritage owing to the lack of characteristic peaks that would be available in SWIR detectors. However it was shown that the hyperspectral equipment can nonetheless be of great assistance for the characterisation of the surface of these works of art. *Figure 4.5* demonstrates the ability of the equipment to analyse the surface of one of the Armenian manuscripts analysed for Paper 1. It is especially powerful when used in conjunction with another technique that is more capable of positively identifying colourants, such as Raman spectroscopy,

in which case VNIR HSI can characterise the heterogeneity of the surface and the different areas of colourant can then be identified. The strengths of VNIR HSI for this purpose are that it can evaluate the surface more rapidly compared to using point techniques alone (in Paper 1 it is alluded to that hyperspectral imaging of the manuscripts could be conducted in 15 minutes, whilst the Raman spectroscopy equipment would need roughly five minutes per point analysed), and that it can point to areas of interest that may have been missed with the naked eye.

7.2.2 Research Question 2

What is the efficacy of VNIR HSI equipment in terms of identifying the spatial location of colourants?

In general this is governed by two properties, the spatial resolution and the spectra of the equipment used. In this case it was found that the utility of the VNIR HSI equipment for this purpose was limited by the mainly visible spectra that it produces in two ways, firstly it was unable to detect colourants that did not reflect in the visible portion of the electromagnetic spectrum, and secondly as Paper 1 demonstrated it could not sufficiently differentiate between different colourants with spectra that were similar in the range detected.

This made it less capable than techniques such as multispectral imaging, that would have been able to map colourants such as Egyptian blue, and possibly detect colouration in the infrared region as well. As it was, only the reflectance spectra of a red colourant

could be reliably detected across the surface of the shrine. Though the presence of Egyptian blue is known, the VNIR HSI equipment was unable to detect it.

While the size of the shrine did greatly increase the scanning time, and the heterogeneity of the surface further complicated the analysis of the data, it was still possible to use the hyperspectral equipment to generate a false colour map of red colouration across the shrine, which enhanced the colouration seen by the naked eye.

7.3.3 Research Question 3

What is the efficacy of the equipment in regards to the monitoring of a subject over a period of time? Is the equipment sensitive enough to provide useful information to conservators with regards to the damage caused by photo-degradation from typical exhibition exposures?

The series of experiments conducted in Paper 3 demonstrate the utility of VNIR HSI for this purpose. The reflectance data obtained is comparable to that obtained from similar techniques such as the DRSP used in this thesis and yet the VNIR HSI equipment is non-destructive, non-contact, and capable of rapidly analysing a much larger area, in more detail. If the precision of the VNIR HSI equipment could be improved it's utility would be significant.

7.3 Future research

For Research question 1, future work could include the expansion of the percentage accuracy to include a more diverse range of pigments, this would of course require a larger sample set, and sufficient artefacts to cover a range of pigments,

binders, and supports, so as to increase the applicability. Mixtures of pigments could also be investigated, due to their prevalence in real world collections.

For Research Question 2 further study could be made into the investigation of mapping faded pigments by the expansion of materials involved in the study. The size of the Shrine proved prohibitive in terms of the quantity of scanning required, and so the number of pigments investigated in this study was limited by necessity. Furthermore it would be most insightful to investigate the mapping of faded pigments on other support media. The sandstone background to the shrine investigation was complex in terms of the hyperspectral data cube, as it provided a background that was highly heterogenous which greatly complicated the analysis.

For Research Question 3 further study could once again involve the expansion of the experiment to incorporate other pigments, dyes, and support media. It could also be expanded so as to allow for more direct comparisons between DRSP and VNIR HSI.

Generally the usefulness of the current equipment has been demonstrated, and future research could focus on the improvement of the equipment. It has been shown that the VNIR wavelength range is insufficient for certain tasks and research and development in the field of hyperspectral imaging should aim to make the higher wavelengths more affordable. It would also be advantageous to increase the spatial resolution of the equipment, as at present multispectral imaging far exceeds hyperspectral imaging in this capacity. Literature has shown an ongoing effort to increase the speed and usefulness of the computational algorithms used to evaluate the hyperspectral data cube which will certainly help the user successfully mine the data generated in a practicable, user friendly manner. One last avenue of research ought to involve the improvement of precision, as this inhibits the usefulness of the data generated.

7.4 Concluding remark – take home message

VNIR HSI has the potential to aid in the work of museum and library conservation teams, both as a routine method, for the monitoring of artefacts, and as part of an analytical suite concerned with the characterisation of a surface. As a compromise between the cost of higher wavelength detectors and the analytical capability that they provide, VNIR HSI has been shown to be capable of providing sufficient analytical data so as to be practicably useful to a conservation team.

The three different experiments have demonstrated the versatility of the equipment for the analysis of different support mediums and the associated colourants, and taken as a whole this thesis has demonstrated that VNIR HSI is useful in the characterisation of colourants, the loss of those colourants over time, and the investigation of the inevitable faded artefact thus this technique can be of use to whole spectrum of desired applications.

Chapter 8 Declaration of Funding

This project was co-funded by EPSRC (as part of the Science and Engineering in Arts, Heritage, and Archaeology Centre for Doctoral Training (SEAHA CDT)) and the University of Oxford through a Fell Fund award. Grant number EP/L016036/1.

Chapter 9 References

- Abdrabou, A., M. Abdalla, *et al.* (2018): Investigation of an ancient Egyptian polychrome wooden statuette by imaging and spectroscopy. *International Journal of Conservation Science* (9)1: 39–54.
- Abdrabou, A., M. Abdallah, *et al.* (2017): Scientific investigation by technical photography, OM, ESEM, XRF, XRD and FTIR of an ancient Egyptian polychrome wooden coffin. *Conservar Patrimonio* 26: 51–63.
- Aceto, M., A. Agostino, *et al.* (2014): Characterisation of colourants on illuminated manuscripts by portable fibre optic UV-visible-NIR reflectance spectrophotometry. *Analytical Methods* (6): 1488–1500.
- Adriaens, A. (2005): Non-destructive analysis and testing of museum objects: An overview of 5 years of research. *Spectrochimica Acta Part B: Atomic Spectroscopy* (60)12: 1503–1516.
- Alfieri, P.V., D. Alves, *et al.* (2020): Non-destructive diagnose of the biodeterioration of heritage assets through an optical microscopy. *Journal of Cultural Heritage*.
- Amanatiadis, S., G. Apostolidis, *et al.* (2021): Consistent Characterization of Color Degradation Due to Artificial Aging Procedures at Popular Pigments of Byzantine Iconography. *Minerals* (11)7.
- Amat, A., C. Miliani, *et al.* (2013): Non-invasive multi-technique investigation of artworks: A new tool for on-the-spot data documentation and analysis. *Journal of Cultural Heritage* (14)1: 23–30.
- Ambers, J. (2004): Raman analysis of pigments from the Egyptian Old Kingdom. *Journal of Raman Spectroscopy* (35)8–9: 768–773.
- Ando, Y., A. Hansuebsai, *et al.* (1997): Digital restoration of faded color images by subjective method. *Journal of Imaging Science and Technology* (41)3: 259–265.
- Anon (1992): *The shrine of Taharqa*. Ashmolean Museum, Oxford.
- Armstrong, C.H. (2015): The two non-blue amuns of the shrine of taharqa at kawa. *Journal of Egyptian Archaeology* (101): 177–195.
- Arrizabalaga, I., O. Gómez-Laserna, *et al.* (2014): Applicability of a diffuse reflectance infrared Fourier transform handheld spectrometer to perform in situ analyses on cultural heritage materials. *Spectrochimica Acta Part A: Molecular and Biomolecular Spectroscopy* (129): 259–267.
- Artforum (2019): Classicist Receives Death Threats from Alt-Right over Art Historical Essay. Available from: <https://www.artforum.com/news/classicist-receives-death-threats-from-alt-right-over-art-historical-essay-68963>.

- Artioli, G. (2010): *Scientific methods and cultural heritage [electronic resource] : an introduction to the application of materials science to archaeometry and conservation science*. Oxford University Press, Oxford.
- Attas, M., E. Cloutis, *et al.* (2003): Near-infrared spectroscopic imaging in art conservation: investigation of drawing constituents. *Journal of Cultural Heritage* (4): 127–136.
- Bacci, M. (1995): Fibre optics applications to works of art. *Sensors and Actuators B: Chemical* (29)1–3: 190–196.
- Bai, D., D.W. Messinger, *et al.* (2019): A hyperspectral imaging spectral unmixing and classification approach to pigment mapping in the Gough & Selden Maps. *Journal of the American Institute for Conservation* (58)1–2: 69–89.
- Bakirov, B., S. Kichanov, *et al.* (2020): Studies of Coins of Medieval Volga Bulgaria by Neutron Diffraction and Tomography. *Journal of Surface Investigation: X-ray, Synchrotron and Neutron Techniques* (14): 376–381.
- Balas, C., V. Papadakis, *et al.* (2003): A novel hyper-spectral imaging apparatus for the non-destructive analysis of objects of artistic and historical value. *Journal of Cultural Heritage* (4): 330s–337s.
- Balta, I., S. Pederzoli, *et al.* (2009): Dynamic secondary ion mass spectrometry and X-ray photoelectron spectroscopy on artistic bronze and copper artificial patinas. *Applied Surface Science* (255)12: 6378–6385.
- Barat, B.R., E. Cano, *et al.* (2021): Design and validation of tailored colour reference charts for monitoring cultural heritage degradation. *Heritage Science* (9)1: 1–9.
- Barnett, J.R., S. Miller, *et al.* (2006): Colour and art: A brief history of pigments. *Optics & Laser Technology* (38)4: 445–453.
- Baronian, S. & F.C. Conybeare (1918): *Catalogue of the Armenian Manuscripts in the Bodleian Library*. The Clarendon Press, Oxford.
- Barrile, V., A. Fotia, *et al.* (2018): Geomatics and augmented reality experiments for the cultural heritage. *Applied Geomatics* (10)4: 569–578.
- Bayarri, V., M.A. Sebastián, *et al.* (2019): Hyperspectral Imaging Techniques for the Study, Conservation and Management of Rock Art. *Applied Sciences* (9)23.
- BBC (2019): When the Parthenon had dazzling colours. Available from: <http://www.bbc.com/culture/story/20180119-when-the-parthenon-had-dazzling-colours>.
- Beeby, A., R. Gameson, *et al.* (2016): Illuminators' Pigments in Lancastrian England. *Manuscripta* (60)2: 143–164.
- Berke, H. (2002): Chemistry in Ancient Times: The Development of Blue and Purple Pigments. *Angewandte Chemie International Edition* (41)14: 2483–2487.

- Berns, R.S., L.A. Taplin, *et al.* (2005): A Comparison of Small-Aperture and Image-Based Spectrophotometry of Paintings. *Studies in Conservation* (50)4: 253–266.
- Berrie, B.H. (2012): Rethinking the History of Artists' Pigments Through Chemical Analysis. *Annual Review of Analytical Chemistry* (5)1: 441–459.
- Berry, M. (1999): A Study of Pigments from a Roman Egyptian Shrine. *AICCM Bulletin* (24)1: 1–9.
- Bitossi, G., R. Giorgi, *et al.* (2005): Spectroscopic Techniques in Cultural Heritage Conservation: A Survey. *Applied Spectroscopy Reviews* (40)3: 187–228.
- Blackburn, G.A. (2007): Hyperspectral remote sensing of plant pigments. *Journal of Experimental Botany* (58)4: 855–867.
- Bloechl, K., H. Hamlin, *et al.* (2010): Text Recovery from the Ultraviolet-Fluorescent Spectrum for Treatises of Archimedes Palimpsest. *SPIE-IS&T* (7531): 753109-1-753109-9.
- Blümich, B., F. Casanova, *et al.* (2010): Noninvasive testing of art and cultural heritage by mobile NMR. *Accounts of chemical research* (43)6: 761–770.
- Boardman, J. & F. Kruse (1994): Automated spectral analysis: a geological example using AVIRIS data, North Grapevine Mountains, Nevada: in Proceedings, ERIM tenth thematic conference on geologic remote sensing. *Environmental Research Institute of Michigan, Ann Arbor, MI, pp. 1-407-1-418.*
- Bonaduce, I., E. Ribechini, *et al.* (2016): Analytical approaches based on gas chromatography mass spectrometry (GC/MS) to study organic materials in artworks and archaeological objects. *Topics in Current Chemistry* (374)1: 6.
- Bonifazi, G., G. Capobianco, *et al.* (2019): Hyperspectral Imaging as Powerful Technique for Investigating the Stability of Painting Samples. *Journal of Imaging* (5)1.
- Boudin, M., M. Van Strydonck, *et al.* (2015): RICH—a new AMS facility at the Royal Institute for Cultural Heritage, Brussels, Belgium. *Nuclear Instruments and Methods in Physics Research Section B: Beam Interactions with Materials and Atoms* (361): 120–123.
- Boukezzoula, R., D. Coquin, *et al.* (2020): A possibilistic regression based on gradual interval B-splines: Application for hyperspectral imaging lake sediments. *Information Sciences* (510): 183–204.
- Bracci, S., O. Caruso, *et al.* (2015): Multidisciplinary approach for the study of an Egyptian coffin (late 22nd/early 25th dynasty): Combining imaging and spectroscopic techniques. *Spectrochimica Acta Part A: Molecular and Biomolecular Spectroscopy* (145): 511–522.
- Bradley, M. (2009): THE IMPORTANCE OF COLOUR ON ANCIENT MARBLE SCULPTURE. *Art History* (32)3: 427–457.

- Brambilla, A., I. Osticioli, *et al.* (2011): A remote scanning Raman spectrometer for in situ measurements of works of art. *Review of Scientific Instruments* (82)063109: 1–8.
- Bratasz, L. & E. Manikowska (2020): Heritage Science - The Benefits of an Interdisciplinary Approach in Protecting Cultural Heritage Interviews. *Santander Art and Culture Law Review (SAACLR)* (2020)2: 17–24.
- Brecoulaki, H. (2019): COLOUR IN ANCIENT ART - (P.) Jockey (ed.) Les arts de la couleur en Grèce ancienne ... et ailleurs. Approches interdisciplinaires. (BCH Supplément 56.) Pp. 508, b/w & colour figs, b/w & colour ills, maps. Athens: École Française d'Athènes, 2018. Paper, €80. ISBN: 978-2-86958-290-3. *The Classical Review* (69)2: 602–605.
- Brocx, M. & V. Semeniuk (2007): Geoheritage and geoconservation - History, definition, scope and scale. *Journal of the Royal Society of Western Australia* (90)2: 53–87.
- Brommelle, N.S. (1964): The Russell and Abney Report on the Action of Light on Water Colours. *Studies in Conservation* (9)4: 140–152.
- Brown, K.L. & R.J.H. Clark (2004): The Lindisfarne Gospels and two other 8th Century Anglo-Saxon/Insular manuscripts: Pigment identification by Raman microscopy. *Journal of Raman Spectroscopy* (35): 4–12.
- Burattini, S. & E. Falcieri (2020): Scanning and transmission electron microscopy in cultural heritage: State of the art. *Microscopie*.
- Burgess, A.E. (1999): The Rose model, revisited. *J. Opt. Soc. Am. A* (16)3: 633–646.
- Burgio, L., R.J.H. Clark, *et al.* (2005): Pigment identification by spectroscopic means: Evidence consistent with the attribution of the painting Young Woman seated at a Virginal to Vermeer. *Anal. Chem.* (77): 1261–1267.
- Burnstock, A., I. Lanfear, *et al.* (2005): 1 Preprints of the 14th Triennial Meeting of the ICOM Committee for Conservation *Comparison of the fading and surface deterioration of red lake pigments in six paintings by Vincent van Gogh with artificially aged paint reconstructions*.
- Burrows, A. (2009): *Chemistry³: introducing inorganic, organic and physical chemistry*. Oxford University Press, Oxford.
- Buti, D., F. Rosi, *et al.* (2013): In-situ identification of copper based green pigments on paintings and manuscripts by reflection FTIR. *Anal Bioanal Chem* (405): 2699–2711.
- C. Li & H. Xu (2009): Automatic Absolute Radiometric Normalization of Satellite Imagery with ENVI/IDL Programming. In: *2009 2nd International Congress on Image and Signal Processing*. , pp. 1–4.
- Cabelli, C.D. & T.F. Mathews (1982): The Palette of Katchatur of Khizan. *The Journal of The Walters Art Gallery* (40): 37–40.

- Cabelli, D.E., M.V. Orna, *et al.* (1984): Analysis of Medieval Pigments from Cilician Armenia. In: *Archaeological Chemistry III*. American Chemical Society, pp. 243–254.
- Canty, M.J. & A.A. Nielsen (2008): Automatic radiometric normalization of multitemporal satellite imagery with the iteratively re-weighted MAD transformation. *Remote Sensing of Environment* (**112**)3: 1025–1036.
- Capitani, D., V. Di Tullio, *et al.* (2012): Nuclear magnetic resonance to characterize and monitor cultural heritage. *Progress in nuclear Magnetic resonance Spectroscopy* (**64**): 29–69.
- Cardeira, A.M., S. Longelin, *et al.* (2016): Analytical characterisation of academic nude paintings by José Veloso Salgado. *Spectrochimica Acta Part A: Molecular and Biomolecular Spectroscopy* (**153**): 379–385.
- Casadio, F., S. Xie, *et al.* (2011): Electron energy loss spectroscopy elucidates the elusive darkening of zinc potassium chromate in Georges Seurat's A Sunday on La Grande Jatte—1884. *Analytical and bioanalytical chemistry* (**399**)9: 2909–2920.
- Casali, F. (2006): X-ray and neutron digital radiography and computed tomography for cultural heritage. *Physical techniques in the study of art, archaeology and cultural heritage* (**1**): 41–123.
- Casey, R.P. (1931): Armenian Manuscripts of St Athanasius of Alexmdra. *Harvard theological review* (**24**)1: 43–59.
- Catelli, E., L.L. Randeberg, *et al.* (2017): An explorative chemometric approach applied to hyperspectral images for the study of illuminated manuscripts. *Spectrochimica Acta Part A: Molecular and Biomolecular Spectroscopy* (**177**): 69–78.
- Cavaleri, T., A. Giovagnoli, *et al.* (2013): Pigments and Mixtures Identification by Visible Reflectance Spectroscopy. *Procedia Chemistry* (**8**): 45–54.
- Centeno, S.A. (2015): Identification of artistic materials in paintings and drawings by Raman spectroscopy: some challenges and future outlook. *Journal of Raman Spectroscopy* (**47**): 9–15.
- Chander, G. & B. Markham (2003): Revised Landsat-5 TM radiometric calibration procedures and postcalibration dynamic ranges. *IEEE Transactions on geoscience and remote sensing* (**41**)11: 2674–2677.
- Chaplin, T.D., R.J.H. Clark, *et al.* (2010): A combined Raman microscopy, XRF and SEM–EDX study of three valuable objects – A large painted leather screen and two illuminated title pages in 17th century books of ordinances of the Worshipful Company of Barbers, London. *A Collection of Invited Papers in Honour of Professor Austin Barnes on the Occasion of His 65th Birthday and His Retirement as Editor of Journal of Molecular Structure* (**976**)1: 350–359.

- Chaplin, T.D., L. Jurado-López, *et al.* (2004): Identification by Raman Spectroscopy of pigments on early postage stamps: Distinction between original 1847 and 1858 - 1862, forged and reproduction postage stamps of Mauritius. *Journal of Raman Spectroscopy* (35): 600–604.
- Chiriu, D., F.A. Pisu, *et al.* (2020): Application of Raman Spectroscopy to Ancient Materials: Models and Results from Archaeometric Analyses. *Materials* (13)11: 2456.
- Clark, R.J.H. (2002): Pigment identification by spectroscopic means: an arts/science interface. *C. R. Chimie* (5): 7–20.
- Clarke, M. (2001): The analysis of medieval European manuscripts. *Studies in Conservation* (46)sup 1: 3–17.
- Colomban, P. (2012): The on-site/remote Raman analysis with mobile instruments: A review of drawbacks and success in cultural heritage studies and other associated fields. *Journal of Raman Spectroscopy* (43): 1529–1535.
- Colombini, M.P. & F. Modugno (2009): *Organic mass spectrometry in art and archaeology*. John Wiley & Sons.
- Coren, F., D. Visintini, *et al.* (2005): Integrating LiDAR intensity measures and hyperspectral data for extracting of cultural heritage.
- Cosentino, A. (2014): Identification of pigments by multispectral imaging; a flowchart method. *Heritage Science* (2)1.
- Cotte, M., P. Dumas, *et al.* (2009): Recent applications and current trends in Cultural Heritage Science using synchrotron-based Fourier transform infrared micro-spectroscopy. *Comptes Rendus Physique* (10)7: 590–600.
- Coupry, C., A. Lautié, *et al.* (1994): Contribution of Raman Spectroscopy to Art and History. *Journal of Raman Spectroscopy* (25): 89–94.
- Creagh, D., V. Otieno-Alego, *et al.* (2017): The use of radiation in the study of cultural heritage artefacts. *Radiation Physics and Chemistry* (137): 216–224.
- Creagh, D.C. & D. Bradley (2007): *Physical Techniques in the Study of Art, Archaeology and Cultural Heritage*. Elsevier Science.
- Cséfalvayová, L., M. Strlič, *et al.* (2011): Quantitative NIR Chemical Imaging in Heritage Science. *Analytical Chemistry* (83)13: 5101–5106.
- Cucci, C. & A. Casini (2020): Chapter 3.8 - Hyperspectral imaging for artworks investigation. In: J. M. Amigo (Ed), *Data Handling in Science and Technology*. Elsevier, pp. 583–604.
- Cucci, C., J.K. Delaney, *et al.* (2016): Reflectance Hyperspectral Imaging for Investigation of Works of Art: Old Master Paintings and Illuminated Manuscripts. *Accounts of Chemical Research* (49)10: 2070–2079.

- Cucci, C., M. Picollo, *et al.* (2015): Hyperspectral remote sensing techniques applied to the non-invasive investigation of mural paintings: a feasibility study carried out on a wall painting by Beato Angelico in Florence. *Optics for Arts, Architecture, and Archeology V* (9527): 1–9.
- Cuttle, C. (1996): Damage to museum objects due to light exposure. *International Journal of Lighting Research and Technology* (28)1: 1–9.
- Daintith, J. & E.A. Martin (2010): *A dictionary of science*. Oxford University Press, USA.
- Daniel, F., A. Mounier, *et al.* (2016): Hyperspectral imaging applied to the analysis of Goya paintings in the Museum of Zaragoza (Spain). *Microchemical Journal* (126): 113–120.
- Davies, G.E. & W.M. Calvin (2017): Mapping acidic mine waste with seasonal airborne hyperspectral imagery at varying spatial scales. *Environmental Earth Sciences* (76)12.
- Deborah, H., S. George, *et al.* (2014): Pigment Mapping of The Scream (1983) Based on Hyperspectral Imaging. *Lecture Notes in Computer Science* (8509): 247–256.
- Delaney, J.K., M. Thoury, *et al.* (2016):(a): Visible and infrared imaging spectroscopy of paintings and improved reflectography. *Heritage Science* (4)6: 1–10.
- Delaney, J.K., M. Thoury, *et al.* (2016):(b): Visible and infrared imaging spectroscopy of paintings and improved reflectography. *Heritage Science* (4)6: 1–10.
- Delaney, J.K., J.G. Zeibel, *et al.* (2009): Visible and infrared reflectance imaging spectroscopy of paintings: pigment mapping and improved infrared reflectography. In: International Society for Optics and Photonics, pp. 739103.
- Delaney, J.K., J.G. Zeibel, *et al.* (2010):(a): Visible and Infrared Imaging Spectroscopy of Picasso's Harlequin Musician: Mapping and Identification of Artistic Materials in situ. *Applied Spectroscopy* (64)6: 584–594.
- Delaney, J.K., J.G. Zeibel, *et al.* (2010):(b): Visible and infrared imaging spectroscopy of picasso's harlequin musician: Mapping and identification of artist materials in situ. *Applied Spectroscopy* (64)6: 584–594.
- Denard, H. (2009): The London Charter for the computer-based visualisation of cultural heritage. Available from: <http://www.londoncharter.org/index.html> (January 1, 2019).
- Dietzel, M., H. Kolmer, *et al.* (2008): Desert varnish and petroglyphs on sandstone - Geochemical composition and climate changes from Pleistocene to Holocene (Libya). *Chemie der Erde* (68)1: 31–43.
- Doménech-Carbó, M.T. & L. Osete-Cortina (2016): Another beauty of analytical chemistry: chemical analysis of inorganic pigments of art and archaeological objects. *ChemTexts* (2)3: 14.

- Dooley, K.A., A. Chieli, *et al.* (2020): Molecular Fluorescence Imaging Spectroscopy for Mapping Low Concentrations of Red Lake Pigments: Van Gogh's Painting The Olive Orchard. *Angewandte Chemie - International Edition* (**59**)15: 6046–6053.
- Dooley, K.A., D.M. Conover, *et al.* (2014): Complementary standoff chemical imaging to map and identify artist materials in an early italian renaissance panel painting. *Angewandte Chemie - International Edition* (**53**)50: 13775–13779.
- Douma, M. (2008):(a): Spectroscopy. In Pigments through the ages. Available from: <http://www.webexhibits.org/pigments/intro/spectroscopy.html> (May 20, 2020).
- Douma, M. (2008):(b): *Spectroscopy. In Pigments through the ages.*
- Douma, M. *Spectroscopy. In Pigments through the ages.*
- Dyer, J. & S. Sotiropoulou (2017): A technical step forward in the integration of visible-induced luminescence imaging methods for the study of ancient polychromy. *Heritage Science* (**5**)1.
- E. Kokkinou, K. Wells, *et al.* (2001): Towards room temperature CCD autoradiography: methods for minimizing the effects of dark current at room temperature. In: *2001 IEEE Nuclear Science Symposium Conference Record (Cat. No.01CH37310)*. , pp. 1624–1628 vol.3.
- Edwards, H.G.M., S.E. Jorge Villar, *et al.* (2004): Raman spectroscopic analysis of pigments from dynastic Egyptian funerary artefacts. *Journal of Raman Spectroscopy* (**35**)8-9: 786–795.
- Elkholy, M.M., M. Mostafa, *et al.* (2020): 921 *Comparative Analysis of Unmixing Algorithms Using Synthetic Hyperspectral Data.*
- Ernst, R.R. (2010): In situ Raman microscopy applied to large Central Asian paintings. *Journal of Raman Spectroscopy* (**41**): 275–287.
- Farges, F. & M. Cotte (2016): X-ray absorption spectroscopy and cultural heritage: highlights and perspectives. *X-Ray Absorption and X-Ray Emission Spectroscopy: Theory and Applications*: 609–636.
- Feathers, J.K. (1997): The application of luminescence dating in American archaeology. *Journal of Archaeological Method and Theory* (**4**)1: 1–66.
- Feller, R.L. (1954): Dammar and Mastic Infrared Analysis. *Science* (**120**)3130: 1069.
- Femenias, A., F. Gatiús, *et al.* (2020): Use of hyperspectral imaging as a tool for Fusarium and deoxynivalenol risk management in cereals: A review. *Food Control* (**108**).
- Festa, G., G. Romanelli, *et al.* (2020): Neutrons for Cultural Heritage—Techniques, Sensors, and Detection. *Sensors* (**20**)2: 502.

- Fieberg, J.E., P. Knutås, *et al.* (2017): “paintings Fade Like Flowers”: Pigment Analysis and Digital Reconstruction of a Faded Pink Lake Pigment in Vincent van Gogh’s Undergrowth with Two Figures. *Applied Spectroscopy* (71)5: 794–808.
- Fischer, C. & I. Kakoulli (2006): Multispectral and hyperspectral imaging technologies in conservation: current research and potential applications. *Reviews in Conservation* (7): 3–16.
- Ford, B.L. (1992): Monitoring Colour Change in Textiles on Display. *Studies in Conservation* (37)1: 1–11.
- France, F.G. (2011): Advanced spectral imaging for non-invasive microanalysis of cultural heritage materials: review of application to documents in the U.S. library of congress. *Applied Spectroscopy* (65): 565–574.
- Fulcher, K. (2017): Evidence for the use of madder as a pigment in Nubia. *The Sudan Archaeological Research Society bulletin* (21).
- Fulcher, K. (2018): Painting Amara West: the technology and experience of colour in New Kingdom Nubia. UCL (University College London)
- Garg, V., A. Senthil Kumar, *et al.* (2017): Spectral similarity approach for mapping turbidity of an inland waterbody. *Journal of Hydrology* (550): 527–537.
- Gasanova, S., S. Pagès-Camagna, *et al.* (2018): Non-destructive in situ analysis of polychromy on ancient Cypriot sculptures. *Archaeological and Anthropological Sciences* (10)1: 83–95.
- Gaudiuso, R., M. Dell’Aglia, *et al.* (2010): Laser induced breakdown spectroscopy for elemental analysis in environmental, cultural heritage and space applications: a review of methods and results. *Sensors* (10)8: 7434–7468.
- Gawade, D.R., S. Ziemann, *et al.* (2021): A Smart Archive Box for Museum Artifact Monitoring Using Battery-Less Temperature and Humidity Sensing. *Sensors* (21)14: 4903.
- Gianoncelli, A., J. Castaing, *et al.* (2008): A portable instrument for in situ determination of the chemical and phase compositions of cultural heritage objects. *X-Ray Spectrometry: An International Journal* (37)4: 418–423.
- Gilberg, M. (1987): Friedrich Rathgen: The Father of Modern Archaeological Conservation. *Journal of the American Institute for Conservation* (26)2: 105–120.
- Giles, C.H. (1965): The fading of colouring matters. *Journal of Applied Chemistry* (15)12: 541–550.
- Goler, S., J.T. Yardley, *et al.* (2016): Characterising the age of ancient Egyptian manuscripts through micro-Raman spectroscopy. *Journal of Raman Spectroscopy*: 1–9.
- Gonzales, R. & R. Woods (2010): *Digital Image Processing*. Pearson Education Inc.

- Gonzalez, V., M. Cotte, *et al.* (2020): X-ray diffraction mapping for cultural heritage science: a review of experimental configurations and applications. *Chemistry–A European Journal* (26)8: 1703–1719.
- Green, A.A., M. Berman, *et al.* (1988): A transformation for ordering multispectral data in terms of image quality with implications for noise removal. *IEEE Transactions on geoscience and remote sensing* (26)1: 65–74.
- Grosjean, D., E. Grosjean, *et al.* (1994): Fading of colorants by atmospheric pollutants: reflectance spectroscopy studies. *Science of The Total Environment* (151)3: 213–226.
- Gürsoy, Ö. & Ş. Kaya (2017): Detecting of Lithological Units by Using Terrestrial Spectral Data and Remote Sensing Image. *Journal of the Indian Society of Remote Sensing* (45)2: 259–269.
- Hadavand, A., M. Mokhtarzadeh, *et al.* (2016): Using pixel-based and object-based methods to classify urban hyperspectral features. *Geodesy and Cartography* (42)3: 92–105.
- Hägele, H. (2013): *Colour in Sculpture: A Survey from Ancient Mesopotamia to the Present*. Cambridge Scholars Publishing.
- Hallmann, A. (2015): Three unusual stelae from Abydos. *Journal of Egyptian Archaeology* (101): 131–152.
- Hanna, S. & M. Norman (1990): The cleaning and removal of surface coatings from a seventh century bc sandstone shrine from nubia. *Studies in Conservation* (35): 23–27.
- Harris Geospatial Solutions, Inc. (2020):(a): Binary Encoding. Available from: <https://www.harrisgeospatial.com/docs/BinaryEncoding.html> (April 24, 2020).
- Harris Geospatial Solutions, Inc. (2020):(b): ENVIRadiometricNormalizationTask. Available from: <https://www.l3harrisgeospatial.com/docs/enviradiometricnormalizationtask.html> (July 21, 2021).
- Harris Geospatial Solutions, Inc. (2020):(c): Minimum Noise Fraction Transform. Available from: <https://www.l3harrisgeospatial.com/docs/minimumnoisefractiontransform.html> (July 27, 2021).
- Harris Geospatial Solutions, Inc. (2020):(d): Perform Classification, MTMF, and Spectral Unmixing. Available from: <https://www.l3harrisgeospatial.com/docs/shperformingclassification.html> (July 28, 2021).
- Harris Geospatial Solutions, Inc. (2020):(e): Pixel Purity Index. Available from: <https://www.l3harrisgeospatial.com/docs/pixelpurityindex.html> (July 27, 2021).

- Harris Geospatial Solutions, Inc. (2020):(f): Principle Components Analysis. Available from:
<https://www.l3harrisgeospatial.com/docs/principalcomponentanalysis.html> (July 28, 2021).
- Harris Geospatial Solutions, Inc. (2020):(g): Spectral Analyst. Available from:
<https://www.l3harrisgeospatial.com/docs/spectralanalyst.html#Spectral> (August 10, 2021).
- Harris Geospatial Solutions, Inc. (2020):(h): Spectral Angle Mapper. Available from:
<http://www.harrisgeospatial.com/docs/SpectralAngleMapper.html> (April 24, 2020).
- Harris Geospatial Solutions, Inc. (2020):(i): Spectral Feature Fitting. Available from:
<http://harrisgeospatial.com/docs/SpectralFeatureFitting.html>.
- Harris Geospatial Solutions, Inc. (2020):(j): Spectral Hourglass Wizard. Available from:
<https://www.l3harrisgeospatial.com/docs/spectralhourglasswizard.html> (July 27, 2021).
- Harris Geospatial Solutions, Inc. (2020):(k): The n-D Visualizer. Available from:
<https://www.l3harrisgeospatial.com/docs/ndimensionalvisualizer.html> (July 27, 2021).
- Hayem-Ghez, A., E. Ravaud, *et al.* (2015): Characterising pigments with hyperspectral imaging variable false-colour composites. *Applied Physics A* (**121**): 939–947.
- Heritage, A., C. Anuzet, *et al.* (2014): The ICCROM Forum on Conservation Science 2013: a collaborative partnership for strategic thinking. In: , pp. 15–19.
- Hou, M., N. Cao, *et al.* (2019): Extraction of Hidden Information under Sootiness on Murals Based on Hyperspectral Image Enhancement. *Applied Sciences* (**9**)17: 3591.
- House of Lords (2012): *Science and Heritage: a follow up - Science and Technology Committee*.
- House of Lords, S. and T.C. (2006): *Science and Heritage: Report with Evidence*.
- Hui, R. (2020): Chapter 4 - Photodetectors. In: R. Hui (Ed), *Introduction to Fiber-Optic Communications*. Academic Press, pp. 125–154.
- Huisman, H., J. de Kort, *et al.* (2019): Erosion of archaeological sites: Quantifying the threat using optically stimulated luminescence and fallout isotopes. *Geoarchaeology* (**34**)4: 478–494.
- Hum-Hartley, S. (1978): Nondestructive Testing for Heritage Structures. *Bulletin of the Association for Preservation Technology* (**10**)3: 4–20.
- ICCROM (2021): Heritage Science. Available from:
<https://www.iccrom.org/section/heritage-science> (August 15, 2021).

- Inglis-Arkell, E. (2019): Ultraviolet light reveals how ancient Greek statues really looked. *Gizmodo*. Available from: <https://io9.gizmodo.com/5616498/ultraviolet-light-reveals-how-ancient-greek-statues-really-looked>.
- Invernizzi, C., T. Rovetta, *et al.* (2018): Mid and near-infrared reflection spectral database of natural organic materials in the cultural heritage field. *International journal of analytical chemistry* (2018).
- Iqbal, M. (2012): *An introduction to solar radiation*. Elsevier.
- Janssens, K., G. Van der Snickt, *et al.* (2016):(a): 374 *Non-Invasive and Non-Destructive Examination of Artistic Pigments, Paints, and Paintings by Means of X-Ray Methods*.
- Janssens, K., G. Van Der Snickt, *et al.* (2016):(b): Rembrandt's "Saul and David" (c. 1652): Use of multiple types of smalt evidenced by means of non-destructive imaging. *Microchemical Journal* (126): 515–523.
- Janssens, K. & R. Van Grieken (2004): *Non-destructive micro analysis of cultural heritage materials*. Elsevier.
- Javier, S. & J.P. Hornak (2018): A nondestructive method of identifying pigments on canvas using low frequency electron paramagnetic resonance spectroscopy. *Journal of the American Institute for Conservation* (57)1–2: 73–82.
- Kaew-On, N., P. Katemake, *et al.* (2020): Monitoring paint and primer samples using multispectral and hyperspectral imaging techniques. *ScienceAsia* (46): 110–116.
- Kang, R., B. Park, *et al.* (2020): Identifying non-O157 Shiga toxin-producing *Escherichia coli* (STEC) using deep learning methods with hyperspectral microscope images. *Spectrochimica Acta - Part A: Molecular and Biomolecular Spectroscopy* (224).
- Karapanagiotis, I. & Y. Chryssoulakis (2006): Investigation of red natural dyes used in historical objects by HPLC-DAD-MS. *Annali di Chimica: Journal of Analytical, Environmental and Cultural Heritage Chemistry* (96)1-2: 75–84.
- Kardjilov, N. & G. Festa (2017): *Neutron methods for archaeology and cultural heritage*. Springer.
- Kirwan, L.P. (1936): Preliminary Report of the Oxford University Excavations at Kawa, 1935-1936. *The Journal of Egyptian Archaeology* (22)2: 199–211.
- Kitchen, K.A. (1996): *The Third Intermediate Period in Egypt (1100–650 BC)*, rev. Warminster: Aris & Phillips.
- Kockelmann, W. & A. Kirfel (2006): Neutron diffraction imaging of cultural heritage objects. In: Citeseer, pp. 1–15.
- Kokaly, R.F., D.G. Despain, *et al.* (2003): Mapping vegetation in Yellowstone National Park using spectral feature analysis of AVIRIS data. *Remote Sensing of Environment* (84)3: 437–456.

- Kopczynski, N., L. de Viguierie, *et al.* (2017): Polychromy in Africa Proconsularis: investigating Roman statues using X-ray fluorescence spectroscopy. *Antiquity* (91)355: 139–154.
- Krmpotić, M., D. Jembrih-Simbürger, *et al.* (2020): The identification of synthetic organic pigments (SOPs) used in modern artist's paints with Secondary Ion Mass Spectrometry with MeV ions. *Analytical Chemistry*.
- Kruse, F.A., A.B. Lefkoff, *et al.* (1993): The spectral image processing system (SIPS)-interactive visualization and analysis of imaging spectrometer data. *Remote Sensing of Environment* (44)2–3: 145–163.
- Kühn, H. (1963): A History of Pigments and Dyestuffs. *Angewandte Chemie International Edition in English* (2)3: 160–161.
- Kurdian, H. (1956): The newly discovered alphabet of the caucasian Albanians. *The Journal of The Royal Asiatic Society of Great Britain and Ireland*: 81–83.
- Laban, N., B. Abdellatif, *et al.* (2020): 921 Reduced 3-D Deep Learning Framework for Hyperspectral Image Classification.
- Labsphere (2021): Labsphere Spectralon Targets. Available from: <https://www.labsphere.com/labsphere-products-solutions/materials-coatings-2/targets-standards/test-child/> (May 13, 2021).
- Langenkämper, A., A. Ulrich, *et al.* (2018): Low-temperature relative reflectivity measurements of reflective and scintillating foils used in rare event searches. *Nuclear Instruments and Methods in Physics Research Section A: Accelerators, Spectrometers, Detectors and Associated Equipment* (884): 40–44.
- Lau, D., P. Kappen, *et al.* (2008):(a): Characterization of green copper phase pigments in Egyptian artifacts with X-ray absorption spectroscopy and principal components analysis. *Spectrochimica Acta - Part B Atomic Spectroscopy* (63)11: 1283–1289.
- Lau, D., C. Villis, *et al.* (2008):(b): Multispectral and hyperspectral image analysis of elemental and micro-Raman maps of cross-sections from a 16th century painting. *Analytica Chimica Acta* (610): 15–24.
- Leeds, E.T. (1942): The new Egyptian sculpture gallery and a shrine of Tirharqa in the Ashmolean museum. *The Museums Journal* (41): 228–231.
- Li, X., D. Lu, *et al.* (2000):(a): Color restoration and image retrieval for Dunhuang fresco preservation. *IEEE Multimedia* (7)2: 38–42.
- Li, X., D. Lu, *et al.* (2000):(b): Virtual Dunhuang mural restoration system in collaborative network environment. *Computer Graphics Forum* (19)3: C-331–C-339.
- Liang, H. (2012): Advances in multispectral and hyperspectral imaging for archaeology and art conservation. *Applied Physics A* (106): 309–323.

- Liang, H., R. Lange, *et al.* (2011): Non-invasive investigations of a wall painting using optical coherence tomography and hyperspectral imaging. *Optics for Arts, Architecture, and Archaeology III* (8084).
- Lint, T.M. van & R. Meyer (2015): *Armenia : masterpieces from an enduring culture*.
- Lomax, S.Q. & T. Learner (2006): A Review of the Classes, Structures, and Methods of Analysis of Synthetic Organic Pigments. *Journal of the American Institute for Conservation* (45)2: 107–125.
- Luo, M.R. (2002): Development of colour-difference formulae. *Review of Progress in Coloration and related Topics* (32)1: 28–39.
- Lynch, P.A., N. Tamura, *et al.* (2007): Application of white-beam X-ray microdiffraction for the study of mineralogical phase identification in ancient Egyptian pigments. *Journal of Applied Crystallography* (40)6: 1089–1096.
- Macadam, M.F.L. (1949): *The temples of Kawa : Oxford University excavations in Nubia*. Published on behalf of the Griffith Institute, Ashmolean Museum, Oxford, by Oxford University Press, London.
- Macholdt, D.S., A.M. Al-Amri, *et al.* (2018): Growth of desert varnish on petroglyphs from Jubbah and Shuwaymis, Ha'il region, Saudi Arabia. *Holocene* (28)9: 1495–1511.
- Magkanas, G., H. Bagán, *et al.* (2021): Illuminated manuscript analysis methodology using MA-XRF and NMF: Application on the Liber Feudorum Maior. *Microchemical Journal* (165): 106112.
- Males, B., L. Oakley, *et al.* (2019): Maximizing the microscope: instrument design and data processing strategies for hyperspectral imaging of cross-sectional cultural heritage samples.
- Manikowska, E., G. Pasternak, *et al.* (2020): Cultural Heritage and Technology Guest Editorial. *Santander Art and Culture Law Review (SAACLR)* (2020)2: 12–16.
- Maravelaki-Kalaitzaki, P., R. Bertoncello, *et al.* (2002): Evaluation of the initial weathering rate of istria stone exposed to rain action, in venice, with x-ray photoelectron spectroscopy. *Journal of Cultural Heritage* (3)4: 273–282.
- Marcus, R.T. (1998): chapter 2 - The Measurement of Color. In: K. Nassau (Ed), *AZimuth*. North-Holland, pp. 31–96.
- Marengo, E., E. Robotti, *et al.* (2003): A Method for Monitoring the Surface Conservation of Wooden Objects by Raman Spectroscopy and Multivariate Control Charts. *Analytical Chemistry* (75)20: 5567–5574.
- Martin Chamberland, Vincent Farley, *et al.* (2004): Development and testing of a hyperspectral imaging instrument for standoff chemical detection.

- Marucci, G., A. Beeby, *et al.* (2018): Raman spectroscopic library of medieval pigments collected with five different wavelengths for investigation of illuminated manuscripts. *Analytical Methods* (**10**)10: 1219–1236.
- Masini, N., G. Leucci, *et al.* (2020): Towards urban archaeo-geophysics in peru. The case study of plaza de armas in cusco. *Sensors (Switzerland)* (**20**)10.
- Mathews, T.F. (1981): A Pigment Analysis of Medieval Armenian Manuscripts. In: W. Hörandner (Ed), *XVI. Internationaler Byzantinistenkongress. Der Österreichischen Akademie Der Wissenschaften*, Vienna, pp. 3.2.
- Mathews, T.F., R.S. Wieck, *et al.* (1994): *Treasures in Heaven: Armenian Illuminated Manuscripts*. The Pierpoint Morgan Library, New York.
- Maybury, I.J., D. Howell, *et al.* (2018): Comparing the effectiveness of hyperspectral imaging and Raman spectroscopy: a case study on Armenian manuscripts. *Heritage Science* (**6**)1: 42.
- Maynard, L. (1975): Restoration of Aboriginal Rock Art: The Moral Problem. *Australian Archaeology* (**3**).
- Mazzuca, C., L. Severini, *et al.* (2020): Polyvinyl alcohol based hydrogels as new tunable materials for application in the cultural heritage field. *Colloids and Surfaces B: Biointerfaces* (**188**): 110777.
- McCreery, R.L. (2000): *157 Raman Spectroscopy for Chemical Analysis*. John Wiley and Sons, Inc.
- van der Meer, F. (2004): Analysis of spectral absorption features in hyperspectral imagery. *International Journal of Applied Earth Observation and Geoinformation* (**5**)1: 55–68.
- Melessanaki, K., V. Papadakis, *et al.* (2001): Laser induced breakdown spectroscopy and hyper-spectral imaging analysis of pigments on an illuminated manuscript. *Spectrochimica Acta - Part B Atomic Spectroscopy* (**56**)12: 2337–2346.
- Melo, M.J., R. Araujo, *et al.* (2016): Colour degradation in medieval manuscripts. *Microchemical Journal* (**124**): 837–844.
- Messenger, C., L. Beck, *et al.* (2020): Thermal analysis of carbonate pigments and linseed oil to optimize CO₂ extraction for radiocarbon dating of lead white paintings. *Microchemical Journal* (**154**): 104637.
- Mignani, A.G., M. Bacci, *et al.* (2003): Equivalent light dosimetry in museums with blue wool standards and optical fibers. *IEEE Sensors Journal* (**3**)1: 108–114.
- Miliani, C., L. Monico, *et al.* (2018): Photochemistry of Artists' Dyes and Pigments: Towards Better Understanding and Prevention of Colour Change in Works of Art. *Angewandte Chemie International Edition* (**57**)25: 7324–7334.

- Montagner, C., R. Jesus, *et al.* (2016): Features combination for art authentication studies: brushstroke and materials analysis of Amadeo de Souza-Cardoso. *Multimedia Tools and Applications* (75): 4039–4063.
- Mori, F., R. Ponti, *et al.* (2006): Chemical characterization and AMS radiocarbon dating of the binder of a prehistoric rock pictograph at Tadrart Acacus, southern west Libya. *Journal of Cultural Heritage* (7)4: 344–349.
- Morigi, M., F. Casali, *et al.* (2010): Application of X-ray computed tomography to cultural heritage diagnostics. *Applied Physics A* (100)3: 653–661.
- Moropoulou, A., K.C. Labropoulos, *et al.* (2013): Non-destructive techniques as a tool for the protection of built cultural heritage. *Construction and Building Materials* (48): 1222–1239.
- Mosca, S., T. Frizzi, *et al.* (2016): Identification of pigments in different layers of illuminated manuscripts by X-ray fluorescence mapping and Raman spectroscopy. *Microchemical Journal* (124): 775–784.
- Mounier, A. & F. Daniel (2015): Hyperspectral imaging for the study of two thirteenth-century Italian miniatures from the Marcadé collection, Treasury of the Saint Andre Cathedral in Bourdeaux, France. *Studies in Conservation* (60)Supplement 1: S200–S209.
- Mounier, A., G.A. Le Bourdon C., *et al.* (2014): Hyperspectral imaging, spectrofluorimetry, FORS, and XRF for the non-invasive study of medieval miniatures materials. *Heritage Science* (2)24: 1–12.
- Moussa, A. & M.F. Ali (2013): Color alteration of ancient Egyptian blue faience. *International Journal of Architectural Heritage* (7)3: 261–274.
- Moutsatsou, A. & A. Alexopoulou (2014): A note on the construction of test panels for the spectral imaging of paintings. *Studies in Conservation* (59)1: 3–9.
- Možina, K., K. Možina, *et al.* (2013): 14 *Journal of Cultural Heritage Non-invasive methods for characterisation of printed cultural heritage*.
- Muir, K., A. Langley, *et al.* (2013): Scientifically investigating Picasso's suspected use of ripolin house paints in Still Life, 1922 and The Red Armchair, 1931. *Journal of the American Institute for Conservation* (52)3: 156–172.
- Mulholland, R., D. Howell, *et al.* (2017): Identifying eighteenth century pigments at the Bodleian library using in situ Raman spectroscopy, XRF and hyperspectral imaging. *Heritage Science* (5)1.
- Nadolny, J. (2003): The first century of published scientific analyses of the materials of historical painting and polychromy, circa 1780-1880. *Studies in Conservation* (48)sup1: 39–51.
- Namowicz, C., K. Trentelman, *et al.* (2009): XRF of cultural heritage materials: Round-robin IV--Paint on canvas. *Powder diffraction* (24)2: 124.

- National Heritage Science Forum (2021): Societal challenges and heritage science research.
- National Heritage Science Steering Group (2010): *National Heritage Science Strategy*.
- Neff, D., L. Bellot-Gurlet, *et al.* (2006): Raman imaging of ancient rust scales on archaeological iron artefacts for long-term rust corrosion mechanisms study. *Journal of Raman Spectroscopy* (37): 1228–1237.
- New House Internet Services B.V. (2021): PTGui. Available from: <https://www.ptgui.com/> (August 7, 2021).
- Nicholson, P.T. & I. Shaw (2000): *Ancient Egyptian materials and technology*. Cambridge University Press.
- Nidamanuri, R.R. & A.M. Ramiya (2014): Spectral identification of materials by reflectance spectral library search. *Geocarto International* (29)6: 609–624.
- Nouri, D., Y. Lucas, *et al.* (2013): Calibration and test of a hyperspectral imaging prototype for intra-operative surgical assistance. In: International Society for Optics and Photonics, pp. 86760P.
- Olin, J.S., M.E. Salmon, *et al.* (1969): Investigations of Historical Objects Utilizing Spectroscopy and Other Optical Methods. *Applied Optics* (8)1: 29–39.
- Orna, M., V. (2013): Artists' Pigments in Illuminated Medieval Manuscripts: Tracing Artistic Influences and Connections - A Review. In: *Archaeological Chemistry VIII (ACS Symposium Series)*. American Chemical Society, pp. 3–18.
- Orna, M.V. & T.F. Mathews (1981): Pigment Analysis of the Glajor Gospel book of V.C.L.A. *Studies in Conservation* (26)2: 57–72.
- Orna, M.V. & T.F. Mathews (1988): Uncovering the Secrets of Medieval Artists. *Analytical Chemistry* (60)1: 47–56.
- Owen, M. (2007): *Practical signal processing*. Cambridge university press.
- Padoan, R., M.E. Klein, *et al.* (2021): Quantitative assessment of impact and sensitivity of imaging spectroscopy for monitoring of ageing of archival documents. *Heritage* (4)1: 105–124.
- Palamara, E., P. Das, *et al.* (2020): Applying SEM-Cathodoluminescence imaging and spectroscopy as an advanced research tool for the characterization of archaeological material. *Microchemical Journal*: 105230.
- Palla, F., M. Bruno, *et al.* (2020): Essential Oils as Natural Biocides in Conservation of Cultural Heritage. *Molecules* (25)3: 730.
- Pallipurath, A., R.V. Vofely, *et al.* (2014): Estimating the concentrations of pigments and binders in lead-based paints using FT-Raman spectroscopy and principal component analysis. *Journal of Raman Spectroscopy* (45): 1272–1278.

- Palomar, T., C. Grazia, *et al.* (2019): Analysis of chromophores in stained-glass windows using Visible Hyperspectral Imaging in-situ. *Spectrochimica Acta Part A: Molecular and Biomolecular Spectroscopy* (**223**): 117378.
- Pan, Z., J. Huang, *et al.* (2013): Multi range spectral feature fitting for hyperspectral imagery in extracting oilseed rape planting area. *International Journal of Applied Earth Observation and Geoinformation* (**25**)1: 21–29.
- Pascual-Izarra, C., N.P. Barradas, *et al.* (2007): Towards truly simultaneous PIXE and RBS analysis of layered objects in cultural heritage. *Nuclear Instruments and Methods in Physics Research Section B: Beam Interactions with Materials and Atoms* (**261**)1–2: 426–429.
- Pérez-Arategui, J. & Á. Larrea (2003): The secret of early nanomaterials is revealed, thanks to transmission electron microscopy. *TrAC Trends in Analytical Chemistry* (**22**)5: 327–329.
- Piccolo, M., C. Cucci, *et al.* (2020): Hyper-Spectral Imaging Technique in the Cultural Heritage Field: New Possible Scenarios. *Sensors* (**20**)10: 2843.
- Pieper, R. & A. Korpel (1983): Image processing for extended depth of field. *Applied Optics* (**22**)10: 1449–1453.
- Pillay, R., J.Y. Hardeberg, *et al.* (2019): Hyperspectral imaging of art: Acquisition and calibration workflows. *Journal of the American Institute for Conservation* (**58**)1–2: 3–15.
- Pires, J. & A. Cruz (2007): Techniques of thermal analysis applied to the study of cultural heritage. *Journal of Thermal Analysis and Calorimetry* (**87**)2: 411–415.
- Plenderleith, H.J. (1998): A history of conservation. *Studies in Conservation* (**43**)3: 129–143.
- Polak, A., T. Kelman, *et al.* (2017): Hyperspectral imaging combined with data classification techniques as an aid for artwork authentication. *Journal of Cultural Heritage* (**26**): 1–11.
- Prisco, J. (2017): What ancient statues really looked like. *CNN*.
- Q. Du, N. Younan, *et al.* (2007): Change Analysis for Hyperspectral Imagery. In: *2007 International Workshop on the Analysis of Multi-temporal Remote Sensing Images.* , pp. 1–4.
- Rebollo, E., L. Nodari, *et al.* (2013): Non-invasive multitechnique methodology applied to the study of two 14th century canvases by Lorenzo Veneziano. *Journal of Cultural Heritage* (**154**): e153–e160.
- Retzlaff, M.-G., J. Hanika, *et al.* (2017): Physically based computer graphics for realistic image formation to simulate optical measurement systems. *Journal of Sensors and Sensor Systems* (**6**)1: 171–184.

- Ricciardi, P., J.K. Delaney, *et al.* (2009): Use of visible and infrared reflectance and luminescence imaging spectroscopy to study illuminated manuscripts: pigment identification and visualisation of underdrawings. *Optics for Arts, Architecture, and Archaeology II* (7391)06: 1–12.
- Ricciardi, P., J.K. Delaney, *et al.* (2013): Use of imaging spectroscopy and in situ analytical methods for the characterisation of the materials and techniques of 15th century illuminated manuscripts. *Journal of the American Institute for Conservation* (52)1: 13–29.
- Ridpath, I. (2018): chromatic aberration.
- Romani, M., G. Capobianco, *et al.* (2020): Analytical chemistry approach in cultural heritage: the case of Vincenzo Pasqualoni's wall paintings in S. Nicola in Carcere (Rome). *Microchemical Journal*: 104920.
- Royal Society of Chemistry (2020): Prehistoric Pigments.
- Royse, J.R. (2009): The Works of Philo. In: *The Cambridge Companion to Philo*. Cambridge University Press, Cambridge, pp. 32–64.
- Sabbatini, L. & I.D. van der Werf (2020): *Chemical Analysis in Cultural Heritage*. Walter de Gruyter GmbH & Co KG.
- Sandak, J., A. Sandak, *et al.* (2021): Nondestructive Evaluation of Heritage Object Coatings with Four Hyperspectral Imaging Systems. *Coatings* 2021, 11, 244.
- Saunders, D. & J. Kirby (1994): Wavelength-dependent fading of artists' pigments. *Studies in Conservation* (39): 190–194.
- Saunders, D. & J.O. Kirby (2004): The Effect of Relative Humidity on Artists' Pigments. *National Gallery Technical Bulletin* (25): 62–72.
- Schlamm, A. & D. Messinger (2010): A Euclidean distance transformation for improved anomaly detection in spectral imagery. *Image Processing Workshop*: 26–29.
- Schulz, W.G. (2009): Science from Art. *Chemical and Engineering News* (87)42: 12–16.
- Science and Heritage Programme (2009): *Science and Heritage Programme: Research Programme Specification March 2009*.
- Scott, D.A. (2016): A review of ancient Egyptian pigments and cosmetics. *Studies in Conservation* (61)4: 185–202.
- Scott, D.A. & L. Swartz Dodd (2002): Examination, conservation and analysis of a gilded Egyptian bronze Osiris. *Journal of Cultural Heritage* (3)4: 333–345.
- Sebar, L.E., E. Angelini, *et al.* (2020): A trustable 3D photogrammetry approach for cultural heritage. In: *IEEE*, pp. 1–6.

- Shen, G., J.A. Fernández Pierna, *et al.* (2020): Local anomaly detection and quantitative analysis of contaminants in soybean meal using near infrared imaging: The example of non-protein nitrogen. *Spectrochimica Acta - Part A: Molecular and Biomolecular Spectroscopy* (**225**).
- Singh, K.D. & D. Ramakrishnan (2017): A comparative study of signal transformation techniques in automated spectral unmixing of infrared spectra for remote sensing applications. *International Journal of Remote Sensing* (**38**)5: 1235–1257.
- Smith, E. & G. Dent (2008): *Modern Raman Spectroscopy: A Practical Approach*. John Wiley & Sons Ltd, Chichester.
- Smith, G.D. & R.J.H. Clark (2004): Raman microscopy in archaeological science. *Journal of Archaeological Science* (**31**): 1137–1160.
- Snijders, L., T. Zaman, *et al.* (2016): Using hyperspectral imaging to reveal a hidden precolonial Mesoamerican codex. *Journal of Archaeological Science: Reports* (**9**): 143–149.
- Sokaras, D. (2020): The new external ion-beam station at the Demokritos Tandem 5.5 MV accelerator: A unique analytical tool in the fields of cultural heritage and environmental science. *HNPS Proceedings* (**16**): 209–218.
- Song, M., E. Li, *et al.* (2020): 516 Spectral Characteristics of Nitrogen and Phosphorus in Water.
- Stanzani, E., D. Bersani, *et al.* (2016): Analysis of artist's palette on a 16th century wood panel painting by portable and laboratory Raman instruments. *Vibrational Spectroscopy* (**85**): 62–70.
- Stevenson, A. & M. Waite (2011): *Concise Oxford English Dictionary*. Oxford University Press.
- Strlic, M. (2015): A brief theory of heritage science. *Heritage science research network*.
- Sun, C., M. Wang, *et al.* (2019): Comparison and analysis of wavelength calibration methods for prism – Grating imaging spectrometer. *Results in Physics* (**12**): 143–146.
- Szökefalvi-Nagy, Z., I. Demeter, *et al.* (2004): Non-destructive XRF analysis of paintings. *Radiation and Archaeometry* (**226**)1: 53–59.
- Tan, K., H. Wang, *et al.* (2020): Estimation of the spatial distribution of heavy metal in agricultural soils using airborne hyperspectral imaging and random forest. *Journal of Hazardous Materials* (**382**).
- Tehfe, M.-A., J. Lalevéé, *et al.* (2012): Iridium complexes incorporating coumarin moiety as catalyst photoinitiators: Towards household green LED bulb and halogen lamp irradiation. *Polymer* (**53**)14: 2803–2808.

- Terras, M. (2010): The digital classicist: Disciplinary focus and interdisciplinary vision. In: *Digital Research in the Study of Classical Antiquity*. Ashgate Publishing, pp. 171–189.
- The Ashmolean Museum (2015): Taharqa's shrine fact sheet. Available from: <http://www.ashmolean.org/education/resources/resources/TaharqaShrineInfoSheet.pdf>.
- Thoms, L.-J. & R. Girwidz (2013): *Experimenting from a Distance: Optical Spectrometry via the Internet*.
- Thuillier, G., L. Floyd, *et al.* (2004): Solar irradiance reference spectra for two solar active levels. *Solar Variability and Climate Change* (34)2: 256–261.
- Troalen, L.G. (2013): Historic dye analysis: method development and new applications in cultural heritage.
- Trumpy, G., D. Conover, *et al.* (2015): Experimental study on merits of virtual cleaning of paintings with aged varnish. *Optics Express* (23)26: 33836–33848.
- Tumanyan, B.E. (1967): On the history of armenian astronomy. *Vistas in Astronomy* (9): 253–259.
- Vandenabeele, P., H.G.M. Edwards, *et al.* (2006): A Decade of Raman Spectroscopy in Art and Archaeology. *Chemical Reviews* (107)3: 675–686.
- Vandenabeele, P., L. Moens, *et al.* (2000): Raman spectroscopic database of azo pigments and application to modern art studies. *Journal of Raman spectroscopy* (31)6: 509–517.
- Vandivere, A., J. Wadum, *et al.* (2020): The Girl in the Spotlight: Vermeer at work, his materials and techniques in Girl with a Pearl Earring. *Heritage Science* (8)1.
- Varella, E.A. (2012): *79 Conservation science for the cultural heritage: applications of instrumental analysis*. Springer Science & Business Media.
- Viles, H., A. Goudie, *et al.* (2011): The use of the Schmidt Hammer and Equotip for rock hardness assessment in geomorphology and heritage science: A comparative analysis. *Earth Surface Processes and Landforms* (36)3: 320–333.
- Vitorino, T., A. Casini, *et al.* (2014): Hyper-Spectral Acquisition on Historically Accurate Reconstructions of Red Organic Lakes. *LNCS* (8509): 257–264.
- Vitorino, T., A. Casini, *et al.* (2015): Non-invasive identification of traditional red lake pigments in fourteenth to sixteenth centuries paintings through the use of hyperspectral imaging technique. *Applied Physics A* (121): 891–901.
- Vogel, A. (1996): Vogel's Qualitative Inorganic Analysis, Revised by Svehla, G. *Logman Scientific*: 112–116.
- Volp, G. & V.H. Grassian (2013): Role(s) of adsorbed water in the surface chemistry of environmental interfaces. *Chemical Communications* (49)30: 3071–3094.

- WANG, J., Y. WANG, *et al.* (2010): Noise model of hyperspectral imaging system and influence on radiation sensitivity. *a a* (4): 1.
- Wang, S., K. Zhou, *et al.* (2018): Effects of weathering, desert-varnish and lichens of rock surface on hyperspectral remote sensing. *Scientia Geologica Sinica* (53)2: 739–748.
- Wang, W., C. Li, *et al.* (2012): A liquid crystal tunable filter based shortwave infrared spectral imaging system: Calibration and characterization. *Computers and Electronics in Agriculture* (80): 135–144.
- Whitmore, P.M. (2002): Pursuing the fugitive: direct measurement of light sensitivity with micro-fading tests. In: *The broad spectrum: Studies in the materials, techniques, and conservation of color on paper.*, pp. 241–244.
- Whitmore, P.M., G.R. Cass, *et al.* (1987): The ozone fading of traditional natural organic colorants on paper. *Journal of the American Institute for Conservation* (26)1: 45–58.
- Whitmore, P.M. & G.R. Cass (1989): The fading of artists' colorants by exposure to atmospheric nitrogen dioxide. *Studies in Conservation* (34)2: 85–97.
- Williams, J. (2009):(a): *The role of science in the management of the UK's heritage.*
- Williams, J. (2009):(b): *The use of science to enhance our understanding of the past.*
- Williams, J. (2009):(c): *Understanding capacity in the heritage science sector.*
- Woolfe, G.J., B.H. Pillman, *et al.* (1998): Restoration of faded images.
- Wu, T., Q. Cheng, *et al.* (2019): The discovery and extraction of Chinese ink characters from the wood surfaces of the Huangchangticou tomb of Western Han Dynasty. *Archaeological and Anthropological Sciences* (11)8: 4147–4155.
- Wu, T., G. Li, *et al.* (2017): Shortwave Infrared Imaging Spectroscopy for Analysis of Ancient Paintings. *Applied Spectroscopy* (71)5: 977–987.
- Xie, T., S. Li, *et al.* (2020): Hyperspectral Images Denoising via Nonconvex Regularized Low-Rank and Sparse Matrix Decomposition. *IEEE transactions on image processing : a publication of the IEEE Signal Processing Society* (29): 44–56.
- Yastikli, N. (2007): Documentation of cultural heritage using digital photogrammetry and laser scanning. *Journal of Cultural Heritage* (8)4: 423–427.
- Yoshizumi, K. & P.C. Crews (2003): Characteristics of fading of wool cloth dyed with selected natural dyestuffs on the basis of solar radiant energy. *Dyes and Pigments* (58)3: 197–204.
- Zacharias, N., F. Karavassili, *et al.* (2018): A novelty for cultural heritage material analysis: transmission electron microscope (TEM) 3D electron diffraction

tomography applied to Roman glass tesserae. *Microchemical Journal* (**138**): 19–25.

Zhao, Y., R.S. Berns, *et al.* (2008): An Investigation of Multispectral Imaging for the Mapping of Pigments in Paintings. *SPIE-IS&T Electronic Imaging* (**6810**): 681007-1-681007-9.

Zoleo, A., D. Confortin, *et al.* (2010): The role of metal ions in the study of ancient paper by electron paramagnetic resonance. *Applied Magnetic Resonance* (**39**)3: 215–223.

Chapter 10 Appendix Proof of submission of manuscripts to journals

Ian Maybury

From: em.sic.0.668592.0d3ab12b@editorialmanager.com on behalf of Prempriya

Mohan

<em@editorialmanager.com>

Sent: 11 October 2019 11:36

To: Ian Maybury

Subject: Submission to Studies in Conservation

CC: "David Howell" david.howell@bodleian.ox.ac.uk, "Melissa Terras"

m.terras@ed.ac.uk, "Heather Viles" heather.viles@ouce.ox.ac.uk

Dear Mr Maybury

We acknowledge receipt of your submission entitled "A Demonstration Of The Utility Of Visible And Near Infrared Hyperspectral Imaging (VNIR HSI) For Monitoring Colour In Collection Items On Display" to Studies in Conservation.

You will be able to check the progress of your paper by logging on to Editorial Manager as an author at the URL <https://www.editorialmanager.com/sic/>: Your username is: Ian

<https://www.editorialmanager.com/sic/1.asp?i=57578&l=IA32XSWG>

Your manuscript will be given a reference number once an Editor has been assigned.

Thank you for submitting your work to this journal.

Kind regards,

Studies in Conservation

In compliance with data protection regulations, you may request that we remove your personal registration details at any time. (Use the following URL:

<https://www.editorialmanager.com/sic/login.asp?a=r>). Please contact the publication office if you have any questions.

Ian Maybury

From: em.jac.0.6681ea.c6b2edf4@editorialmanager.com on behalf of Editorial Office,
Journal of the American Institute for Conservation
<em@editorialmanager.com>
Sent: 10 October 2019 20:00
To: Ian Maybury
Subject: Submission to Journal of the American Institute for Conservation
CC: "David Howell" david.howel@bodleian.ox.ac.uk, "Melissa Terras" m.terras@ed.ac.uk, "Heather Viles" heather.viles@ouce.ox.ac.uk

Dear Mr Maybury

We acknowledge receipt of your submission entitled "Digital restoration using visible and near infrared hyperspectral imaging (VNIR HSI): An investigation into the pigmentation on the west wall of the Shrine of Taharqa" to Journal of the American Institute for Conservation.

You will be able to check the progress of your paper by logging on to Editorial Manager as an author at the URL <https://www.editorialmanager.com/jac/>:

Your username is: ian.maybury@stx.ox.ac.uk

<https://www.editorialmanager.com/jac/1.asp?i=22992&l=HL16LCHM>

Your manuscript will be given a reference number once an Editor has been assigned.

Thank you for submitting your work to this journal.

Kind regards,

Journal of the American Institute for Conservation

In compliance with data protection regulations, you may request that we remove your personal registration details at any time. (Use the following URL: <https://www.editorialmanager.com/jac/login.asp?a=r>). Please contact the publication office if you have any questions.